Downstream Effects of the Pelton Round Butte Hydroelectric Project on Bedload Transport, Channel Morphology, and Channel-bed Texture, Deschutes River, Oregon

Prepared for PGE by:

Gordon E. Grant
U.S. Forest Service, Pacific Northwest Research Station

Heidi Fassnacht
Department of Geosciences,
Oregon State University

Ellen M. McClure
Philip Williams and Associates, Ltd.

Peter C. Klingeman
Department of Civil, Construction, and Environmental Engineering
Oregon State University

April 1999

Downstream Effects of the Pelton Round Butte Hydroelectric Project on Bedload Transport,
PGE April 1999

For copies of this report, write:

Portland General Electric
Hydro Licensing Department
Attn: Marty May
121 SW Salmon St.
Portland, OR 97204

2591

Downstream Effects of the Pelton Round Butte Hydroelectric Project on Bedload Transport, Channel Morphology, and Channel-bed Texture, Deschutes River, Oregon

Prepared for PGE by:

Gordon E. Grant
U.S. Forest Service, Pacific Northwest Research Station
3200 Jefferson Way, Corvallis, Oregon, 97331

Heidi Fassnacht
Department of Geosciences
Oregon State University, Corvallis, Oregon, 97331

Ellen M. McClure
Philip Williams and Associates, Ltd.
770 Tamalpais Drive, Suite 401,Corte Madera, CA, 94925

Peter C. Klingeman
Department of Civil, Construction, and Environmental Engineering
Oregon State University, Corvallis, Oregon, 97331

April 1999

TABLE OF CONTENTS

[Blank]

LIST OF FIGURES

LIST OF FIGURES (Continued)

LIST OF FIGURES (Continued)

[Blank]

LIST OF TABLES

[Blank]

LIST OF SYMBOLS

A	cross-sectional area
β	statistical model coefficient
β_0	y intercept or D_{50} when all other β values equal zero
β_1	River Kilometer
β_2	equals 0 for 1995 and equals 1 for 1996
β_3	equals 1 for moderate levels of *Ceratophyllum demersum*
β_4	equals 1 for high levels of *Ceratophyllum demersum*
CD	level of *Ceratophyllum demersum*
$\bar{d}$	hydraulic mean depth ($\bar{d} = A/T$)
D_{50s}	channel-bed surface particle diameter for which 50% of sample is finer
D_i	geometric mean of i^{th} grain-size range
F_a	frequency of flow required to move some index value (i.e. D_{50}) of the surface or subsurface grain-size distribution after river impoundment
F_b	frequency of flow required to move some index value (i.e. D_{50}) of the surface or subsurface grain-size distribution before river impoundment
g	gravitational acceleration
γ_f	specific weight of fluid (water)
μ	estimated mean
Q	water discharge
Q_S	total volumetric bedload transport rate, or sediment discharge
Q_{sa}	sediment supply after river impoundment
Q_{sb}	sediment supply before river impoundment
Q_{cr}	critical discharge, water discharge producing threshold transport conditions
Q_{in}	water discharge into Round Butte Reservoir
Q_{out}	water discharge out of the Pelton Round Butte Dam Complex
Q_{Sin}	bedload transported by Q_{in}
Q_{Sout}	bedload transported by Q_{out}
RK	River Kilometer
ρ_s	density of sediment
ρ_f	density of fluid (water)
S_e	downstream slope of the energy grade line, or energy slope
T	top width, or the width of the free surface of the fluid at the top of the channel
τ	shear stress
τ_{ave}	average shear stress for a site
τ_{cr}	critical shear stress
τ_{cr50s}	shear stress required to entrain the median particle diameter of the channel-bed surface material
τ^*_{cr}	dimensionless critical shear stress or Shields stress
τ^*_{cr50s}	Shields stress for median diameter of channel-bed surface

[Blank]

ABSTRACT

We report on a four-year investigation on the effects of the Pelton Round Butte dam complex on the geomorphology of the lower Deschutes River, Oregon. A conceptual model relating predicted changes below dams to the frequency of streamflows that transport sediment and the rate of sediment supply is developed. Field, laboratory, and historical data provide the basis for testing this model for the Deschutes River. We evaluated the frequency and magnitude of streamflows and bedload transport prior to and following dam construction using hydraulic and bedload transport models. These models constrained the range of flows required to initiate bedload transport from 270 to 460 m^3/s (9,530 to 16,240 ft^3/s). Such flows occur, on average, less than 1% of the time and are substantially less frequent than on other alluvial rivers. The lower range of modeled estimates for initiation of bedload transport agree well with analyses of historical change at long-term cross sections, which show general scour and fill beginning at approximately 250 m^3/s (8,830 ft^3/s). Dam operations have had only minimal effects on streamflow and frequency and magnitude of bedload transport. Surveys of Round Butte Reservoir (Lake Billy Chinook) reveal very low sedimentation rates of approximately 10 metric tons/km^2/yr (30 standard tons/mi^2/yr) over the 34-year period since construction of Round Butte Dam. These rates are quite low for western rivers. Consistent with the conceptual model, field studies of channel response below the dams indicate only minor changes to channel cross section. Degradation of the channel, which was occurring prior to dam construction, is at least an order of magnitude lower than for other dammed rivers. Detailed analyses of longitudinal trends in surface and subsurface grain sizes and bed armoring indicate that the dams have had only minimal effects on channel-bed texture. A major (100-year) flood in February 1996 produced only modest changes to channel morphology, primarily in the vicinity of tributary junctions where sediment input from tributaries contributed to local changes in island and bar morphology. These studies paint a coherent picture of the Deschutes River under its current flow and geomorphic regime as an extremely stable alluvial system. Evidence indicates that its stability is due to a hydrologically uniform flow regime and low rates of sediment supply. Both of these factors arise from the river's unique geological setting and have not been substantially altered by dams or their operation.

[Blank]

INTRODUCTION

Dams and reservoirs alter the movement of water, sediment, wood, and organisms through rivers, and therefore can have potentially significant effects on alluvial systems. Previous studies on the effects of dams on alluvial channels, however, show that predicting the magnitude, timing, extent, or duration of dam effects is complex (e.g., Petts, 1979, 1980; Wilma and Wolman, 1984). Physical changes to channels downstream of dams can range from minimal to significant, and can vary from bed degradation and narrowing to changes in channel-bed texture or armoring to bed aggradation, bar construction, and widening (Petts 1979, Williams and Wolman 1984; Chien, 1985; Galay et al., 1985; Gilvear and Winterbottom, 1992; Collier et al., 1996). Factors contributing to this variability include the relation between pre- and post-dam flow regimes, the size distribution and erodibility of bed and bank materials, the frequency of flows capable of transporting bedload and shaping the channel, and the availability of sediment supplied from tributaries and other sources.

These complex and interacting factors limit our ability to predict the effect of any given dam on the downstream channel. Field and modeling studies are typically required to evaluate downstream changes and relate them directly to the dam or its operation. Such studies are becoming increasingly important as the operating rules and licenses for both Federal and non-Federal dams are renewed, in light of changing societal expectations and objectives for river management.

This paper reports results from the Deschutes River Geomorphology Study, a four-year effort conducted by scientists at the U.S. Forest Service Pacific Northwest Research Station, Oregon State University, and the U.S. Geological Survey (USGS) to examine the effects of the Pelton Round Butte Hydroelectric Project (hereafter "the Project") on the Deschutes River. The Project is located in north-central Oregon, 161 km (100 mi.) upstream from the confluence of the Deschutes and Columbia Rivers (Figure 1). The study was funded by Portland General Electric (PGE) as part of a series of independent scientific studies to evaluate the effects of the Project and reservoir operation on key resources, under the Federal Energy Regulatory Commission (FERC)

[Blank]

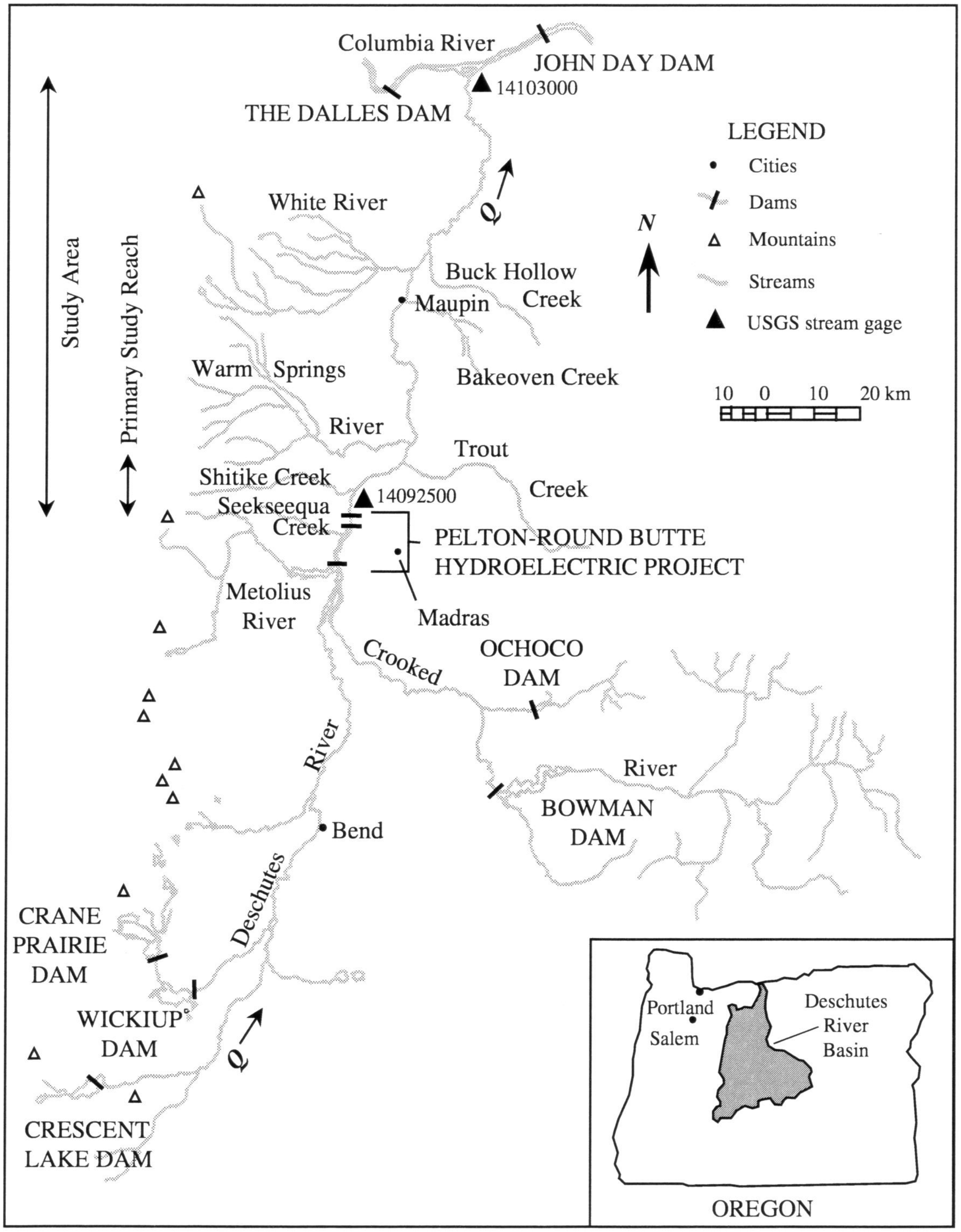

Figure 1. The Deschutes River basin. Major water storage projects shown in block lettering. Base map from Aney et al. (1967).

relicensing process for the Project. This paper, along with the companion paper by O'Connor et al. (in prep.), represent the final report of the study.

In this paper, we report and synthesize the results of coordinated studies carried out to evaluate the magnitude and extent of changes to bedload transport, channel morphology, and textural properties of the channel bed downstream of the Project. Major components include the results of 1) field data collection, historical streamflow analysis, and computer modeling to estimate the frequency and magnitude of streamflow and bedload transport both prior to and following Project construction; 2) historical cross-section and aerial photograph analyses and field observations to identify temporal trends in cross section and channel planform; and 3) field data collection, laboratory work, and statistical analyses to evaluate longitudinal trends in bed-material properties downstream of the Project. More detailed discussions of these results are contained in the Master's theses of Fassnacht (1998) for item 1 and McClure (1998) for part of item 2 and all of item 3. Item 2 includes more detailed analyses conducted following completion of these two Master's theses.

The studies described here continue a 30-year history of research on the effects of Project dams on gravel recruitment and quality in the lower Deschutes River. Previous studies (Aney et al., 1967; Huntington, 1985) focused primarily on the character and distribution of fish habitat without an overarching geomorphic context for interpreting channel conditions. Because of differences in approach and methods, results from these earlier studies are of only limited use in interpreting historical trends. In our work, we have tried to place the Project and its operation within the overall geomorphic setting of the entire Deschutes River basin, including its geological and historical framework and the impacts of other dams and reservoirs upstream of the Project. Full development of these ideas are contained in the companion paper by O'Connor et al., (in prep.).

TECHNICAL BACKGROUND AND APPROACH

Geomorphic theory and previous studies on effects of dams on alluvial rivers provide some basis for predicting general trends in how the Deschutes River might respond to river impoundment. Dams influence the two primary factors — water and sediment — that determine the shape, size, and overall morphology of the river. The degree of flow regime alteration varies by dam and management objectives. Dams also trap the vast majority of sediment derived from upstream reaches. With increasing distance downstream, sediment supply is restored by inputs from tributaries, hillslopes, and channel storage. The variability in channel responses downstream of dams reflects this complex interplay between the degree of flow regime alteration, the frequency of flows capable of transporting sediment, and the rate at which new sediment is supplied to the channel relative to the amount trapped by the dam (Williams and Wolman, 1984).

We organized our studies of the lower Deschutes River using a simple conceptual model of channel changes in response to altered flow regime and sediment supply. The relation of these two variables can be thought of in terms of a matrix representing four end-member cases in a continuum of possible responses (Figure 2). According to this model, we expect that the effect of clear water releases on the channel downstream of the Project will vary in relation to the frequency of flows that can transport sediment and in relation to sediment supply from tributaries. Where bed transport events occur frequently and sediment supply is low following impoundment (Figure 2, lower right-hand corner), increased coarsening/armoring of the bed and possibly erosion of channel bed, bar, and island deposits should occur (Leopold et al., 1964; Williams and Wolman, 1984; Galay et al., 1985). Where bedload transporting flows are infrequent and sediment supply is high (Figure 2, upper left-hand corner), predicted channel responses include channel aggradation (Church, 1995; Collier et al., 1996), widening (Xu, 1996), and/or abrupt shifts in the longitudinal pattern of surface bed material near sediment sources (Church and Kellerhals, 1978; Petts, 1984). Bars and islands may form near tributary confluences. Where both frequency of bedload transport events and sediment supply are low (Figure 2, lower left-hand corner), little or no change may occur to the downstream channel other

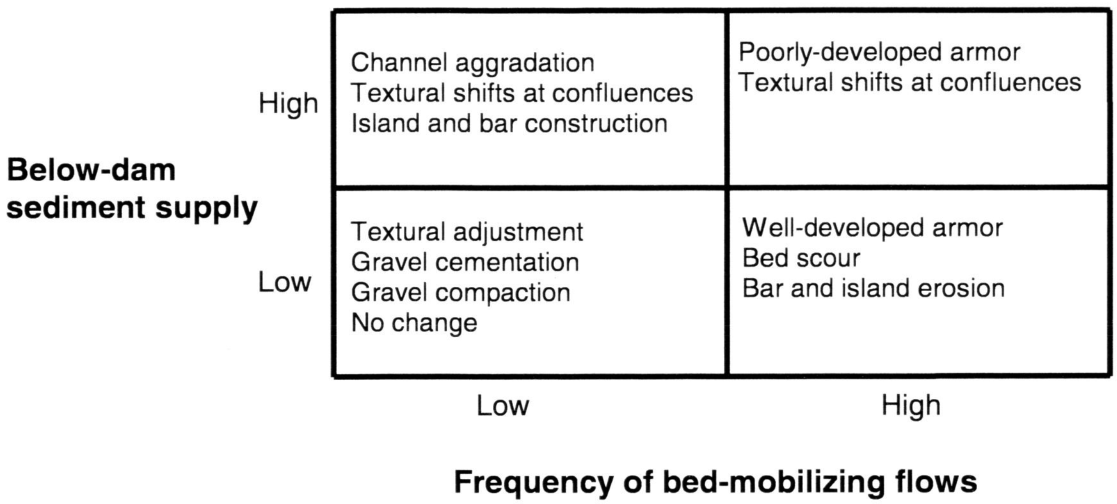

Figure 2. Summary of possible major downstream geomorphic impacts of river impoundment. Modified from Grant et al. (1995).

than subtle textural shifts in the grain-size distribution. On the other hand, high introduced sediment loads and frequent transport events (Figure 2, upper right-hand corner) may give rise to poorly sorted or armored channels with abundant fine sediment (Dietrich et al., 1989). Multiple responses may be observed on the same river as flow, sediment supply, bed material size, channel slope, geology, or channel morphology change with distance from the point of regulation or with time.

Our approach was to use field surveys, historical records, and modeling to establish where the Deschutes River fits into this conceptual model, in terms of the frequency of bed-mobilizing flows, below-dam sediment supply, and the associated downstream effects. Components of this study focused on two aspects of the proposed conceptual model: 1) characterization of the Deschutes with respect to the two axes, and 2) documentation of any impacts downstream of the Project. We then evaluated whether observed responses were consistent with calculated pre- to post-dam changes in flow regime and bedload transport.

To estimate the frequency of transport events both prior to and following construction of the Project, bedload transport modeling was conducted. The percentage of time that threshold transport conditions were exceeded was calculated, based on hydraulic modeling and analysis of historical streamflow records. The robustness of the modeling results was further confirmed by detailed analysis of long-term cross-section change in relation to discharge. These results suggested extremely low bedload transport rates that would be difficult to capture in a field program.

Although we did not calculate a sediment budget for the entire river, repeat surveys of Project reservoirs provide first-order estimates of pre-dam sediment supply to the lower river. In addition, historical cross-section analysis was used to estimate the approximate volume of sediment supplied from storage in the channel bed downstream of the dam. Field observations and aerial photographs were used to assess relative inputs of bed material from tributaries during high flow events.

Downstream effects of the Project were examined by using sequential aerial photographs to assess channel morphology changes through time and using historical cross sections to measure channel aggradation or scour. A field program was designed to evaluate changes in the grain-size distribution of the channel bed below the Project.

There were no pre-dam or prior post-dam grain-size measurements along the lower Deschutes River. Therefore, two "snapshots" in time of downstream longitudinal trends in the size of the surface and subsurface bed material prior to and following a large flood were used to evaluate the extent and magnitude of channel response. We also calculated an armoring ratio, defined as $D_{50\,surface}/D_{50\,subsurface}$, where D_{50} represents the median grain-size diameter of either the surface or subsurface. We modified the simple conceptual model described above (Figure 2) to incorporate predicted post-dam trends in grain size in relation to the controlling variables of sediment supply and frequency of mobilizing flows. The axes of the modified model are dimensionless ratios of post- to pre-dam differences in flow regime and sediment supply (Figure 3). We define F_a as the frequency of flow required to move some index value (i.e., D_{50}) of the surface or subsurface grain-size distribution after impoundment, and F_b as that same frequency before impoundment. The ratio F_a/F_b therefore represents the relative change in frequency of bed-mobilizing flows. If we similarly define Q_{sb} and Q_{sa} as the sediment supply prior to and following dam emplacement, respectively, then the ratio Q_{sa}/Q_{sb} can be used to indicate the relative change in sediment supply. Again, there is a continuum of responses between four end-member cases.

In the case of both ratios approximating unity, there should be little longitudinal trend in the size of surface or subsurface bed material or degree of armoring with downstream distance (Figure 3, Type B). This case represents the case of a regulated river with little or no modification to flow or sediment supply, perhaps because natural (pre-dam) supply rates are very low. If the sediment supply remains relatively unchanged but F_a/F_b is small (i.e., dam operation dramatically reduces the frequency of bedload transport events), then as tributaries supply more sediment than flows are able to entrain, bed material textural shifts may occur, depending on the contrast between mainstem and tributary grain sizes (Figure 3, Type A). For rivers where F_a/F_b remains largely unchanged but Q_{sa}/Q_{sb} is small, the bed is likely to degrade and coarsen immediately downstream of the dam because entrained sediment is not replaced by material transported from upstream (Figure 3, Type D). Both the surface and subsurface may

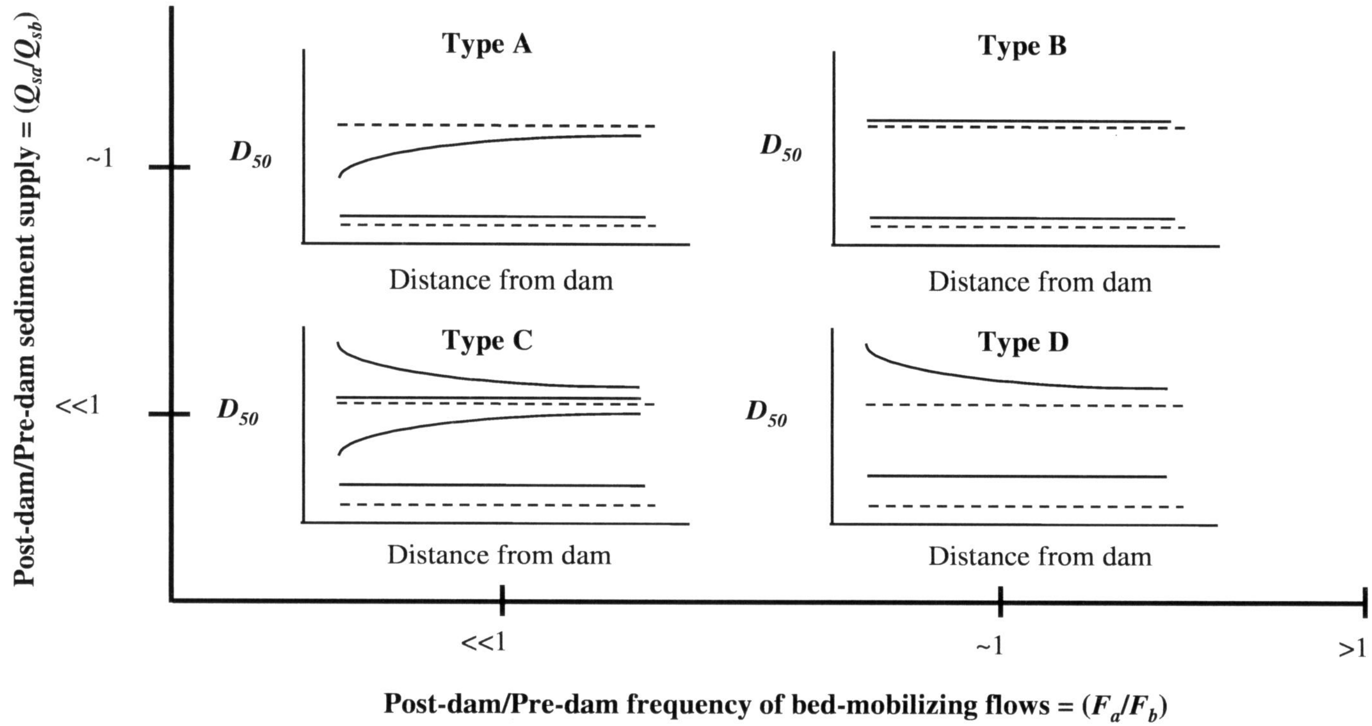

Figure 3. Conceptual model of longitudinal trends of surface and subsurface particle size (here D_{50}) with distance from a dam. Within each quadrant of the graph, the upper dashed lines indicate pre-dam surface particle sizes. Upper solid lines and curves represent possible post-dam surface trends. Lower dashed lines indicate pre-dam subsurface particle sizes. Lower solid lines represent possible post-dam subsurface trends. Armoring ratios are represented by the ratio of the surface and subsurface values.

become progressively coarser with time and with proximity to the dam in response to the decline in supply of sediment. Where both F_a/F_b and Q_{sa}/Q_{sb} are small, a wide range of responses are possible, depending on the interplay between the supply and transport processes (Figure 3, Type C).

Results from the multiple analyses conducted within the scope of this study all support the two conceptual models presented above. The morphologic and textural responses noted downstream of the Project are consistent with the low frequency of bed-mobilizing flows and low sediment supply to the lower Deschutes River (Figure 2), and with post- to pre-dam ratios near unity for both factors (Figure 3). Taken together, these different lines of evidence paint a coherent and consistent picture of the Deschutes River and Project effects.

STUDY AREA

The study area is located in the 27,200 km^2 (10,500 mi^2) Deschutes River basin in north-central Oregon (Figure 1). Three major subbasins comprise the watershed upstream of the Project: the Crooked River, upper Deschutes River, and Metolius River subbasins. The Crooked River drains the Ochoco Mountains to the east. The upper Deschutes River drains the area to the south and southwest. The Metolius River flows from the Cascade Mountains to the west.

The Project (FERC No. 2030), a three-dam complex on the mainstem Deschutes River, is located directly downstream from the confluence of the three subbasins (Figure 1). The Project includes Round Butte Dam [River Kilometer (RK) 178.0, River Mile (RM) 110.6], Pelton Dam (RK 165.4, RM 102.8), and the Reregulating Dam (RK 161.2, RM 100.2). The Pelton and Reregulating Dams were constructed between 1956 and 1958, and Round Butte Dam was constructed between 1962 and 1964.

The study area was the lower Deschutes River, the 161 km (100 mi.) of the river extending from the Reregulating Dam to the confluence of the Deschutes and Columbia Rivers (Figure 1). Within this larger study area a primary study reach, extending 21 km (13 mi.) between the Reregulating Dam and Trout Creek tributary (RK 140.5, RM 87.3), was selected for more intensive study because the greatest effects of the Project were expected to be most pronounced in the reach closest to the Project. All data used in the bedload transport study were collected within the primary study reach. For the channel-bed texture study, both the primary study reach and the entire study area were considered.

General Description

The lower Deschutes River has a drainage area of approximately 6,940 km^2 (2,680 mi^2) and ranges in elevation from about 425 m (1390 ft) at the Reregulating Dam to about 50 m (170 ft) its mouth. The river has six perennial tributaries along its lower 161 km: Shitike Creek, Trout Creek, Warm Springs River, Bakeoven Creek, White River, and Buck Hollow Creek (Figure 1). Smaller intermittent streams enter via side canyons along the entire lower river. Alluvial fans at tributary junctions constrain stream width locally and deflect the channel.

The lower Deschutes River is deeply incised into the volcanic, volcaniclastic, and sedimentary units that surround it. Where the river flows through resistant formations, (e.g., Columbia River Basalt), the river is confined in a narrow canyon 100–600 m (330–1970 ft) deep (Aney et al., 1967) and floodplains and terraces are rare. Where the river is bordered by softer formations, (e.g., John Day Formation rhyolitic tuffs), the valley is wider and some terraces and limited floodplains occur. The width of the lower river ranges from 10–170 m (30–560 ft), with an average width of 70 m (230 ft, Aney et al., 1967).

Islands and submerged bars are key morphologic and ecologic features and are commonly associated with tributary fans and channel-margin expansions and constrictions. Exposed bars are rare. For the purposes of this study, islands were defined as vegetated mid-channel or channel-margin deposits bounded by water and with surfaces above the average water surface elevation. Bars are unvegetated mid-channel and channel-margin deposits that are submerged and usually lobate in form.

Bed material, mainly composed of basalt, ranges in size from silts to boulders, with the majority of particles being gravel and cobbles. Patches of sand are associated with marginal deposits and downstream ends of islands, which typically occur in relatively wide sections of the river, and are locally colonized by submerged aquatic vegetation. Roughness elements consist primarily of the gravel, cobbles, and boulders that comprise the channel bed, with only occasional riffles and rapids. For most of its length the lower river has low to moderate sinuosity and a very uniform channel gradient of about 0.23% (Aney et al., 1967; McClure, 1998).

Native riparian species include white alder (*Alnus rhombiofolia*), willow (*Salix spp.*), sedges, rushes, and perennial grasses (Nehlsen, 1995). Although several macrophytes populate portions of the lower Deschutes, *Ceratophyllum demersum* (identification, S. Gregory, OSU, oral communication, 1998) is by far the most abundant and is concentrated in the reach closest to the Project. This floating macrophyte occupies zones of shallow, slow-moving waters (Haslam, 1987) and is anchored by shoots penetrating bed material.

Hydrologic Setting

The upper Deschutes River basin drains highly porous and permeable Pliocene and Pleistocene basalts, which are fed by snowfields through a relatively undissected and poorly integrated stream network with many springs (Manga, 1996; Grant, 1997). The Deschutes River experiences only small seasonal discharge variations because it receives large groundwater contributions (Gannett et al., 1996). Most of this groundwater enters the Crooked, upper Deschutes, and Metolius Rivers upstream of Round Butte Dam, but below irrigation withdrawal points (unpublished data, USGS, 1999). Uniform groundwater flows and the relatively small volume of Lake Billy Chinook's (Round Butte Reservoir's) annual used storage (see River Regulation, below) contributes to the river's extremely stable flow. Henshaw et al. (1914) noted that the river's streamflow regime was more uniform than that of any river of comparable size or larger in the USA.

There are two active USGS stream gaging stations on the mainstem lower Deschutes River: station 14092500 (Deschutes River near Madras, Oregon) located at RK 161.1 (RM 100.1) just downstream from the Reregulating Dam, and station 14103000 (Deschutes River at Moody near Biggs, Oregon) located at RK 2.3 (RM 1.4) near the mouth (Figure 1). The Madras gage has been moved twice in association with dam construction (unpublished report, USGS, 1994). Stream gage and streamflow characteristics of the lower Deschutes River are shown in Table 1.

A flow duration curve constructed for the Madras gage from 1925–1996 illustrates the extraordinary uniformity of river flows (Figure 4). The mean monthly discharge with a 90% exceedance probability is less than two times that with a 10% exceedance probability. The difference between the 1% and 99% exceedance probability discharges is less than a factor of three.

Since 1924, the lower Deschutes River has experienced two exceptionally large floods: the floods of December 1964 and February 1996 (Table 1). Both occurred as the result of rain-on-snow events. During the December 1964 flood, Round Butte Dam caught the flood peak, which filled the reservoir for the first time, almost a year ahead of schedule.

River Regulation

The waters of the Deschutes River are regulated by eight major water storage projects (Figure 1, Table 2) and numerous irrigation diversions. The dams in the basin retain a total of 129 x 10^7 m^3 (1,045,800 ac-ft) of water, 76% of which is permitted annual active storage (though only 32% on average is used). The Crooked River subbasin has two major structures — Ochoco and Bowman Dams (Figure 1) — with major storage allocated to flood control. Together, these two dams are responsible for 32% of the average used annual active storage in the basin. There are three irrigation water storage projects in the upper Deschutes subbasin: Crane Prairie, Wickiup, and Crescent Lake Dams (Figure 1). These three dams, together, account for 61% of the average used

Table 1. Stream gage and streamflow characteristics of the lower Deschutes River.

	Madras gage	Moody gage	Reference
Stream gage characteristics			
Period of Record	Jan 1924–June 1933 Aug 1929–Nov 1956 Nov 1957–present	Oct 1897–Dec 1899 Jul 1906–present	1, 2
Location, River Kilometer (River Mile)	165.4 (102.8) 164.8 (102.4) 161.1 (100.1)	2.3 (1.4)	1, 2
Drainage Area km^2 ($mi.^2$)	20,274 (7,820)	27, 195 (10,500)	1
Streamflow characteristics m^3/s (ft^3/s)			
Mean Annual Flows			
Range	101–174 (3,560–6,150)	121–209 (4,290–7,380)	4
Average	128 (4,517)	163 (5,739)	4
Maximum Recorded Flows [a]	637 (22,500)	1,991 (70,300)	1
Largest Flood Peaks [b]			
February 8, 1996			
Instantaneous flow	541 (19,100)	1,991 (70,300)	1
Mean daily flow	504 (17,800)	1,821 (64,300)	1
December 1964	December 28, 1964	December 22, 1964	3
Instantaneous flow	447 (15,800)	1,906 (67,300)	1, 3
Mean daily flow	428 (15,100)	1,767 (62,400) [c]	3
Minimum Recorded Flows [a]	26 (916)	68 (2,400)	1

References:
1 = Hubbard et al. (1997)
2 = USGS (1994)
3 = USGS (1965)
4 = USGS (1997b,c)

[a] Maximum instantaneous flow regardless of whether due to storm event or anthropogenic causes.
[b] Maximum instantaneous and mean daily flows resulting from storm events.
[c] Occurred on December 23, 1964 (USGS, 1965).

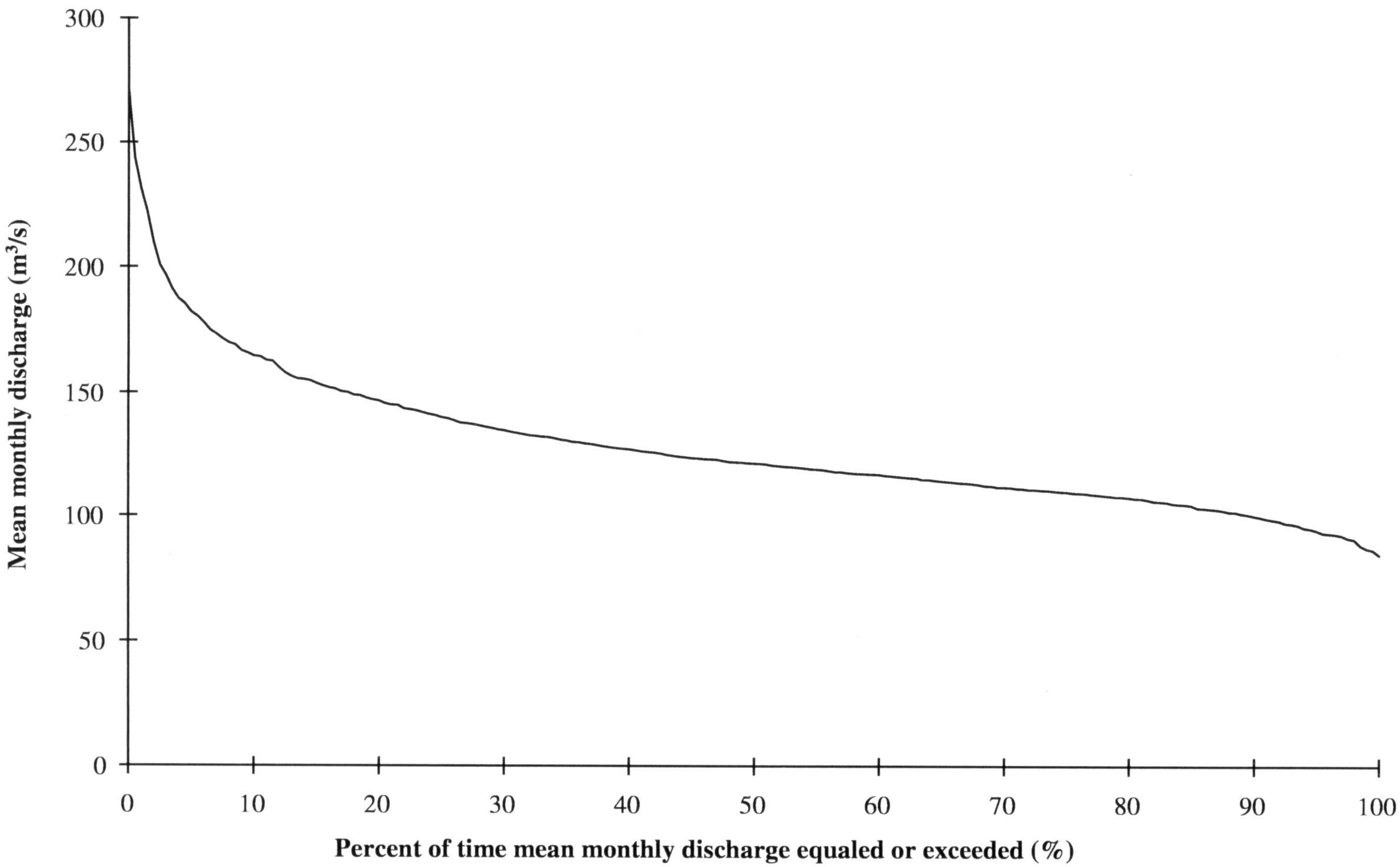

Figure 4. Flow duration curve for the Deschutes River near Madras: water years 1925–1996.

Table 2. Storage characteristics of major water storage projects in the Deschutes River basin.

Project (Reservoir)	River	Year Construction Began	Purpose of Dam	Total Storage m^3 (acre-ft)	Permitted Annual Active Storage m^3 (acre-ft)	Average Used Annual Active Storage m^3 (acre-ft)	Drainage Area km^2 (mi^2)
Ochoco (Ochoco)	Ochoco Creek	1918 [a, b]	Flood control Irrigation	5.92×10^7 (48,000) [a, b]	5.7×10^7 (46,500) [a, b]	3.26×10^7 (26,400) [c]	750 (290) [b]
Crane Prairie (Crane Prairie)	Deschutes	1922 [d]	Irrigation	6.82×10^7 (55,300) [d, f]	6.6×10^7 ($54{,}000 \times 10^4$) [e]	3.45×10^7 (28,000) [c]	660(250) [e, f]
Crescent Lake (Crescent Lake)	Crescent Creek	1922 [d, f]	Irrigation	11.3×10^7 (91,600) [f, h]	11×10^7 (91,600) [f]	3.62×10^7 (29,300) [c]	150(60) [f]
Wickiup (Wickiup)	Deschutes	1939 [h]	Irrigation	24.7×10^7 (200,000) [d, i]	24.7×10^7 (200,000) [i]	18.0×10^7 (146,200) [c]	660 (250) 1,040 (400) [h, i]
Pelton (Lake Simtustus)	Deschutes	1956 [i]	Hydroelectric	3.82×10^7 (31,000) [j]	0.46×10^7 (3,700) [j]	0 [j]	19,950? (7,700) [f]
Pelton Reregulation	Deschutes	1956 [i]	Flow reregulation Hydroelectric	0.43×10^7 (3,500) [j]	0.31×10^7 (2,500) [j]	0 [j]	20,250 (7,820) [k]
Bowman (Prineville)	Crooked	1958 [b, k]	Flood control Irrigation	19.1×10^7 (154,500) [b, l]	19×10^7 (152,800) [b, l]	9.38×10^7 (76,100) [c]	7,280 (2,810) [b]
Round Butte (Lake Billy Chinook)	Deschutes	1962 [i]	Hydroelectric	56.1×10^7 (455,000) [j]	30×10^7 (242,000) [j]	2.86×10^7 (23,200) [j]	19,410 (7,490) [k]
TOTAL				128×10^7 (1,038,900)	97.8×10^7 (793,100)	40.6×10^7 (329,200)	

Table 2. (Continued)

[a] U.S. Army Corps of Engineers (1959).
[b] U.S. Department of the Interior, Bureau of Reclamation (1966).
[c] Wayne Skladal, Central Region WRD, Bend, Oregon, written communication, 1999.
[d] U.S. Department of Interior, Bureau of Reclamation (unpublished report).
[e] K. Gorman, Watermaster, Central Oregon Irrigation District, Bend, Oregon, oral communication, 1997. Original dam had around the same storage capacity as listed. The dam was rebuilt in the 1940s improving its structural support. The hydrologic drainage boundary is uncertain due to inter-basin groundwater exchange.
[f] Johnson (1985).
[g] G. Cartwright, Field Supervisor, Tumalo Irrigation District, Bend, Oregon, oral communication, 1997. Storage values are for post-1956.
[h] Northwest Power Planning Council (1986). Values given under total storage are maximum capacity.
[i] U.S. Department of the Interior, Water and Power Resources Service (1981).
[j] Portland General Electric (1996).
[k] Hubbard et al. (1994).
[l] U.S. Army Corps of Engineers (1961).

annual active storage. There are no storage projects in the Metolius River subbasin. On the mainstem Deschutes are the three Project dams: Round Butte Dam, Pelton Dam, and the Reregulating Dam. Round Butte Dam impoundsLake Billy Chinook, the basin's largest reservoir, holding over 40% of the total water stored in the Deschutes River basin (Fassnacht, 1998; Table 2). Round Butte Dam has been operated using only 7% of the average annual active storage used in the basin. Pelton Dam and the Reregulating Dam have no annual active storage. The purpose of the Reregulating Dam is to provide constant discharge to the lower Deschutes River while allowing daily peaking power production from Pelton Dam upstream. The Reregulating Dam, thus, stores water and evens flow on a daily basis. Downstream of the Project, the Deschutes River flows uninterrupted to its confluence with the Columbia River.

Upstream of the Project near Bend, substantial quantities of water are diverted for irrigation, with as much as 94% of monthly streamflow being diverted at the height of the irrigation season (Fassnacht, 1998). However, about 85 m^3/s (3,000 ft^3/s), or 270 x 10^7 m^3 (220 x 10^4 ac-ft), of groundwater inflow is estimated to enter the Deschutes system annually below major irrigation diversions and above Lake Billy Chinook (M. W. Gannet, USGS, written communication, 1999). This is six times the annual used active storage in the basin. As a result, even with the presence of the water storage projects upstream, the lower Deschutes River has been able to maintain its historically stable discharge.

Sediment Sources

Sediment in the Deschutes River comes from a variety of sources over a wide range of temporal and spatial scales. Volcanism and glaciation have played an important role in shaping the land surrounding the Deschutes River over the last several million years. During the Miocene and Pliocene, volcanism associated with construction of the ancestral and modern Cascade Mountains episodically contributed extraordinary volumes of detrital material to the Deschutes River and adjacent fluvial basins, primarily as airfall, pyroclastic flows, and hyperconcentrated flood flows (Smith, 1991). Pleistocene meltwater streams and more recent jokulhlaups (glacial-outburst floods) from the eastern slopes of the High Cascades transported glacial debris downstream to the waters of the Deschutes (O'Connor et al., in press). Large rotational mass failures and rapid fluvial erosion of volcanic or glacial deposits delivered large quantities of material to the Deschutes River via tributaries. The Missoula floods — catastrophic releases of water derived from large glacially dammed lakes located in western Montana — inundated the lower-most Deschutes River to upstream of Maupin and delivered sediment upstream via flood waters and rafted icebergs (O'Connor et al., in prep.).

More recent and proximal sediment sources to the Deschutes River include canyon-wall landslides and rock-falls, debris flows from tributary side canyons, and fluvial erosion of previously deposited material from both the main channel and its tributaries. Volcanic and glacial activity continue to play a role in sediment delivery, though to a lesser degree than in the geologic past. The White River (RK 75.2, RM 46.7), which drains White River Glacier on the east side of Mount Hood, is likely responsible for much of the fine-grained sediment entering the lower Deschutes River. The most recent eruption of Mount Hood and resulting pyroclastic flows down the White River occurred about 200 years ago (Scott et al., 1997). Valley floors in the White River drainage were completely buried all the way to the Deschutes River by past lahars from Mount Hood (Scott, et al., 1997). The upper White River canyon is partially filled by at least 60 km (37 mi.) of lahar and fluvial deposits (Swanson et al., 1989). Suspended sediment transport in the lower White River is about 490 metric tons/month (540 standard tons/month) in September/October and 54,000 metric tons/month (59,000 standard tons/month) in November/December (Bonneville Power Administration, 1985). Based on field observations (e.g., new deposits), Shitike Creek (RK 156.1, RM 97.0) and Warm Springs River (RK 135.5, RM 84.2) both deliver gravel and cobbles to the mainstem during high discharge events, such as the February 1996 flood. Shitike Creek is the only substantial tributary in the primary study reach. Very limited data exist on the absolute or relative amounts of sediment delivered from tributaries downstream of the Project.

METHODS

Bedload Transport Study

FIELD METHODS

Ten sites were selected within the primary study reach (sites labeled A through J, Figure 5) representing three hydraulic environments characteristic of the lower Deschutes River: straight, contraction, and expansion zones (Figure 6). Straight zones are reaches where the channel banks are roughly parallel (Figure 6a); contraction zones are those where the channel narrows abruptly downstream (Figure 6b); and expansion zones are reaches where the channel widens abruptly downstream (Figure 6c). In the Deschutes River channel, contractions and expansions are often the result of tributary alluvial fans constricting the main river channel (e.g., Figure 6b). Field data were collected for all ten sites, but because of time constraints, data from only five of the ten sites were examined (Sites B, D, E, H, and I).

Study sites were selected and cross sections and channel-bed particle-size distributions measured during the summer of 1995. Cross-section data were collected at each site along four to seven transects oriented approximately perpendicular to the main direction of flow. The number of transects measured per site was based on each site's morphologic complexity. Transects were placed upstream of, through, and downstream of hydraulically important features (e.g., channel expansions). Where the water was more than 0.5 m deep, cross-sectional profiles were measured using an Acoustic Doppler Current Profiler (ADCP) mounted on a jet boat and operated by USGS personnel. On dry land or where the water was less than about 0.5 m deep, elevations were surveyed using a total-station instrument and a prism mounted on a stadia rod.

Particle-size distributions of the channel-bed surface for hydraulic and bedload transport modeling calculations were estimated for each site using a modified pebble-count technique (Wolman, 1954). Approximately 100 particles per site, on average, were selected at pre-designated intervals along a survey tape oriented parallel to streamflow on

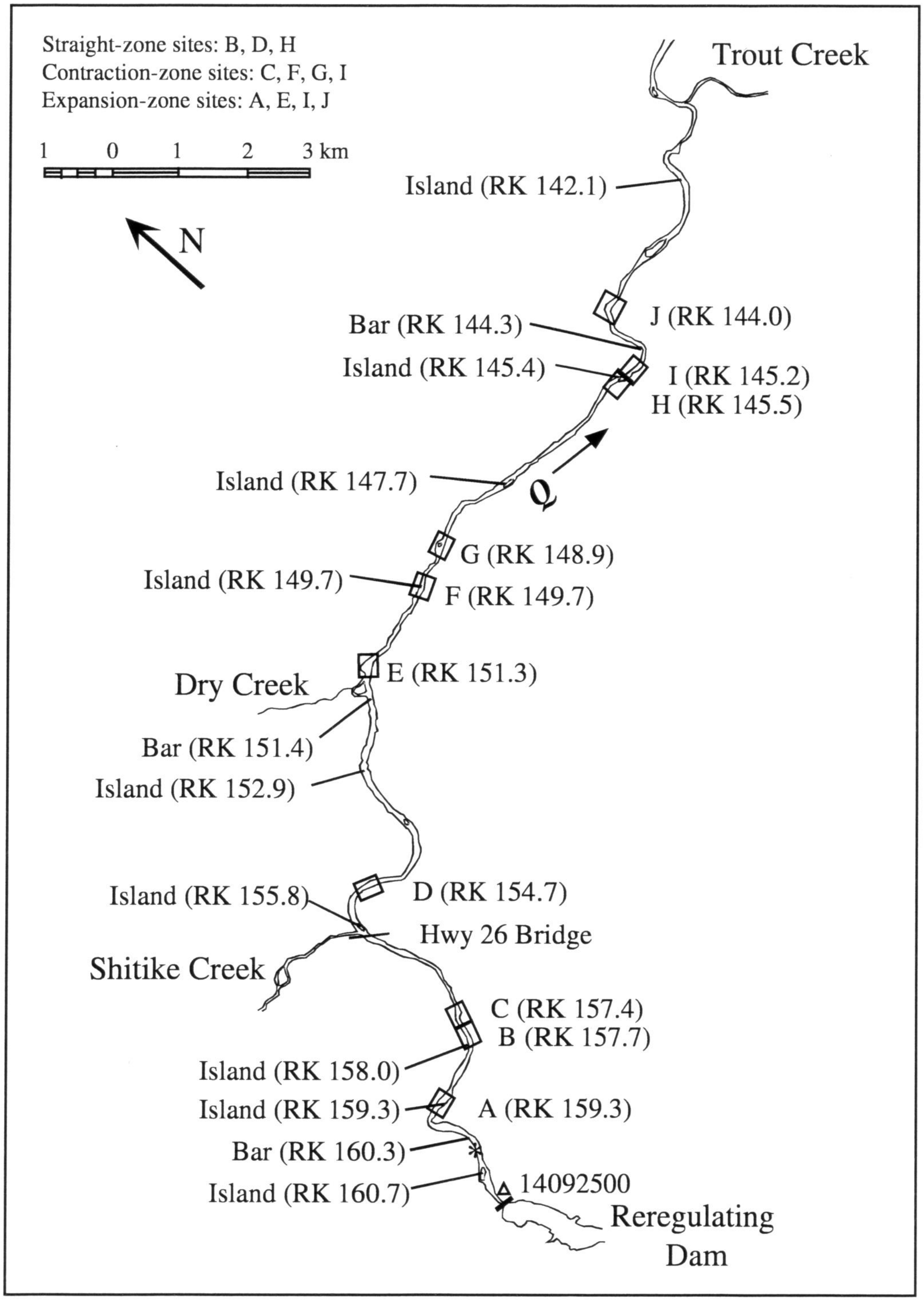

Figure 5. Primary study reach and sites for bedload transport and channel-bed textural studies. Bedload transport study sites (A - J) located within boxes and labeled on right side of river. Channel-bed textural study site locations indicated by lines and labeled on left side river. USGS Madras stream gage station shown by triangle. USGS measurement cross section shown by asterix. Base map from Appel (1986).

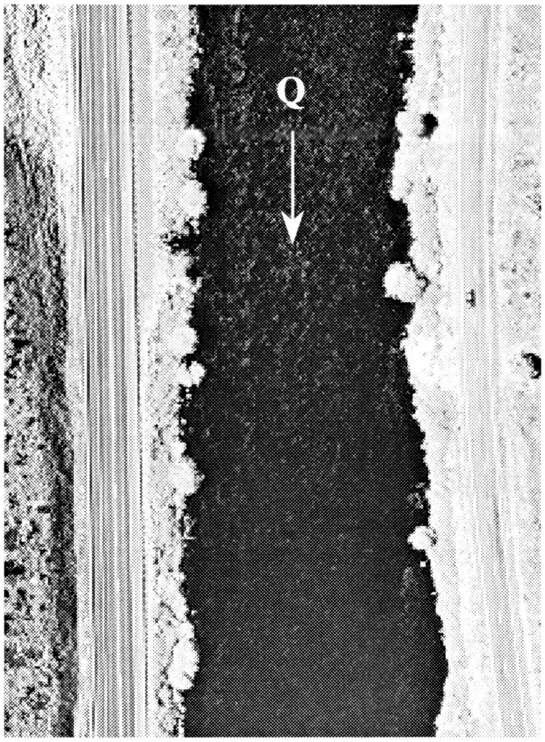

(a) straight zone

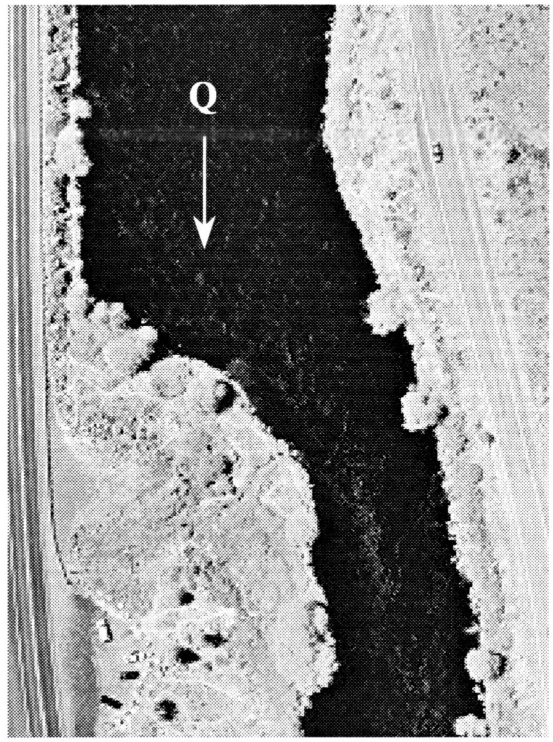

(b) contraction zone

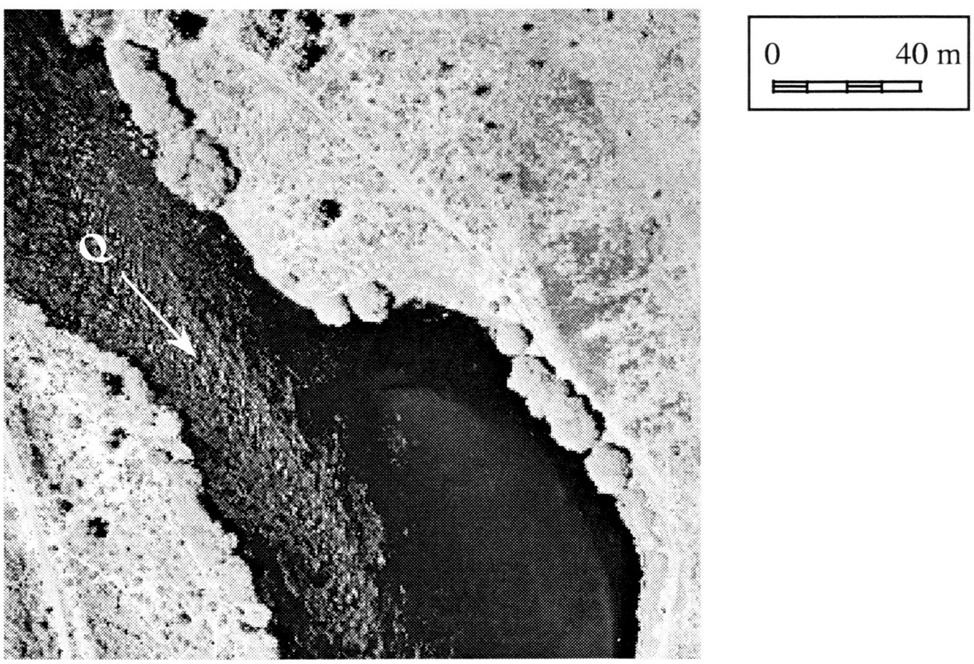

(c) expansion zone

Figure 6. Three hydraulic environments characteristic of the lower Deschutes River: (a) straight, (b) contraction , and (c) expansion zones.

shallow submerged bars and along island and channel margins within each site. Deep water and high velocities precluded sampling the channel bed near the thalweg. Visual inspection made from a drift boat of deeper regions of the river, however, suggested that the range of grain sizes in the channel bed (including the margins)was relatively narrow, though grain-size ranges did vary noticeably from site to site. These observations were supported by the results of the channel-bed texture study (McClure, 1998). Therefore, particle-size distributions measured along channel margins represent a more reasonable estimate of the overall particle-size distribution for calculating hydraulic roughness than in other, more variable rivers.

Following the record flood in February 1996, we revisited all sites in the spring and summer to reference the flood's high-water line against the 1995 survey points using a stadia rod and hand level.

Discharges for September 1995 and February 1996 (the dates for which we obtained field measurements of water surface elevation) were derived from mean daily flow data from nearby USGS gage stations. For the site located above Shitike Creek confluence (Site B, Figure 5), discharge was assumed equal to that measured at the Madras gage (station 14092500). For sites located downstream of the Shitike Creek confluence (Sites D, E, H, and I; Figure 5), discharge was assumed equal to the sum of the discharges measured at the Madras and Shitike Creek gages (Shitike Creek values from USGS station 14092885). Discharges for September 1995 ranged from 96 to 105 m^3/s (3,390 to 3,710 ft^3/s) over the five sites. For February 1996, the range was from 510 to 586 m^3/s (18,010 to 20,690 ft^3/s), based on provisional data from the USGS. Intermediate discharge values of 100, 200, 300, 400, and 500 m^3/s (3,530; 7,060; 10,590; 14,130; and 17,660 ft^3/s) were used in the data analysis to provide a range of discharge values.

Direct measurements of bedload transport were not made because of the logistics of installing bedload traps, scour chains, or marked particles in a large river. In addition, field evidence suggested extremely low bedload transport rates that would be difficult to capture in a field program. Consequently, bedload transport was calculated using the Parker (1990) model (see Data Analysis below).

Initiation of Bedload Transport

Mean shear stresses (τ) were estimated for each site over a range of discharges by combining field measurements of channel geometry and particle size with the one-dimensional step-backwater curve model HEC-RAS (US Army Corps of Engineers, 1995a, b). Shear stresses were calculated using the hydraulic mean depth values generated by HEC-RAS and the relation

$$\tau = \gamma_f \bar{d} S_e \tag{1}$$

where τ is shear stress, γ_f is the specific weight of the fluid (water), $\bar{d}$ is hydraulic mean depth ($\bar{d} = A/T$ where A is area and T is top width), and S_e is downstream slope of the energy grade line, or energy slope. The shear stress required to entrain the median particle diameter of the channel-bed surface material, (here called critical shear stress, τ_{cr50s}) was determined for each study site from the relation (Shields, 1936)

$$\tau^*_{cr50s} = \frac{\tau_{cr50}}{(\rho_s - \rho_f) g D_{50s}} \tag{2}$$

where τ^*_{cr50s} is dimensionless critical shear stress, or Shield's stress, for median particle diameter of channel-bed surface (D_{50s}), ρ_s is the density of the sediment, ρ_f is the density of the fluid (water), and g is gravitational acceleration. For particles coarser than sand, τ^*_{cr} is essentially constant. We chose a value of $\tau^*_{cr50s} = 0.047$; the same as that used by Meyer-Peter and Mueller (1948) for coarse-bedded rivers.

The HEC-RAS model was run for discharges ranging from September 1995 summer low flows to February 1996 flood flows to obtain the hydraulic mean depth for these discharges. Hydraulic mean depth was used with Equation 1 to then calculate shear stresses for a site over a range of discharges. Shear stress was plotted against discharge to construct a rating curve for each site (e.g., Figure 7). Critical shear stresses were then

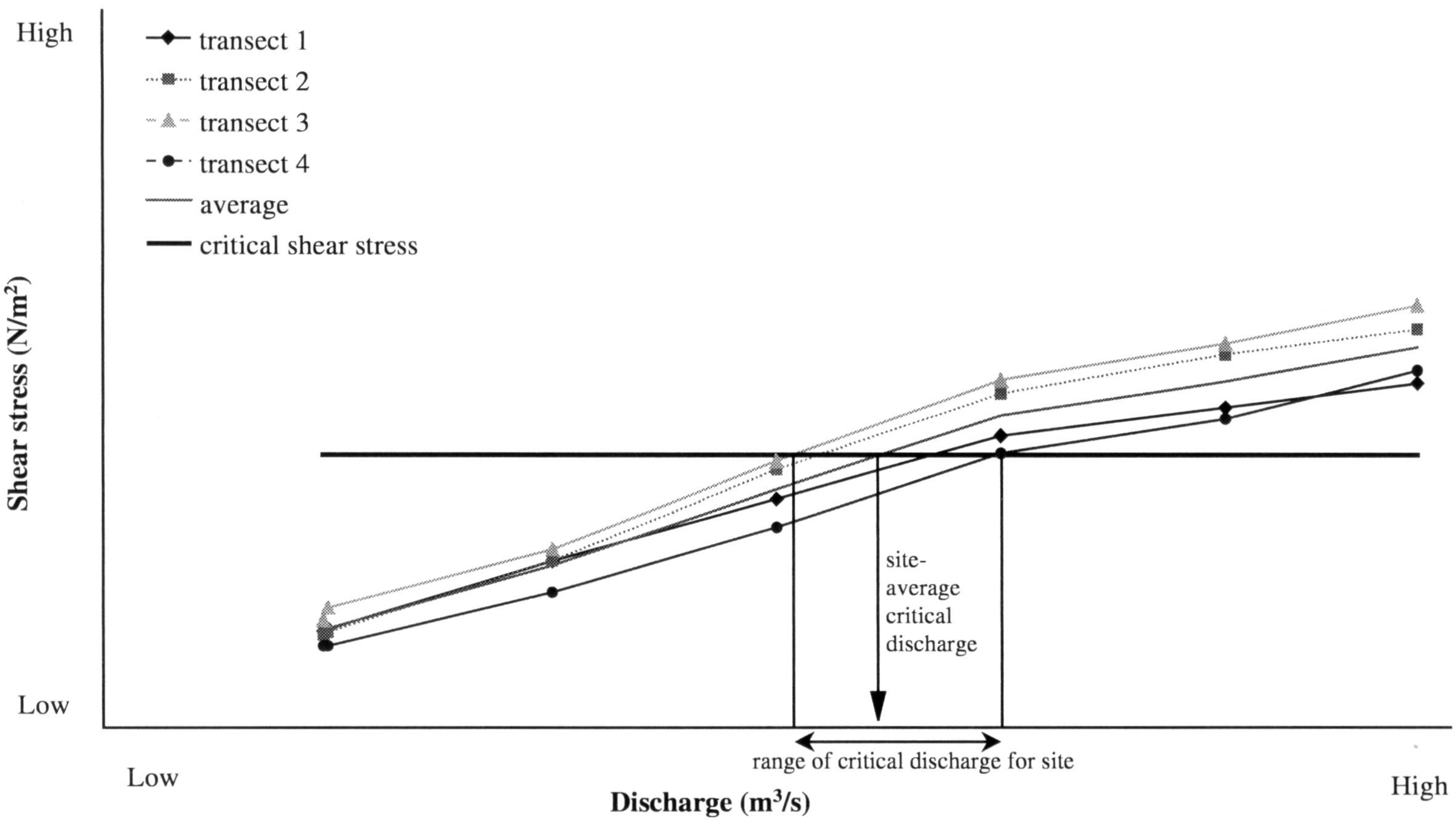

Figure 7. Example discharge (Q) vs. shear stress (τ) rating curve. Critical discharge was determined from the point of intersection of the Q vs. τ and τ_{crit} curves. The average Q vs. τ curve was used to produce a site-average critical discharge.

calculated (Equation 2) for each site and superimposed on the site's rating curve to estimate the discharge required to produce threshold transport conditions (critical discharge, Q_{cr}) at that site (Figure 7).

We analyzed the sensitivity of the calculated critical discharges and corresponding shear stresses to important parameters; the energy slope (S_e), median particle diameter of the channel-bed surface (D_{50s}), and Shields stress for the median diameter of the channel-bed surface (τ^*_{cr50s}). The parameters were changed, one at a time, by $\pm$ 10%, while all other independent parameters were held constant. The energy slopes were varied by plus or minus one half of a standard deviation to maintain similitude with observed values. The effect on critical discharge was then evaluated. To evaluate the robustness of the model to changes in more than one parameter at a time, the three parameters evaluated were changed simultaneously to either increase or decrease critical discharge.

Bedload Transport Analysis

Rating curves of the predicted bedload transport rate (Q_s) versus water discharge (Q) were constructed for each site for a range of discharges by combining field measurements of channel geometry and particle size with hydraulic data derived from the HEC-RAS model as input to the Parker (1990) one-dimensional bedload transport model for gravel mixtures. This bed surface-based model was derived from an existing, empirical, subsurface-based relation developed entirely from field data (Parker et al., 1982). Full description of our method is given in Fassnacht (1998).

Particle-size ranges were chosen to correspond to those designated by the Wentworth scale. The discharge values for which bedload transport were calculated were the same as those used in the hydraulic analysis.

Historical Streamflow Analysis

We examined annual flow duration curves for the period of record (1925–1996) to evaluate changes in flow frequency with time. Annual curves were constructed from mean daily flow data to examine time periods of equal length (one year). Flow duration curves were also constructed to compare two 30-year time intervals: 1925–1955 (pre-Project) and 1966–1996 (post-Project).

Analysis of the Frequency and Magnitude of Bedload Transport

Results from the hydraulic, sensitivity, and bedload transport analyses were combined with historical streamflow and reservoir storage data to make a first-order approximation of frequency and magnitude of bedload transport in the primary study reach, and to examine the effects of the Project on water and sediment discharges. The highest calculated critical discharge value for all sites examined was used in this analysis because, at this discharge, bedload transport should occur at all sites and our interest was in the condition of general bedload transport throughout the primary study reach. The sensitivity analysis of the critical discharge calculation, where the three parameters tested were varied simultaneously, provided a range of what we considered maximum deviation of the critical discharge value. Therefore, these "alternate" critical discharge values were also evaluated in determining the frequency of bedload transport.

The frequency of bedload transport was calculated using historical daily streamflow records by determining the number of days over the period of record during which the calculated critical discharge (or the alternate values) were equaled or exceeded. A calculation of transport frequency was also made that attempted to take into account temporal variability in resistance to transport (Reid et al., 1985). To do this, different transport thresholds were used on the rising and falling limbs of storm hydrographs. On the rising limb of the hydrographs, we considered bedload transport to begin at the calculated critical discharge, and on the falling limb we considered transport to continue to discharges 40 m^3/s (1,410 ft^3/s) below the calculated critical discharge value. Bedload transport was considered to cease at this lower discharge value because, at this point, predicted daily volumetric bedload transport was less than 10 m^3 (350 ft^3), which was considered the detection limit.

The quantity of bedload moved per day was predicted at one example site (Site B) over the period of record using the sediment rating curve calculated in the bedload transport analysis and the method described above for accommodating some form of temporal variability in the resistance to transport. Calculated daily bedload transport values were regrouped by water year to examine the pattern of bedload transport over time. Days during which bedload transport was predicted to have occurred were called "transport days," and a continuous series of these days were called a "transport event."

Calculated bedload transport values were evaluated against results from a reservoir sedimentation survey conducted recently by PGE. Methods used in the survey are described in O'Connor et al. (in prep.).

Project Effects on Discharge and Bedload Transport

Hydrographs of mean daily inflow and outflow were developed for the Project using data provided by DE&S Consulting and from USGS gage stations (USGS 1997a, b, c) for post-dam storm events whose discharge exceeded threshold transport conditions. DE&S determined inflow from the Project using reservoir elevation data and elevation-storage rating curves. Reservoir outflow equaled the discharge measured at the USGS Madras stream gage. For the two earliest storms examined, reservoir elevation data were not available. Consequently, inflows for these two storms were estimated by adding together discharges of the three main rivers tributary to the reservoir as measured at USGS gages 14087400 (Crooked River below Opal Springs, near Culver, Oregon), 14076500 (Deschutes River near Culver, Oregon), and 14091500 (Metolius River near Grandview, Oregon). Inflow calculations based on data from these three gages did not account for any discharge derived from approximately 850 km^2 (330 mi^2) of drainage area between the gages and Round Butte Dam (4% of the total drainage area). The result is an underestimation of reservoir inflow. To gain some idea of the amount by which inflow might be underestimated, inflows were calculated using data from the three upstream gages for the storm events for which reservoir elevation data were available. The inflows by the two different methods were then compared and differences determined. The average of the percent differences between the two methods was applied to the inflow calculations for the two storm events not having reservoir elevation data.

From the inflow and outflow hydrographs, the quantity of bedload transport through the sites was calculated using sediment rating curves derived from the bedload transport analysis. Bedload transport calculations for sites located below Shitike Creek and for all events except those in 1996, reflect only the bed material moved by streamflow measured at the Madras gage. Shitike Creek, which joins the Deschutes upstream of Site D, was ungaged during these events and, therefore, the influence of this tributary could not be taken into account.

Channel Morphology Study

HISTORICAL CHANGES IN CHANNEL CROSS SECTION

Discharge measurements and corresponding cross-section measurements have been collected by the USGS for the Deschutes River near Madras station (14092500) from January 1924 to the present. Cross-section measurements from this gage were analyzed for changes in channel-bed elevation and area over the period of record. Comparisons of channel change between pre- and post-dam time periods are complicated by movement of the gage and associated cableway twice in connection with dam construction. All movement of the measurement cross section occurred before any dams in the Project were closed. The locations and time periods over which measurements were made for the three locations of the Madras gage are shown in Table 1. Channel change described in this analysis does not necessarily represent channel change experienced over the river as a whole. Measurement cross sections are specifically chosen for their stability and are, therefore, expected to show less change than elsewhere in the river.

To determine if there had been long-term aggradation or degradation of the streambed over time at the Madras gage site, minimum streambed elevation was examined over the period of record using the method outlined in Smelser and Schmidt (1998). In addition, cross-sectional areas were calculated for every third USGS cross section measurement from 1957 to the present. Areas below a depth of 2 m from an arbitrary datum (highest water-surface elevation during period of record examined) were calculated using the method outlined in Fassnacht (1998) Appendix E.3. Simple linear regressions were done to determine if changes observed within a single gage location were significant. Cross sections prior to 1957 were not included because of the pronounced stability of the streambed at the two previous upstream gage locations. Smaller-scale temporal patterns were also examined by looking at changes in cross-section shape and area for measurements spanning individual high discharge events. To investigate thresholds of general bed mobility over the cross section, measurements spanning reasonable discharge ranges [every 57 m^3/s (2,000 ft^3/s) starting at 113 m^3/s (4,000 ft^3/s)] were evaluated.

Historical Changes in Channel Planform

Black and white aerial photographs from 1944 (scale approximately 1:22,400), 1951 (scale 1:20,000), 1956 (scale 1:20,000), 1968 (scale 1:20,000), and 1972 (scale 1:20,000); infrared photographs from 1995 (scale 1:2,000); and video stills from 1996 (scale varies; ~1:2,000) were examined to evaluate planform changes over the study area with time. Detailed analysis was focused on the primary study reach, where photographic coverage was best. Particular attention was paid to changes associated with major flood events and at tributary junctions.

Channel-Bed Texture Study

FIELD AND LABORATORY METHODS

Islands and submerged bars were sampled to analyze longitudinal trends in bed material because they represent dominant depositional features of the river and allow comparisons between similar depositional environments (Kondolf, 1997). Sampled sites included islands and bars in comparable hydraulic settings, along which sampling grids could be safely established under low flow conditions. Around each island, four distinctive geomorphic "environments" were sampled: the head (upstream end), side (side abutting main flow), side channel (side bordering secondary channel), and tail (downstream end) (Figure 8). Head and tail environments of selected bars were also sampled. Results presented here focus on comparison of grain-size distributions from heads of islands and bars, since these are the most consistent hydraulic environments between these two types of depositional features. Analysis of other geomorphic environments shows similar trends (McClure, 1998).

In the summer of 1995, 12 islands and bars were sampled in the primary study reach (Figure 5). To document changes following the February 1996 flood, these sites were resampled during the summer of 1996. Eleven island heads in the lowermost 140 km of the river were also sampled during the summer of 1996 to extend the analysis downstream to the Columbia River (Figure 9).

Sampling of the Channel-bed Surface

Surface bed material was sampled at each site by measuring intermediate (b-axis) particle diameter for three standard 100-particle pebble counts (Wolman, 1954) conducted on three overlapping 10 m by 10 m grids (Figure 8). Smaller particles were binned into a <2 mm category in the field. Sample grids were centered along a line, parallel to flow, through the island or bar and spaced no more than 3 m from vegetated

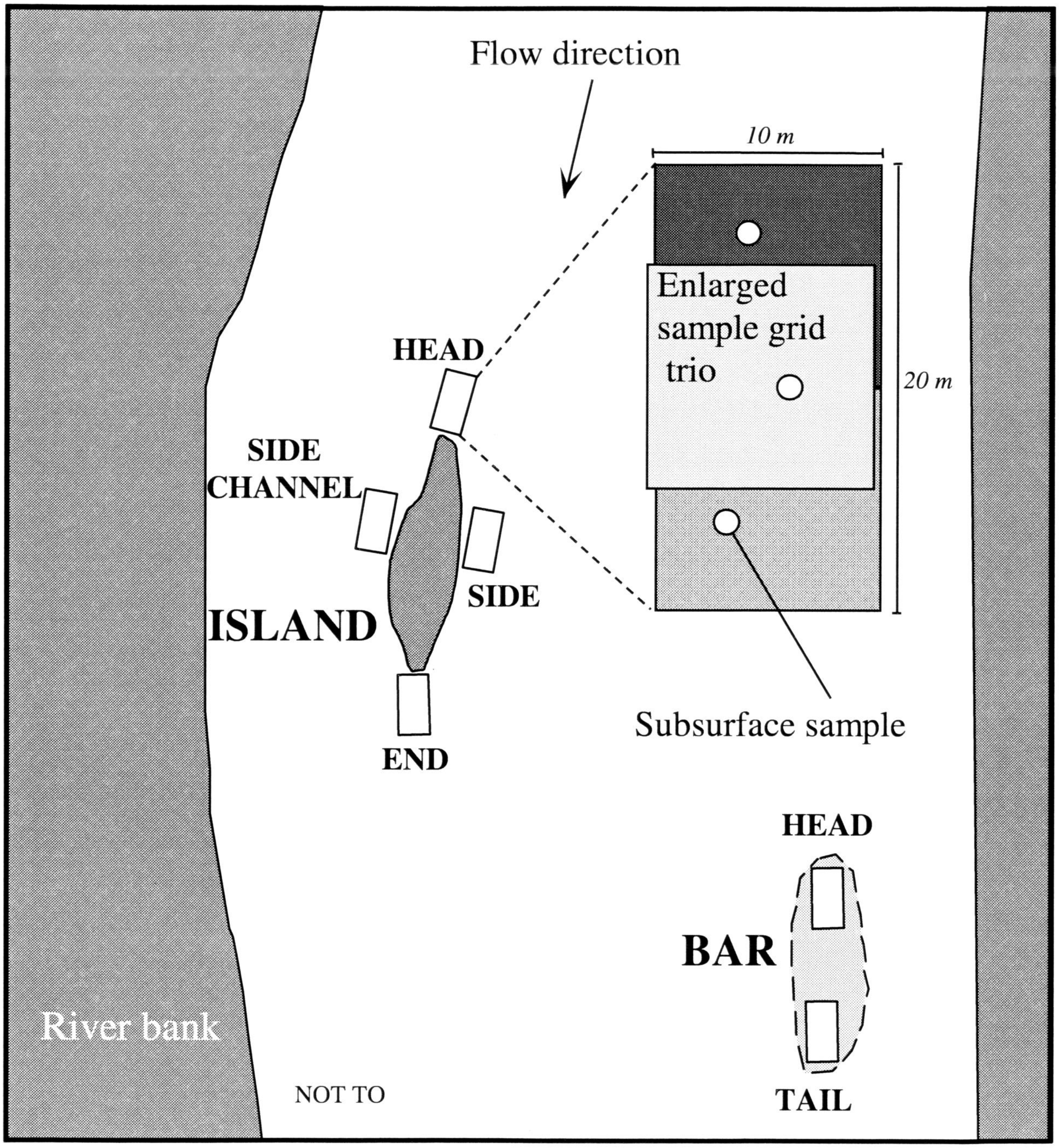

Figure 8. Schematic of sampling design at vegetated island and submerged bar. The location of head, side, side channel, and tail environments are shown as smaller rectangles. Squares represent grids for pebble counts of surface bed material. Circles indicate positions of subsurface samples.

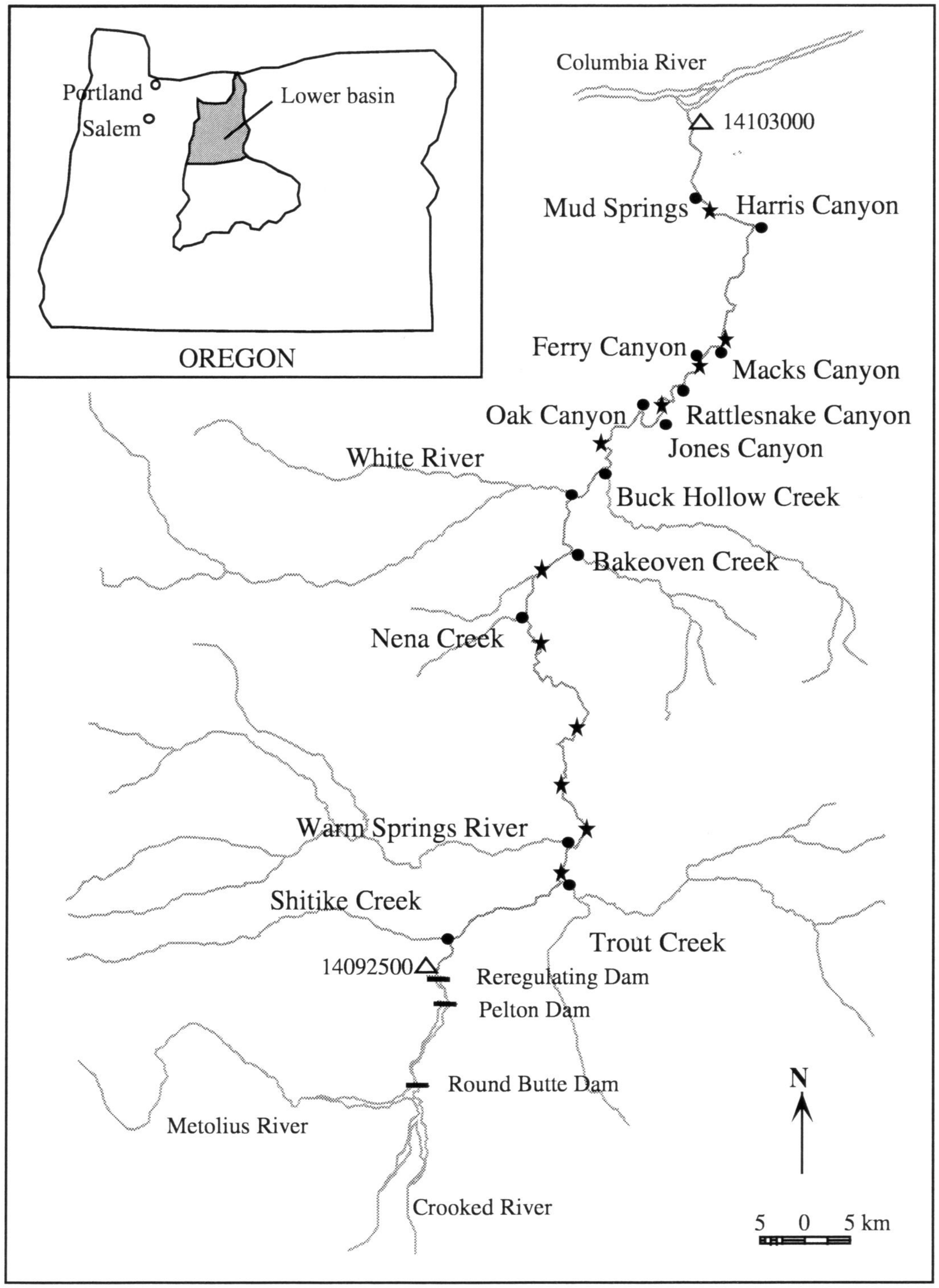

Figure 9. Lower Deschutes River basin. Channel-bed textural study mainstem sample sites downstream of the primary study reach (i.e., below Trout Creek) are indicated by stars. Tributaries sampled are named and sample sites indicated by dots. USGS Madras (14092500) and Moody (141030000) gaging stations are shown by triangles

island perimeters (Figure 8). The use of a grid system ensured independence of samples. Along with each particle measurement, the presence or absence of the macrophyte *C. demersum* was noted. Since the plant can trap fine sediment on the bed surface, it was necessary to account for its abundance in later analyses.

Although Wolman (1954) suggested that measuring 100 particles was sufficient for sampling, Rice and Church (1996) recommend 400-stone samples to improve estimates of all percentiles to within a tenth of a phi unit within 95% confidence limits. In this study, pebble counts from a single area were pooled to form individual pebble counts of 200 to 600 particles for each site (Table 3). This effectively reduced the sample number to 1 for each island or bar head and, therefore, restricted the total number of sampled island and bar heads in both years to 23. As a result, statistical methods were focused on estimating longitudinal variability between island and bar heads, rather than variability between pebble counts at each island or bar head.

Grain-size measurements from tributaries were used to identify local sources of sediment that could affect textural patterns within the mainstem. Tributaries sampled include Shitike Creek in the primary study reach and 13 tributaries farther downstream (Figure 9). Pebble counts of 400 particles were conducted along reaches of 2 to 10 channel widths by pacing back and forth between the bankfull channel margins. For each tributary, sampling was conducted near the confluence with the lower Deschutes but above the zone where water backing up into tributaries during high flow events is likely to influence the tributary channels.

Sampling of the Channel-bed Subsurface

At each site on the mainstem Deschutes River where surface sampling was conducted, particles below the surface armor layer were also sampled. The armor layer, identified as the layer of particles extending to the depth of the largest surface particle, was removed by hand, and subsurface material extending to a depth between one to two times the thickness of the armor layer was scooped into a bucket. To prevent washing of

Table 3. Summary of sample size of surface and subsurface bed material by year and environment.

	Number of 100-particle pebble counts conducted					Volume of subsurface bed material retained (kg)				
	1996	1995				1996	1995			
River Kilometer of site	Head	Head	Side	Side channel	End	Head	Head	Side	Side channel	End
PRIMARY STUDY REACH										
160.7	3	3	3	3	3	21.1	47.6	71.7	59.1	51.5
160.3	3	6	n/a	n/a	6	20.5	57.3	n/a	n/a	52.5
159.3	3	3	6	3	6	25.4	61.4	55.9	56.6	59.4
158.0	3	6	---	---	---	22.8	68.0	---	---	---
155.8	3	6	2	---	---	22.3	53.5	64.8	---	---
152.9	3	6	3	6	6	23.7	59.9	55.3	57.9	44.8
151.4	3	2	n/a	n/a	---	19.7	58.7	n/a	n/a	---
149.7	3	2	2	2	2	21.1	62.0	72.4	60.7	62.2
147.7	3	3	3	3	3	23.4	60.4	72.7	57.0	65.9
145.4	3	2	2	---	---	23.2	127.5	60.5	---	---
144.3	3	2	n/a	n/a	---	22.4	59.1	n/a	n/a	---
142.1	3	6	3	2	2	23.5	45.7	49.2	55.0	62.5
ENTIRE STUDY AREA										
138.9	3	n/a	n/a	n/a	n/a	25.0	n/a	n/a	n/a	n/a
133.5	3	n/a	n/a	n/a	n/a	26.4	n/a	n/a	n/a	n/a
123.9	3	n/a	n/a	n/a	n/a	20.6	n/a	n/a	n/a	n/a
114.1	3	n/a	n/a	n/a	n/a	23.4	n/a	n/a	n/a	n/a
97.4	3	n/a	n/a	n/a	n/a	18.2	n/a	n/a	n/a	n/a
83.6	3	n/a	n/a	n/a	n/a	27.8	n/a	n/a	n/a	n/a
64.5	3	n/a	n/a	n/a	n/a	21.6	n/a	n/a	n/a	n/a
51.2	3	n/a	n/a	n/a	n/a	21.0	n/a	n/a	n/a	n/a
42.3	3	n/a	n/a	n/a	n/a	22.7	n/a	n/a	n/a	n/a
38.6	3	n/a	n/a	n/a	n/a	24.8	n/a	n/a	n/a	n/a
15.2	3	n/a	n/a	n/a	n/a	27.4	n/a	n/a	n/a	n/a

NOTE: n/a = not applicable, "---" = not sampled fine sediment downstream, a sawed-off 55-gallon barrel cylinder was worked vertically into the submerged bed. Water collected in the scoop was also added to the bucket to retain finer particles put into suspension during the sampling process.

At least one subsurface sample was collected beneath each pebble count grid in the summer of 1995 (Figure 8). For both 1995 and 1996, individual samples averaged about 20.3 kg by dry weight. Bulk samples from 1995 were pooled to form samples averaging 60.9 kg for each site. To expedite sampling in the summer of 1996, only a sample from the middle grid was obtained. All samples were dried in the laboratory and sieved using a progression of U.S. Standard sieves: 4 in., 3 in., 2 in., 1.5 in., 1 in., 0.75 in., 0.5 in., 0.375 in., 0.25 in., #4, #8, #16, #30, #50, #100, #200, #230, and pan (thus spanning the range from 101.6 mm to <0.063 mm).

Data Analysis

For surface and subsurface samples, percentiles of the grain-size distribution (D_5, D_{16}, D_{25}, D_{50}, D_{75}, D_{84}, D_{95}) on the phi scale were computed by site and then recalculated as millimeters. From these values, the armoring ratio was calculated for each site as $D_{50\ surface}$ (mm)/$D_{50\ subsurface}$ (mm). Trask sorting coefficients were computed as $[D_{75}\ (\text{mm})/\ D_{25}\ (\text{mm})]^{1/2}$ (Krumbein and Pettijohn, 1938); higher values indicate poorer sorting.

Statistical models were developed to evaluate any longitudinal trend in grain size and for changes following the 1996 flood, while accounting for the abundance of *C. demersum* at each site. Because grain-size percentiles in a single grain-size distribution are inherently interdependent, only D_{50} values underwent statistical testing.

The surface, subsurface, and armoring data were analyzed separately using multiple linear regression. Separate statistical analyses were conducted for data from the primary study reach (1995 and 1996) and for that from the entire study area (1996 only). Analysis of the three data sets for these two reach lengths resulted in six statistical models.

Each model of surface grain size, subsurface grain size, and armoring included variables for location (RK) and year. Since these two variables were designed to identify spatial and temporal patterns rather than to build a predictive model, they were not dropped from the model even if they were not statistically significant. Models for surface grain size also included a variable for the abundance of *C. demersum*; however, this variable was dropped from the model if it was not significant. Interactions between variables were tested at the 0.05 significance level. For each model, interaction terms with 2-sided p-values exceeding 0.05 were dropped. Following these guidelines, final models were developed. For each final model, the effect of influential points was evaluated. Significance of variables in the final models was assessed at the 0.05 significance level.

RESULTS

Bedload Transport Study

INITIATION OF BEDLOAD TRANSPORT

Modeled estimates of critical discharge were quite consistent for four of the five sites examined, with site-averaged values ranging from 310 to 340 m3/s (10,950 to 12,010 ft3/s) as measured at the Madras gage (Table 4). A critical discharge value for Site H could not be determined using the analysis technique employed, because critical shear stress was above the Q vs. ? curve calculated for the site. This implied that critical discharge at Site H was greater than the discharge of the February 1996 flood. Field observations following the February 1996 flood (e.g., fresh gravel deposits), however, suggested that material was moved through Site H. We suspect that hydraulic parameters controlling the site were not adequately represented by field measurements. The consistency of results from the remaining four sites and the field evidence strongly suggested that the hydraulic values modeled for Site H were anomolously high, and we

Table 4. Calculated critical discharge (Q_{cr}) ranges and site averages as measured at the Madras gage for Sites B, D, E, H, and I. Ranges indicate the extent of variation found in critical discharge values calculated for individual transects at a site. Site averages represent the average of critical discharge values found within the range of values at a site. Bed critical discharges were calculated as an average critical discharge over the channel bed (i.e. using hydraulic depth). Critical discharge for the channel thalweg are included for comparison (i.e. using maximum depth).

Site	RK (RM)	Zone type [a]	Range of bed Q_{cr} @ Madras m^3/s (ft^3/s)	Site-averaged — bed Q_{cr} @ Madras m^3/s (ft^3/s)	Range of thalweg Q_{cr} @ Madras m^3/s (ft^3/s)	Site-averaged. — thalweg Q_{cr} @ Madras m^3/s (ft^3/s)
B	157.8 (98.0)	S	310–380 (10,950–13,420)	340 (12,010)	250–300 (8,830–10,590)[b]	270 (9,530)[b]
D	154.7 (96.1)	S	290–380 (10,240–13,420)	320 (11,300)	130-200 (4,590–7,060)[b]	160 (5,650)[b]
E	151.3 (94.0)	E	240–490 (8,480–17,300)	330 (11,650)	80–420 (2,830-14,830)[b]	220 (7,770)[b]
H	145.5 (90.4)	S		[c]	[c]	[c]
I	145.2 (90.2)	C/E	230–490 (8,120–17,300)	310 (10,950)	80–230 (2,830–8,120)[b]	120 (4,240)[b]

[a] E = expansion zone, S = straight zone, C = contraction zone
[b] assuming that channel-bed here comprised of same sized material as was measured in shallower water
[c] critical discharge could not be calculated because predicted critical shear stress exceeded the range of shear stresses

defined by the Q_{cr} vs τ curve.

treated the site as an outlier, removing it from further analysis. The model also predicted that bed material would begin to move in the channel thalweg before bed material over the entire cross section was mobilized (Table 4). Here we focus on the remaining straight zone sites (Sites B and D), which most closely fit the assumptions of the one-dimensional flow model.

The sensitivity of the hydraulic analysis to variations in the energy slope (S_e), median particle diameter of the channel-bed surface (D_{50s}), and Shields stress for the median diameter of the channel-bed surface (τ^*_{cr50s}) was site-dependent. Site D was more sensitive, on average, to both individual and multiple-parameter variation than Site B. Critical discharges for Sites B and D that resulted from varying the three tested parameters simultaneously to decrease critical discharge were both 270 m^3/s (9,530 ft^3/s) and were 420 m^3/s and 500 m^3/s (14,830 ft^3/s and 17,660 ft^3/s), respectively (average 460 m^3/s, 16,240 ft^3/s), when parameters were varied to increase critical discharge. These values (270 m^3/s and 460 m^3/s) represent a range of what we will consider maximum deviation of the critical discharge value for these sites in the primary study reach.

Bedload Transport Analysis

Employing the Parker (1990) model, we predicted transport of all particle sizes to begin between approximately 300 and 400 m^3/s (10,590 and 14,130 ft^3/s), with predicted bedload transport rates increasing with discharge (Figure 10). These findings are consistent with the critical discharge of 340 m^3/s (12,010 ft^3/s) calculated in the hydraulic analysis for D_{50}-sized bed material. The Parker (1990) model was derived for conditions when transport is controlled by hydraulic conditions rather than particle availability (Parker et al., 1982); therefore, transport rates represented here are those that occur following exceedance of threshold transport conditions and disruption of the channel-bed armor layer. Because of differences in static and dynamic coefficients of friction, particle interlocking, and particle hiding, bed material can typically be transported at discharges much lower than those necessary to entrain them (Reid et al., 1985). To take into account

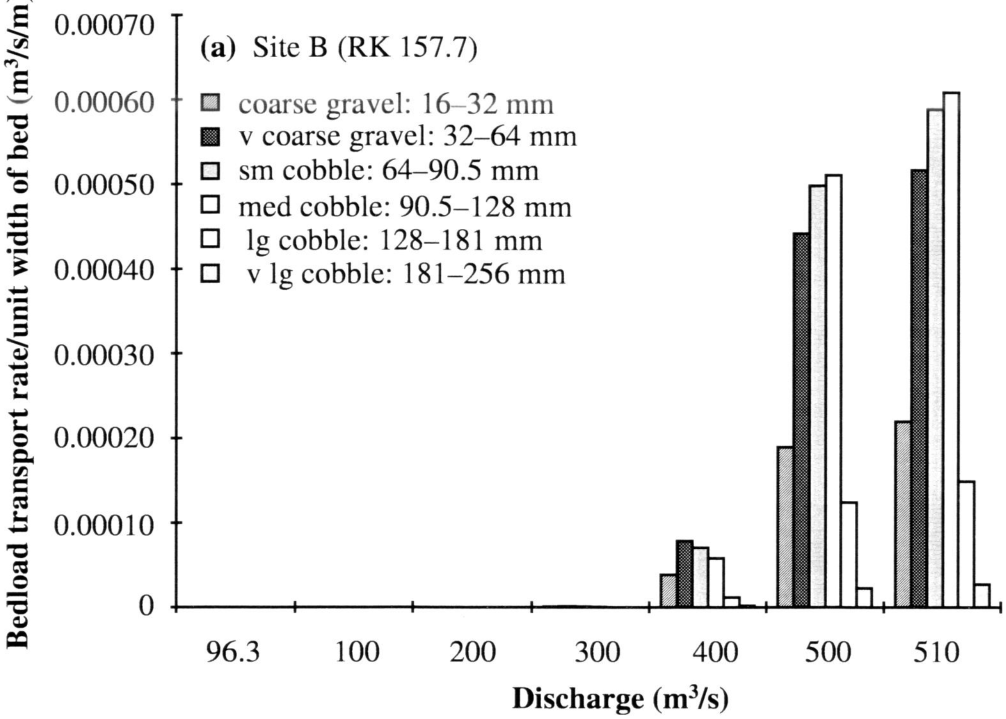

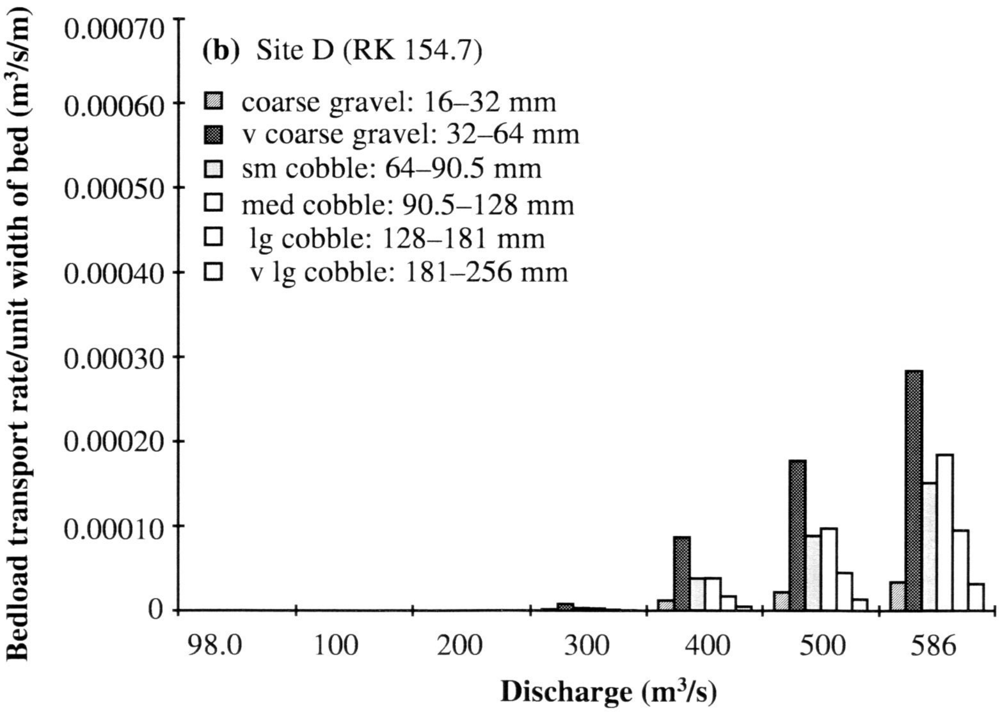

Figure 10. Calculated bedload transport rates per unit gravel-bed width for (a) Site B and (b) Site D. General bedload transport was predicted to begin between 300 m^3/s (~10,590 ft^3/s) and 400 m^3/s (~14,130 ft^3/s) with smaller particle sizes being moved preferentially throughout the range of discharges examined.

some degree of continued transport following entrainment, bedload transport was considered to continue to a discharge of 280 m^3/s (9,890 ft^3/s), at which point, the volume of material transported (measured in m^3/day) fell into single digits.

HISTORICAL STREAMFLOW ANALYSIS

Examination of annual flow duration curves showed that the highest mean daily flows on an annual basis over the period of record ranged from 150 to 510 m^3/s (5,300 to 18,010 ft^3/s), with most falling between 150 and 300 m^3/s (5,300 and 10,590 ft^3/s, Figure 11). Comparison of the curves did not reveal any dramatic changes in flow frequency over the period of record (Figure 11). This would suggest that any changes in streamflow due to the Project are subtle or are operating on different time scales than that of mean daily flows.

Comparison of the 30-year flow duration curves similarly did not reveal any dramatic changes in flow frequency between the pre- and post-Project time periods (Figure 12). Some differences between curves reflect the influence of climatic differences between the two periods; severe drought occurred from the mid-1920s through much of the 1930s, affecting the pre-Project curve, and the largest flood of record affected the post-Project curve. Consequently, differences observed between the curves cannot be attributed to the Project alone. Despite these climatic differences, the curves for these two time periods are still quite similar, underscoring the remarkably slight variation in flow for the Deschutes River prior to and following closure of the Project.

Determining any effect of the Project on streamflow using flow duration curves is confounded by the presence of five other dams and six major flow diversions upstream of the Project. In addition, water storage (both natural and anthropogenic), water diversions, irrigation return-flow, climate change, and interbasin groundwater exchange influence the pattern of streamflow in the basin and act as confounding variables. A comprehensive statistical analysis and water budget are required to determine changes in streamflow due to Project operation but were not conducted as part of this study.

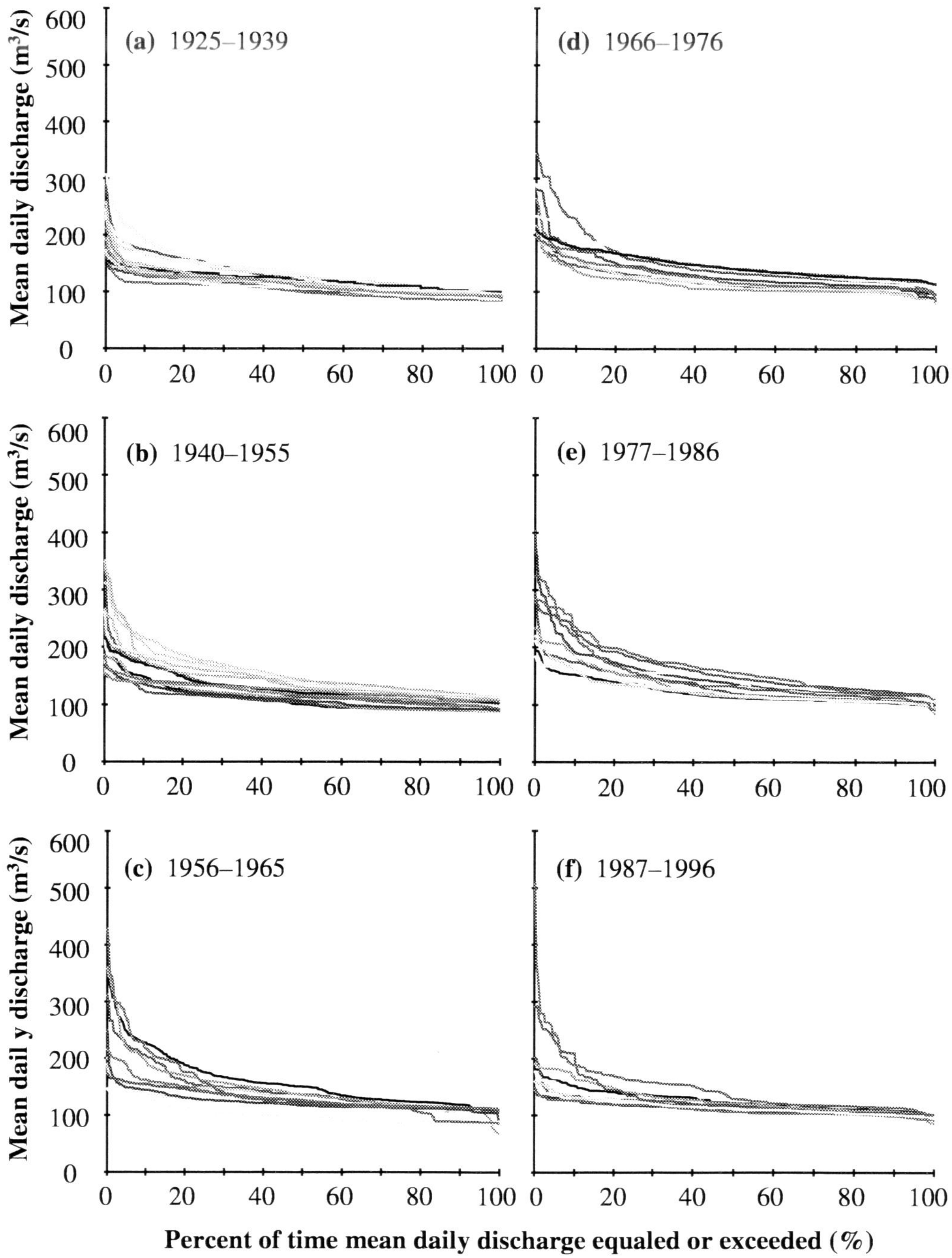

Figure 11. Annual flow duration curves (Deschutes River near Madras gage) for water years (a) 1925–1939, (b) 1940–1955, (c) 1956–1965, (d) 1966–1976, (e) 1977–1986, and (f) 1987–1996.

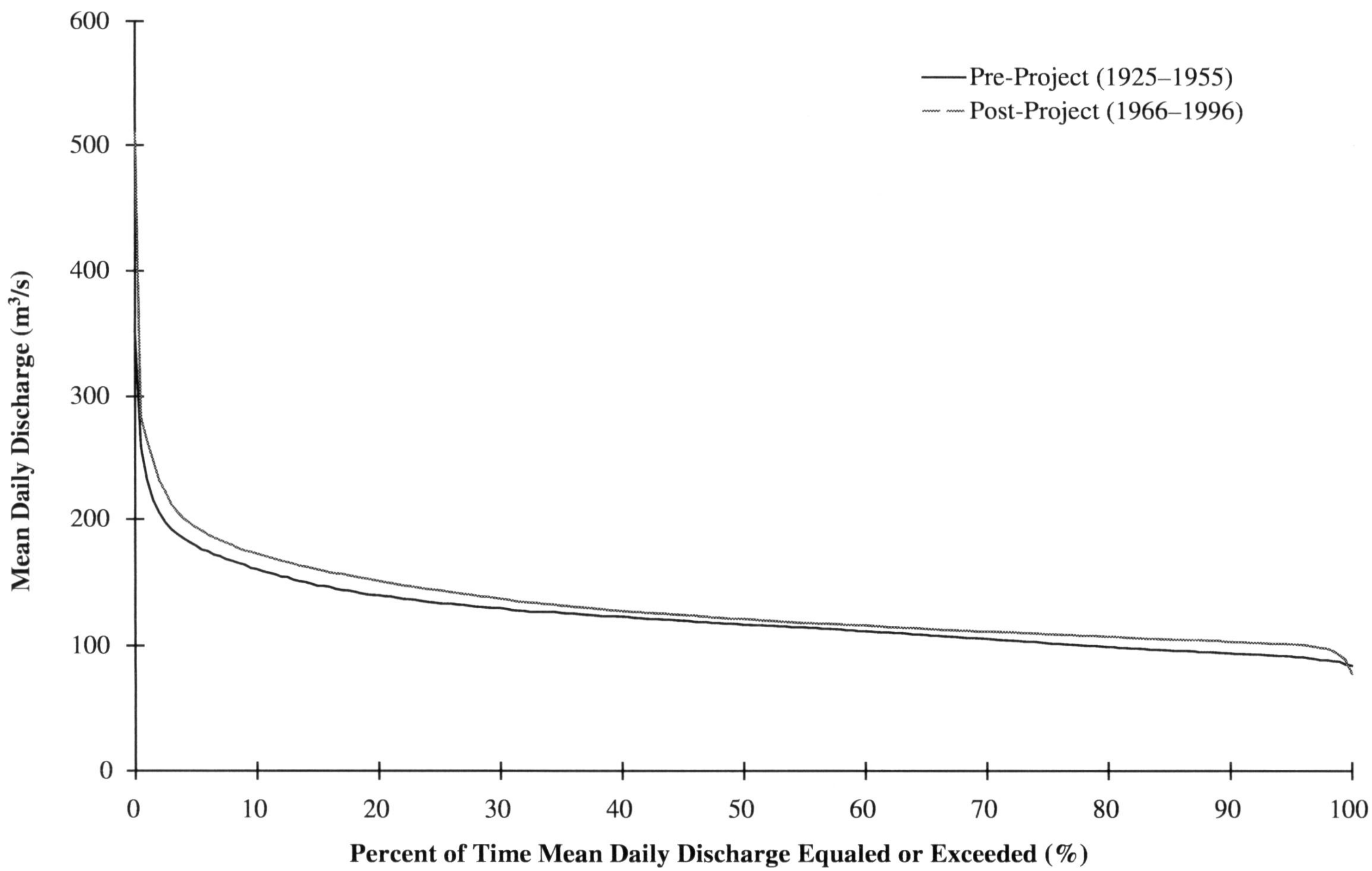

Figure 12. 30-year flow duration curves for pre-Project (water years 1925–1955) and post-Project (water years 1966–1996) time periods. A flow of 300 m^3/s is equivalent to ~10,590 ft^3/s and a flow of 400 m^3/s is equivalent to ~14,130 ft^3/s.

Our results predicted events capable of mobilizing channel-bed material to be rare for sites examined in the primary study reach. There have only been 26 transport days during the 72-year flow record during which mean daily discharge equaled or exceeded 340 m^3/s (12,010 ft^3/s), the predicted threshold for bedload transport (Table 5). These estimates are robust with respect to model parameter sensitivity, as the combined effects of reasonable uncertainties on the hydraulic modeling indicate that bedload transport has occurred less than 1% of the time over the period of record (Table 5). Even if bedload transport is assumed to begin at 340 m^3/s (12,010 ft^3/s) but continue to 280 m^3/s (9,890 ft^3/s), transport is still predicted to occur during well below 1% of the time (Table 5).

Table 5. Frequency and magnitude of critical discharge exceedance over the period of record for calculated critical discharges of 270, 340, and 460 m^3/s (9,530, 12,010, and 16,240 ft^3/s).

Q_{cr} (m^3/s)	# days $Q \geq Q_{cr}$	% of record $Q \geq Q_{cr}$	# storm events	# days $Q > Q_{cr}$ by	
				>10%	>20%
270	181	0.7	29	96	48
340	26	0.1	11	6	5
460	1	0.004	1	1	0
340[a]	69	0.3	11	6	5

[a] taking into account transport initiating at 340 m^3/s but continuing until 280 m^3/s.

Predicted bedload transport rates for Site B (RK 157.7, RM 98.0) ranged from 2,000 to 3,000 m^3/yr (2,620 to 3,920 yd^3/yr), with two notable exceptions, for the years during which general bedload transport was predicted to occur over the period of record (Figure 13). The exceptions occurred during water years 1965 and 1996 as a result of the December 1964 and February 1996 floods, respectively. The 1964 flood was predicted to have transported 6,530 m^3 (8,540 yd^3), or 7%, of all material calculated to have moved through Site B since 1925. The flood of February 1996 was predicted to have transported the most material through Site B of any event on record, with an estimated 14,900 m^3 (19,490 yd^3) of bedload moved. This volume was equal to 42% of all material predicted to have been transported through Site B since 1925.

PROJECT EFFECTS ON DISCHARGE AND BEDLOAD TRANSPORT

Post-Project transport events were predicted to have occurred in December 1964, January 1965, March 1972, February 1982, and February 1996. The 1964 event occurred prior to the Project being fully operational but was included in the analysis because this flood had the largest recorded inflow to the Project (PGE, 1996), the second highest discharge recorded downstream of the Project (Hubbard et al., 1997), and its peak was captured by Round Butte Dam, whose reservoir was filling for the first time. For simplicity, we refer to the four storms following filling of the reservoir as "post-filling" events; all five events together are called "post-dam" events.

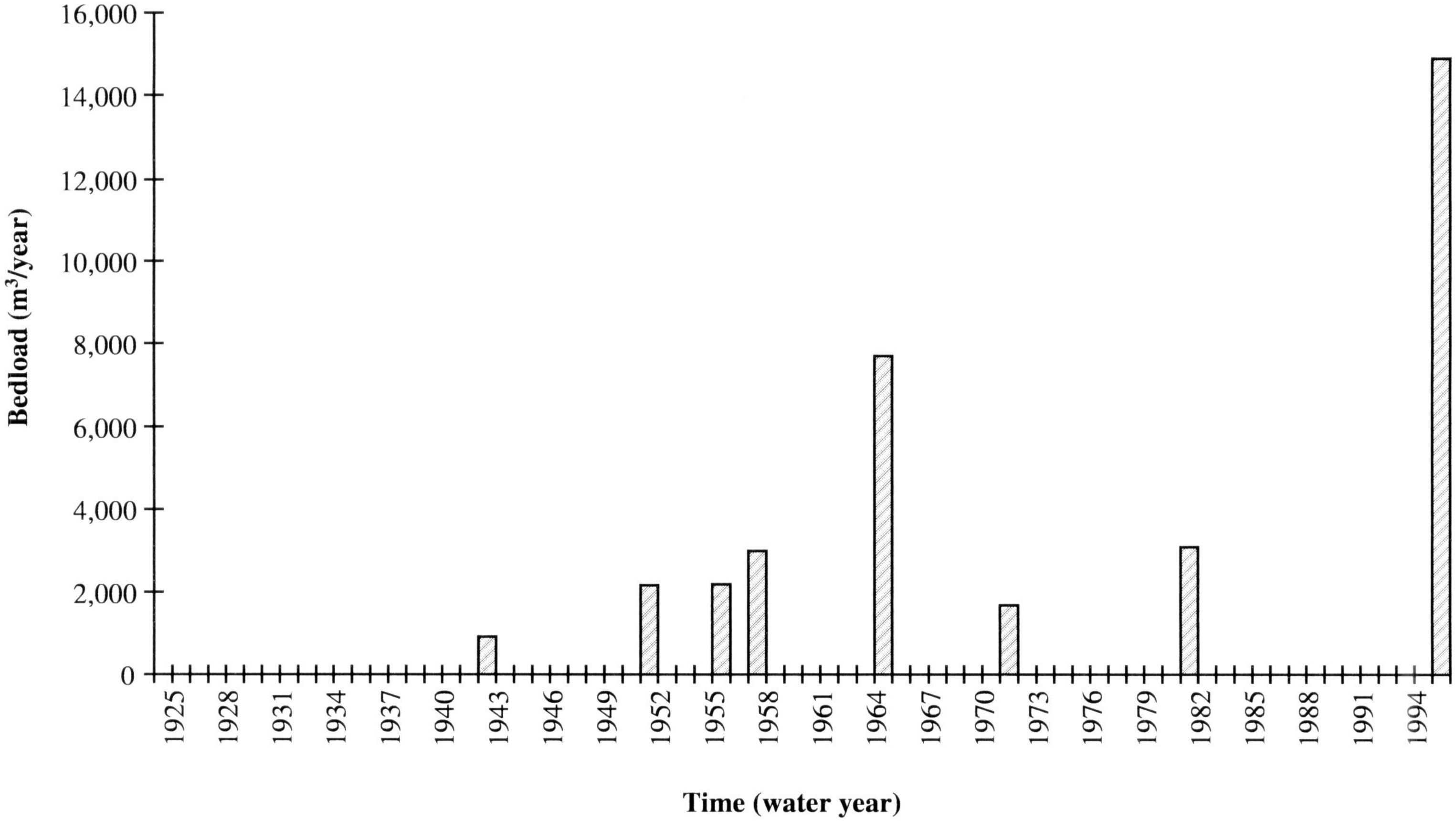

Figure 13. Predicted volume of bedload moved per year at Site B (RK 157.7) during water years 1925–1996.

A comparison of hydrograph shapes for Project inflows and outflow showed that for all post-dam transport events, the Project stored water (i.e., inflow > outflow) on the rising limb of the hydrograph and released water (i.e., inflow < outflow) during and/or following the peak of the hydrograph (Figure 14). In all cases but the 1964 event, however, the amount of water stored and released was minimal compared to the overall discharge for the event and, in most cases, the majority of change in the hydrograph due to the Project occurred at discharges that were less than critical for transport. Although changes in the hydrograph at flows less than critical discharge are not important in the context of bedload transport or channel morphologic change, consequences of such flow reduction or enhancement to suspended sediment transport and ecological parameters are unknown.

The Project had no effect on the timing of post-filling-event flow peaks, but delayed the peak of the 1964 event by four days (Table 6). The Project had no effect or slightly increased the magnitude of all post-filling flow peaks (0 to 8%) and decreased the magnitude of the 1964 flow peak by 32% (Table 6). These magnitudes of flow increases are small, probably in the range of discharge measurement error during large flow events. Because of unusual circumstances surrounding the 1964 event, and the finding that no other post-dam transport event was affected in the same way, we consider the decreased and delayed flood peak caused by the Project to be unique to the 1964 event.

Using the inflow and outflow discharges previously derived, the quantity of bedload transported per day by reservoir inflows and outflows was predicted and compared for each post-dam transport event for Sites B and D. The results indicated that at Sites B and D the Project increased bedload transport by 0 to 27% (average 10%) for the four post-filling events and decreased transport by 69 to 86% (average 78%) for the 1964 event (Table 7). Because reservoir inflows during the 1964 flood exceeded the upper limits of the sediment rating curve for Site B, transport rates for this event had to be extrapolated.

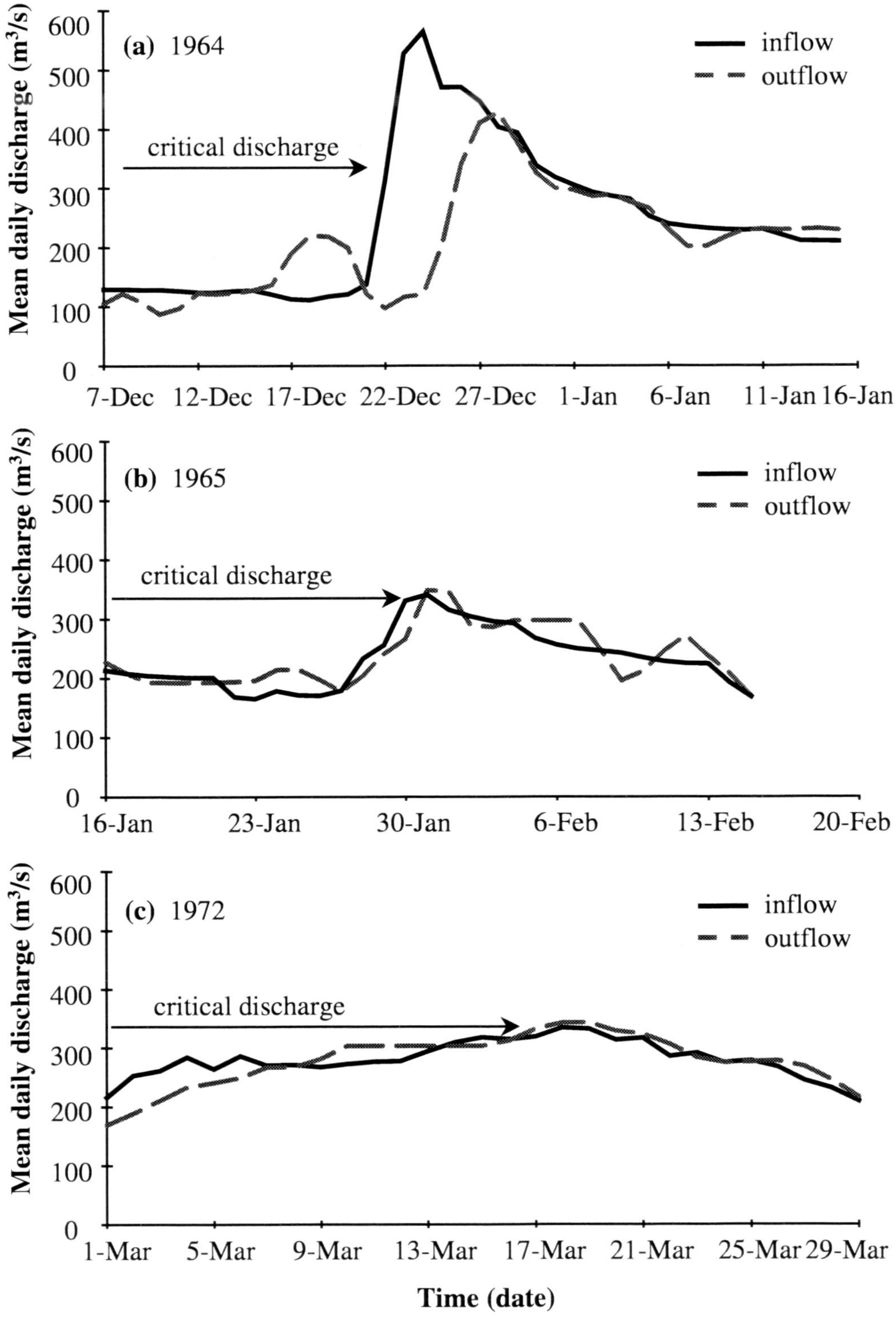

Figure 14. Round Butte reservoir inflows and Project outflows for all post-dam transport events: (a) December 1964, (b) January 1965, (c) March 1972, (d) February 1982, and (e) February 1996. Note that x-axes cover different length time periods.

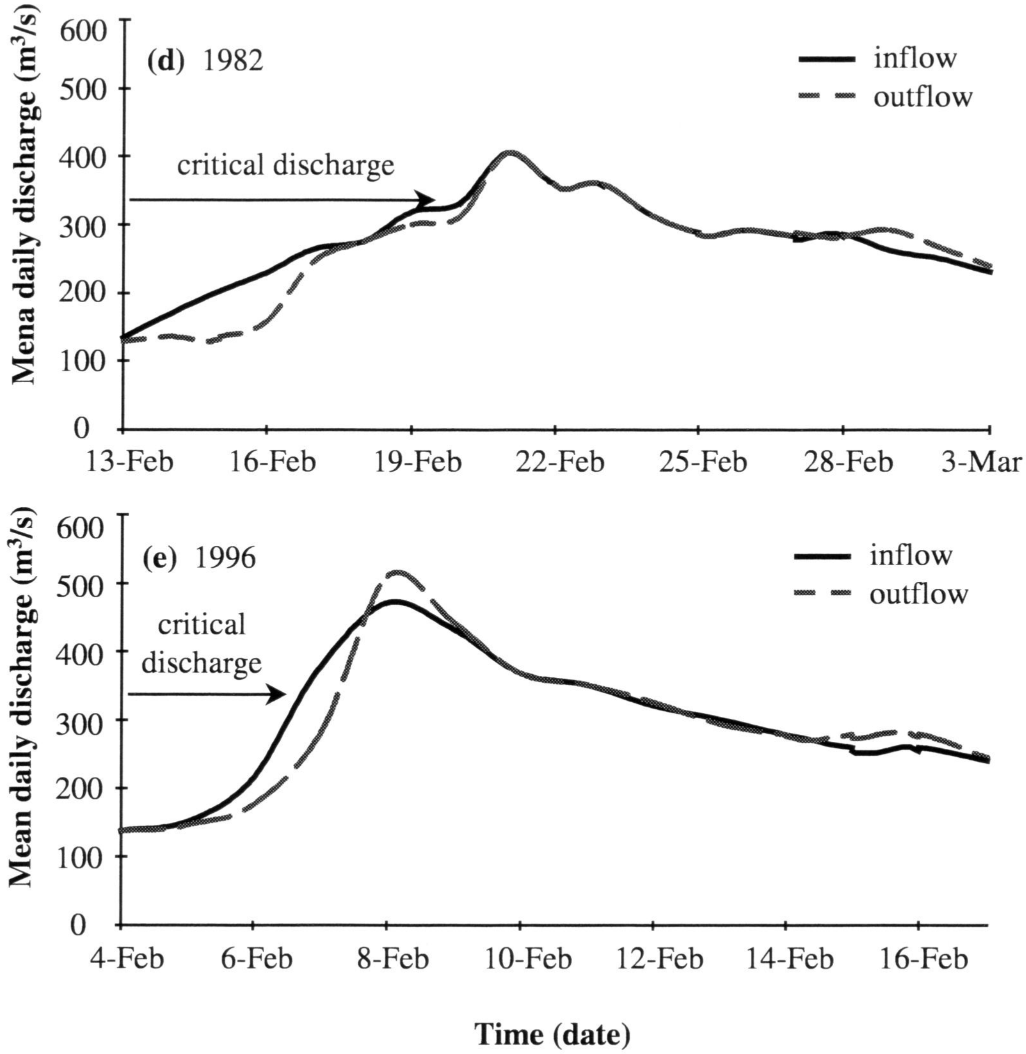

Figure 14. (Continued)

Table 6. Timing and magnitude of highest flow peaks for reservoir inflows (Q_{in}) and outflows (Q_{out}) for post-dam transport events. All discharges are mean daily flow.

Transport Event	Magnitude of Highest Flow			Date of Highest Flow		
	Q_{in} (m^3/s)	Q_{out} (m^3/s)	% change	Q_{in}	Q_{out}	Days peak lagged
Dec 1964	564?	428	-32	12/24/64	12/28/64	4
Jan 1965	341?	348	2	1/31/65	1/31/65	0
Mar 1972	334	343	3	3/18/72	3/18–3/19/72	0
Feb 1982	405	405	0	2/21/82	2/21/82	0
Feb 1996	471	510	8	2/8/96	2/8/96	0

? = estimated value because of lack of reservoir water elevation data

Table 7. Total bedload transported by reservoir inflows ($Q_{s\ in}$) and outflows ($Q_{s\ out}$) for five post-dam transport events. Reservoir inflows approximate streamflows that would occur in the absence of the Project. Transport calculations for Site D (except in 1996) do not take into account the discharge contributed by Shitike Creek as the creek was not gaged at this time.

Site	Transport event	$Q_{s\ in}$ (m^3)	$Q_{s\ out}$ (m^3)	% change in $Q_{s\ in}$
B	Dec 1964	48,000	6,526	-86
D	Dec 1964	13,900	4,301	-69
B	Jan 1965	1,100	1,200	9
D	Jan 1965	1,400	1,600	14
B	Mar 1972	0 [a]	1,700	--
D	Mar 1972	0 [a]	1,900	--
B	Feb 1982	3,100	3,100	0
D	Feb 1982	3,000	3,100	3
B	Feb 1996	11,700	14,900	27
D	Feb 1996	9,700	10,400	7

a: $Q_{s\ in}$ here = 0 because $Q_{s\ in}$ was less than the predicted critical discharge of 340 m^3/s (Figure 14c).

Channel Morphology Study

HISTORICAL CHANGES IN CHANNEL CROSS SECTION

Comparison of USGS historical cross section measurements for the gage near Madras revealed that the channel bed was degrading at a very slow but statistically significant rate both prior to and following construction of the Project (2-sided p-value = 0.05 for 1924–1933; 2-sided p-value << 0.001 for 1929–1956 and 1957–1998) as indicated by decreasing minimum streambed elevations (Figure 15). Although absolute degradation rates between pre- and post-dam time periods cannot be compared because the measurement cross section was moved when the Project was constructed in 1957, the slopes of the 1929–1957 and post-1957 trend lines are quite similar. The largest decreases in minimum streambed elevation after 1957 appeared to be associated with high discharge events, particularly those exceeding the predicted critical discharge of 340 m^3/s (12,010 ft^3/s, Figure 15b). Prior to 1957, the measurement cross section was located in a boulder-and bedrock-controlled section (USGS, 1957, unpublished data) and, therefore, was not as affected by large flood events as the more alluvial post-1957 site (Figure15a). Net degradation since 1957 was estimated at less than 0.05 m (0.2 ft, Figure 15b). For the post-1957 gage site, cross sectional area was found to increase with time at a very small but statistically significant rate (2-sided p-value << 0.001), indicating a very slight increase in channel capacity over time (Figure 16). Pre-1957 areas were not calculated because of the extreme stability of the site (Figure 17).

Examination of changes in individual cross sections during and following high discharge events showed channel scour during high discharge events and partial to total refill of scoured areas in the weeks to months following the event (Figure 18). Maximum scour experienced at the Madras gage measurement cross section was 0.8 m on river right

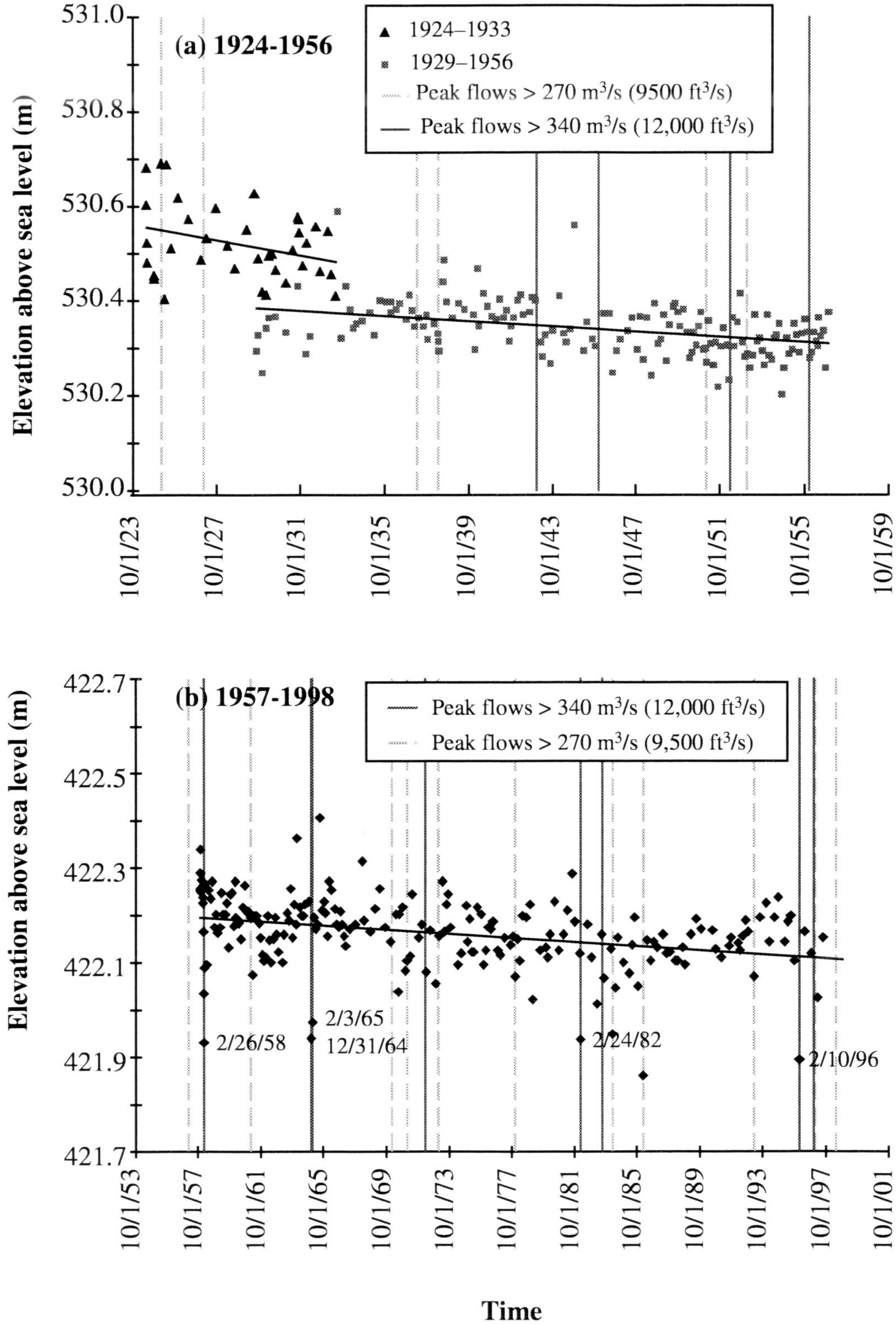

Figure 15. Minimum streambed elevation (elevation of channel thalweg) of the USGS measurement cross-section for the Deschutes River near Madras gage, (a) 1924–1956 and (b) 1957–1998.

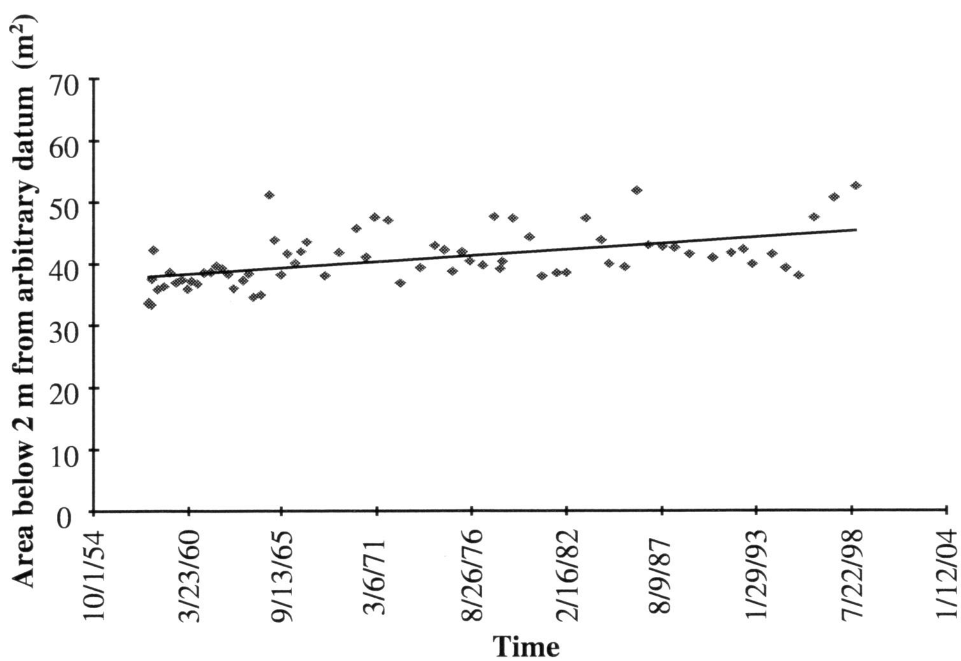

Figure 16. Area of USGS measurement cross section below 2 meters from arbitrary datum (Deschutes River near Madras gage). Areas calculated for every third measurement from 1957–1998. The slope of the trend line is significantly different than zero.

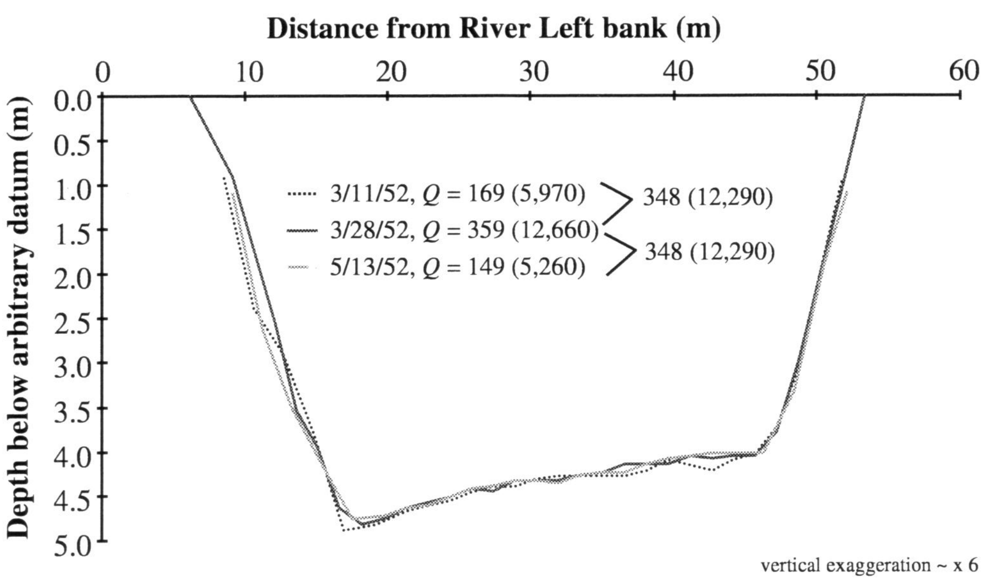

Figure 17. Cross-sectional profiles at the USGS measurement cross section for the Deschutes River near Madras gage before, during, and after a large flood in March 1952. Date, instantaneous discharge at time of measurement [in m^3/s and [ft^3/s)], and highest mean daily discharge between measurements [in m^3/s and (ft^3/s)] indicated for each cross-section measurement.

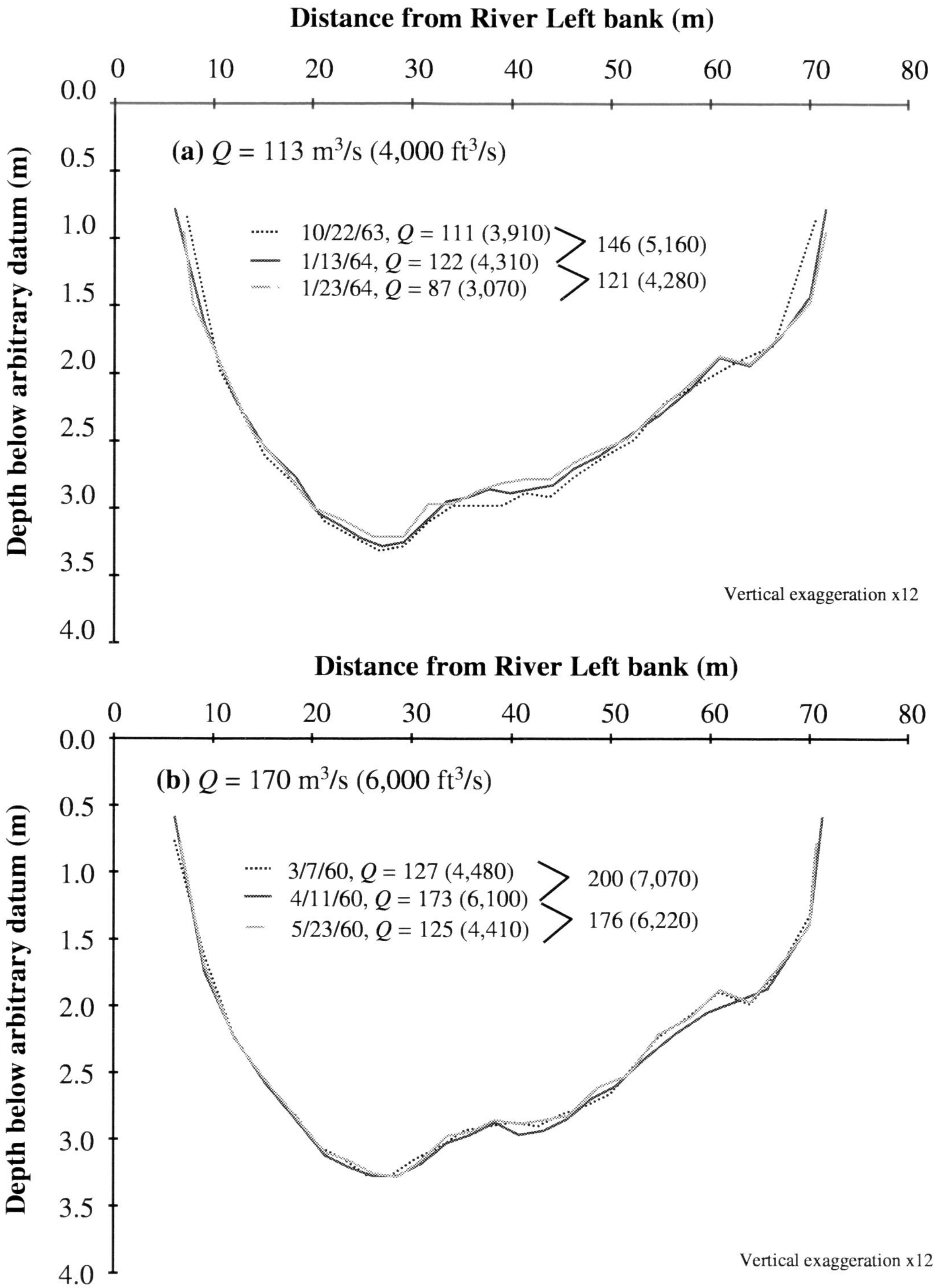

Figure 18. Cross-sectional profiles at the USGS measurement cross section for the Deschutes River near Madras gage. Changes in profiles between measurements spanning different discharge ranges were used to estimate discharges at which general transport begins over the channel bed. The date, instantaneous discharge at the time of measurement (in m^3/s [ft^3/s]), and the highest discharge between measurements (in m^3/s and [ft^3/s]), are indicated.

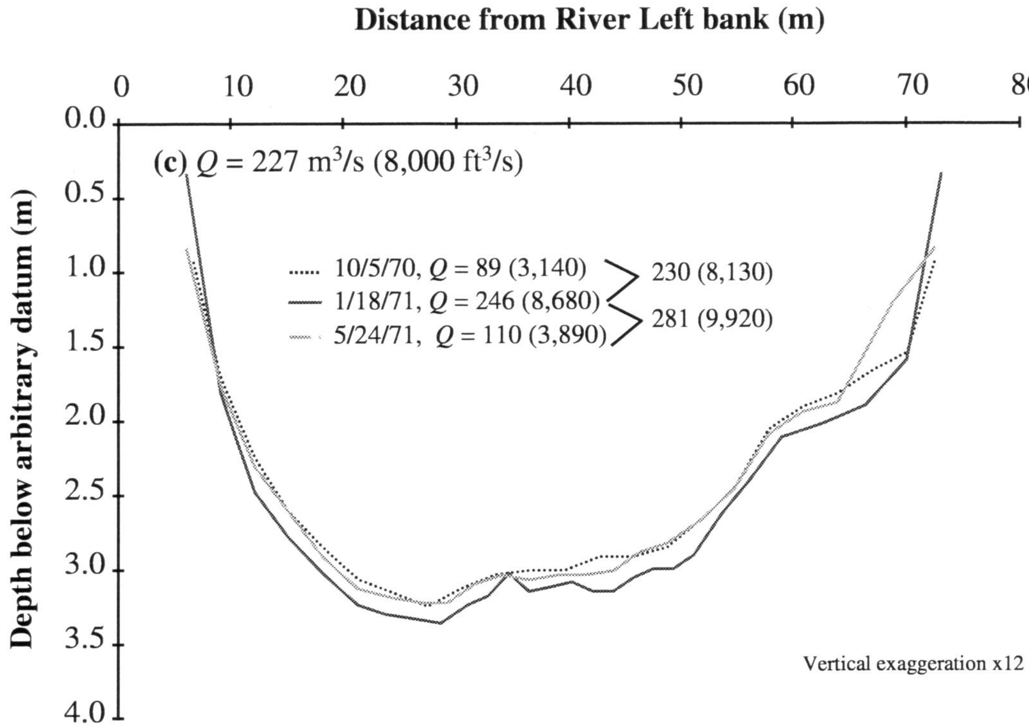

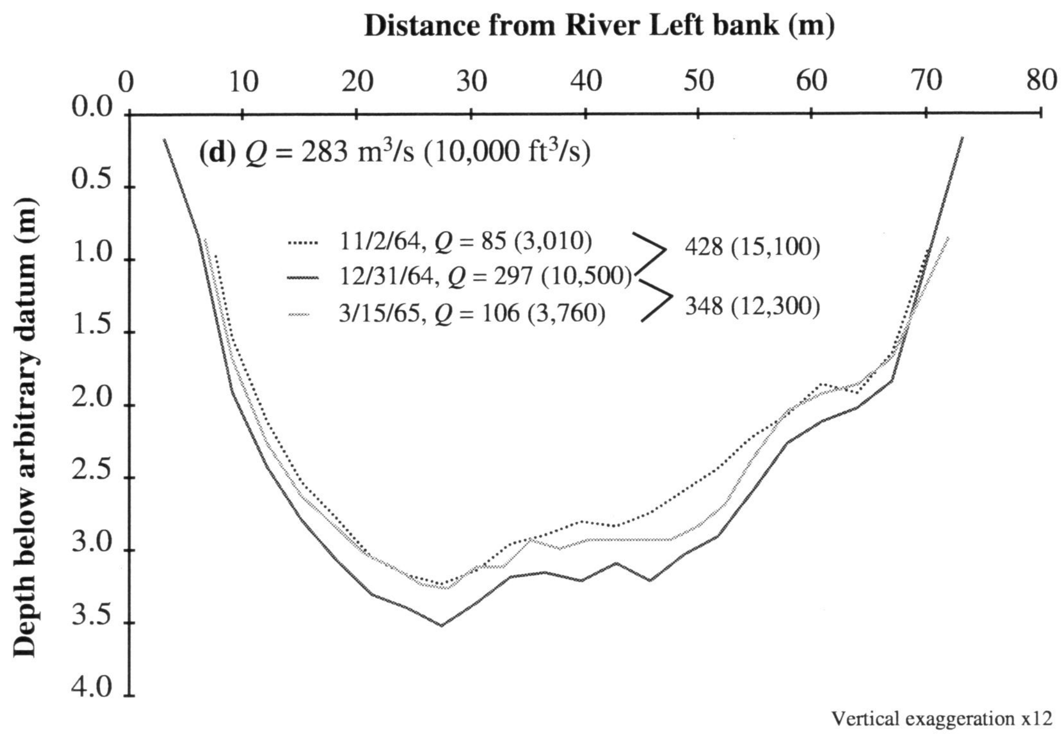

Figure 18. (Continued)

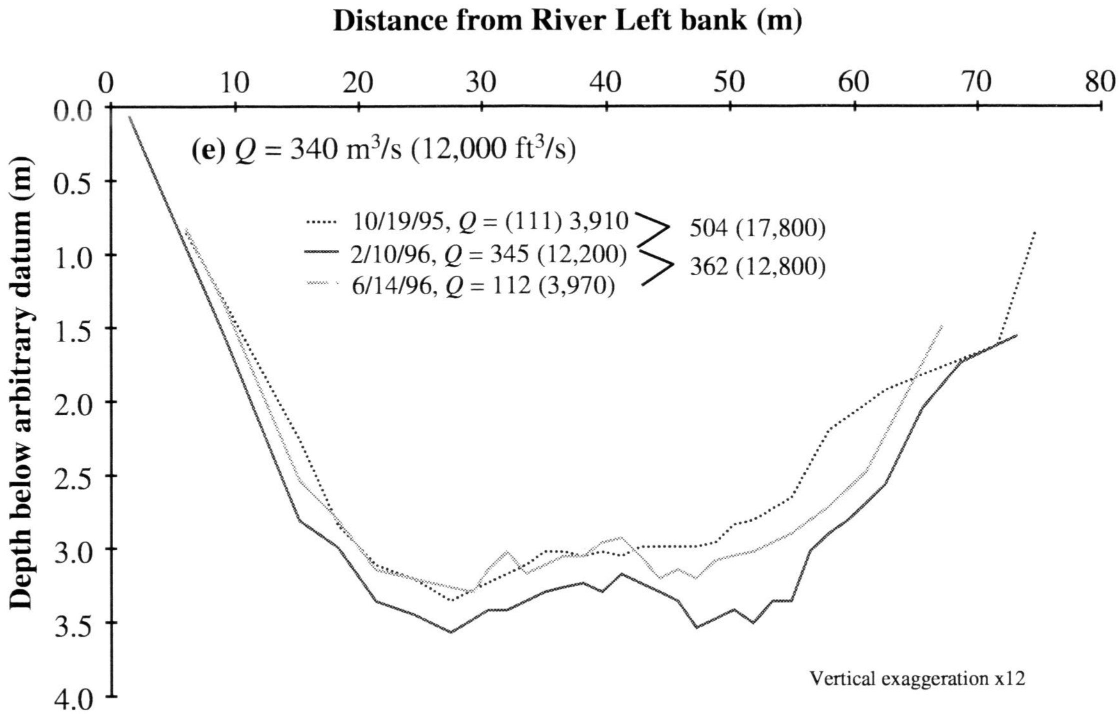

Figure 18. (Continued)

during the February 1996 flood (Figure 18e). By the next cross section measurement four months later, 0.5 m of the original 0.8 m scour had refilled (Figure 18e). The magnitude of channel "rebound" was quantified by evaluating the maximum change in cross-sectional area over the time period spanning events (Figure 19). Rebound magnitude appeared to be strongly associated with the magnitude of the peak discharge experienced during the measurement period evaluated (Figure 19). Similar channel rebound was noted much further downstream at the measurement cross section for the Deschutes River at Moody gage (14103000; McClure, 1998)

Thresholds for general channel-bed entrainment at the Madras gage site appeared to be exceeded beginning around 250 m^3/s (8,800 ft^3/s; Figure 18c, d, e). At these discharges and higher, the entire cross section exhibited change. Channel change was concentrated in the thalweg for smaller discharges of about 150 m^3/s (5,300 ft^3/s; Figure 18a, b). These results are generally in close agreement with the lower bound of critical thresholds predicted from the hydraulic models for both the cross-section average and the thalweg (Table 4).

Historical Changes in Channel Planform

Aerial photographs from 1944, 1951, 1956, 1968, 1972, 1995, and 1996 illustrate stable channel boundaries and island perimeters throughout most of the study area. Even at the confluences with the Warm Springs and the White Rivers, which likely supply the largest volumes of sediment to the mainstem, photographs bracketing major flood events did not reveal changes in planform geometry. Islands and bars in the primary study reach, however, were typically found to grow or be modified during large floods but underwent little change during intervening periods of time. The supply of gravel from tributaries during these high flow events may play a critical role in changes to islands and bars. Historical photographs showed cycles of bar and island construction at the confluence of Shitike Creek following the 1964 and 1996 floods (Figure 20). The photographs document the following sequence: 1) large floods deposit new bars; material

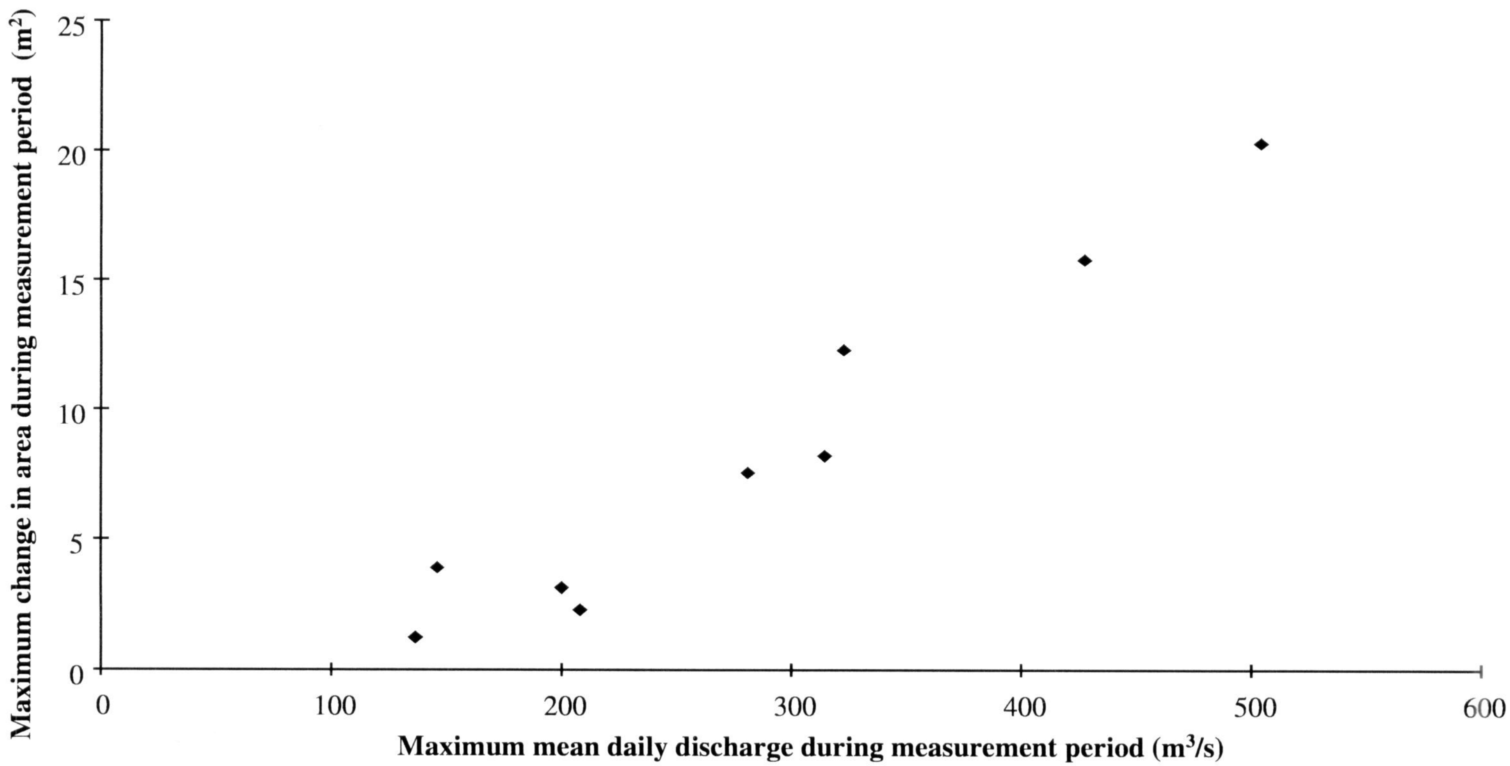

Figure 19. Maximum change in area between cross sections during measurement periods examined in historical cross-section analysis (e.g. Figure 18) versus maximum mean daily discharge that occurred during the same measurement period. A flow of 300 m^3/s is equivalent to ~10,590 ft^3/s and 400 m^3/s to ~14,130 ft^3/s.

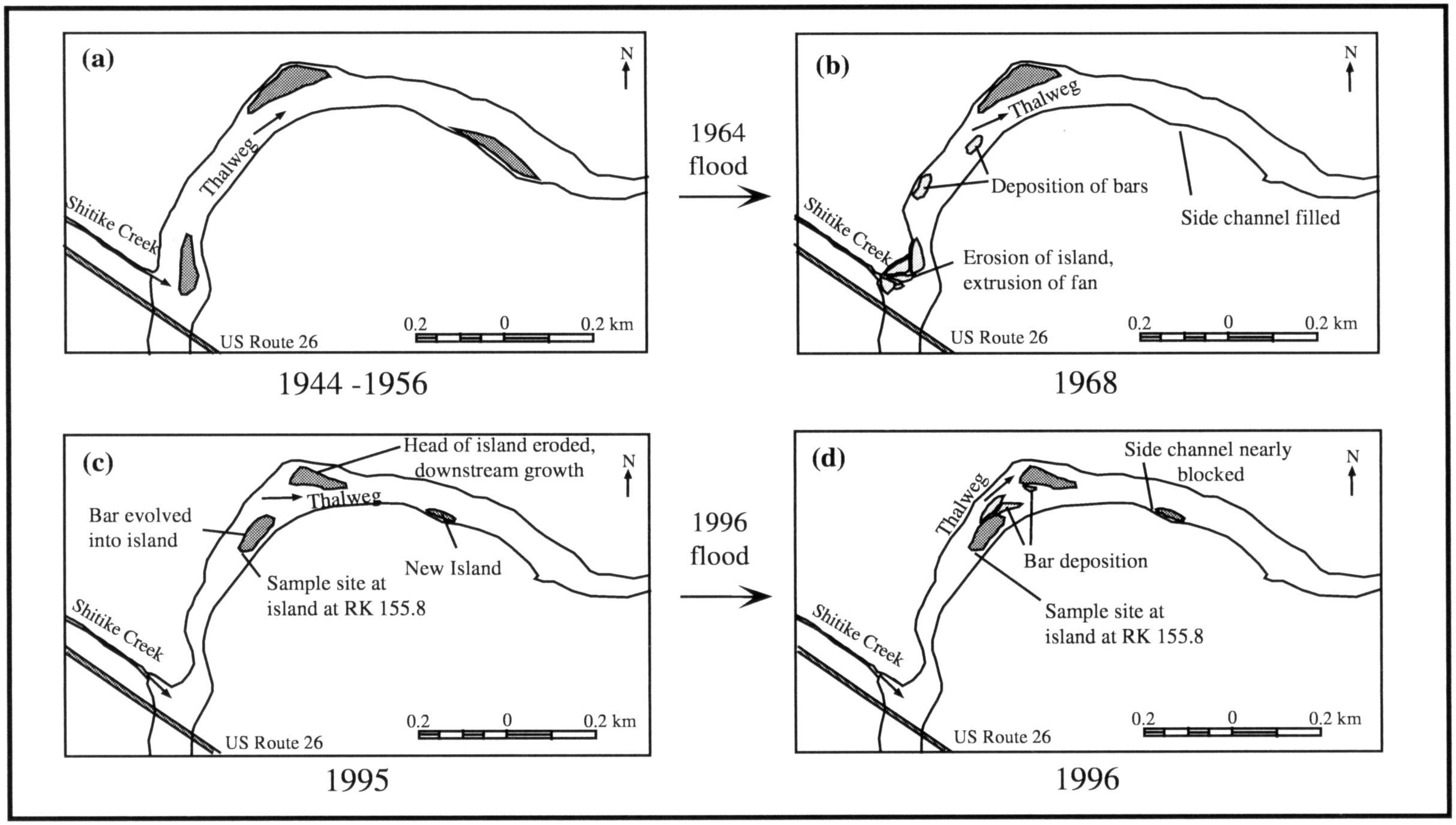

Figure 20. Schematic showing major planform changes in the Deschutes River near Shitike Creek observed in historical aerial photographs. Darker lobate shapes indicate islands. Lighter lobate shapes are submerged bars.

in these bars is derived from nearby tributaries and/or the main channel bed (Figure 20b, d); 2) subsequent lower intensity flows modify deposits; vegetation stabilizes bars, converting them to islands (Figure 20 between b and c); and 3) subsequent floods deposit sediment in the lee of stable islands or may form new bars (Figure 20d).

A few other changes in island morphology were noted in the historical photographic record of the primary study reach. Just below the Dry Creek confluence, an island on river left was present from at least 1944 through 1956, but by 1968 had been reduced to a small gravel bar, still present in 1998. From at least 1944 to the present an island situated only about 60 m upstream of this island has persisted, so changes have been extremely localized. Photographs of the lowermost river are too sparse to correlate any changes with high flow events.

Huntington (1985) argues that islands near the Project have provided a natural source for gravel recruitment that has partially offset losses in sediment supply from upstream of the Project. Photographic analyses did not show major changes in island morphology immediately downstream of the Project over the period 1944 to 1996. Overhanging vegetation and the scale of photographs makes it impossible to discern small changes in island size at most sites, however.

Channel-Bed Texture Study

The final statistical models developed using multiple linear regression were:

Primary Study Reach

$$|\mu(\text{surface } D_{50})| = \beta_0 + \beta_1(RK) + \beta_2(YEAR) + \beta_3(CD) + \beta_4(CD)$$

$$|\mu(\text{subsurface } D_{50})| = \beta_0 + \beta_1(RK) + \beta_2(YEAR)$$

$$|\mu(\text{armor})| = \beta_0 + \beta_1(RK) + \beta_2(YEAR)$$

Entire Study Area

$$|\mu(\text{surface } D_{50})| = \beta_0 + \beta_1(RK)$$

$$|\mu(\text{subsurface } D_{50})| = \beta_0 + \beta_1(RK)$$

$$|\mu(\text{armor})| = \beta_0 + \beta_1(RK)$$

where μ = the estimated mean of the grain parameter indicated, RK = River Kilometer, $YEAR$ = year, CD = the level of *C. demersum*, and β values represent coefficients in each regression model (β_0 = y intercept or D_{50} when all other β values equal zero, β_1 = RK, β_2 = 0 for 1995, β_2 = 1 for 1996, β_3 = 1 for moderate levels of *C. demersum*, β_4 = 1 for high levels of *C. demersum*). The coefficients and associated 2-sided p-values for each model are displayed in Table 8. Results from multiple regression analyses were variable but largely showed no significant longitudinal or temporal trends.

The following sections describe the individual models developed for the primary study reach and for the entire study area. In addition, Trask sorting coefficients are reported.

Particle-Size Trends over the Primary Study Reach

Bed-surface Particle Size

In the primary study reach, bed surface D_{50} values at island and bar heads ranged from 30 mm to 95 mm (average 70 mm) during 1995 and 1996 (Figure 21). There was little or no apparent trend in surface D_{50} with distance downstream from the Project (Figure 21). Results from multiple linear regression show no evidence for a change in surface D_{50} with distance, even after accounting for year and abundance of *C. demersum* (Table 8). One influential point was identified in the regression. When this point was removed from the final model for comparison, the results remained unchanged.

Table 8. Summary of regression results for the primary study reach and entire study area. Asterisks indicate statistically significant (<0.05) p-values.

	Surface D_{50} (mm)		Subsurface D_{50} (mm)		Armoring ratio (mm/mm)	
Independent variables	Value of β Coefficient	2-sided p-value	Value of β Coefficient	2-sided p-value	Value of β Coefficient	2-sided p-value
PRIMARY STUDY REACH						
Constant (Low *C. dem.*, 1995)	-34.30	0.68	110.74	0.044*	-21.00	0.062
River Kilometer	0.73	0.19	-0.56	0.11	0.16	0.034*
YEAR (0 for 1995, 1 for 1996)	6.53	0.32	-6.54	0.14	1.68	0.07
C. demersum: (1 for moderate)	1.54	0.84	n/a	n/a	n/a	n/a
C. demersum: (1 for high)	-28.12	0.0052*	n/a	n/a	n/a	n/a
ENTIRE STUDY AREA						
Constant	87.68	<0.0001*	30.14	0.0003*	2.59	0.07
River Kilometer	-0.13	0.23	-0.08	0.14	0.02	0.14

n/a = not applicable

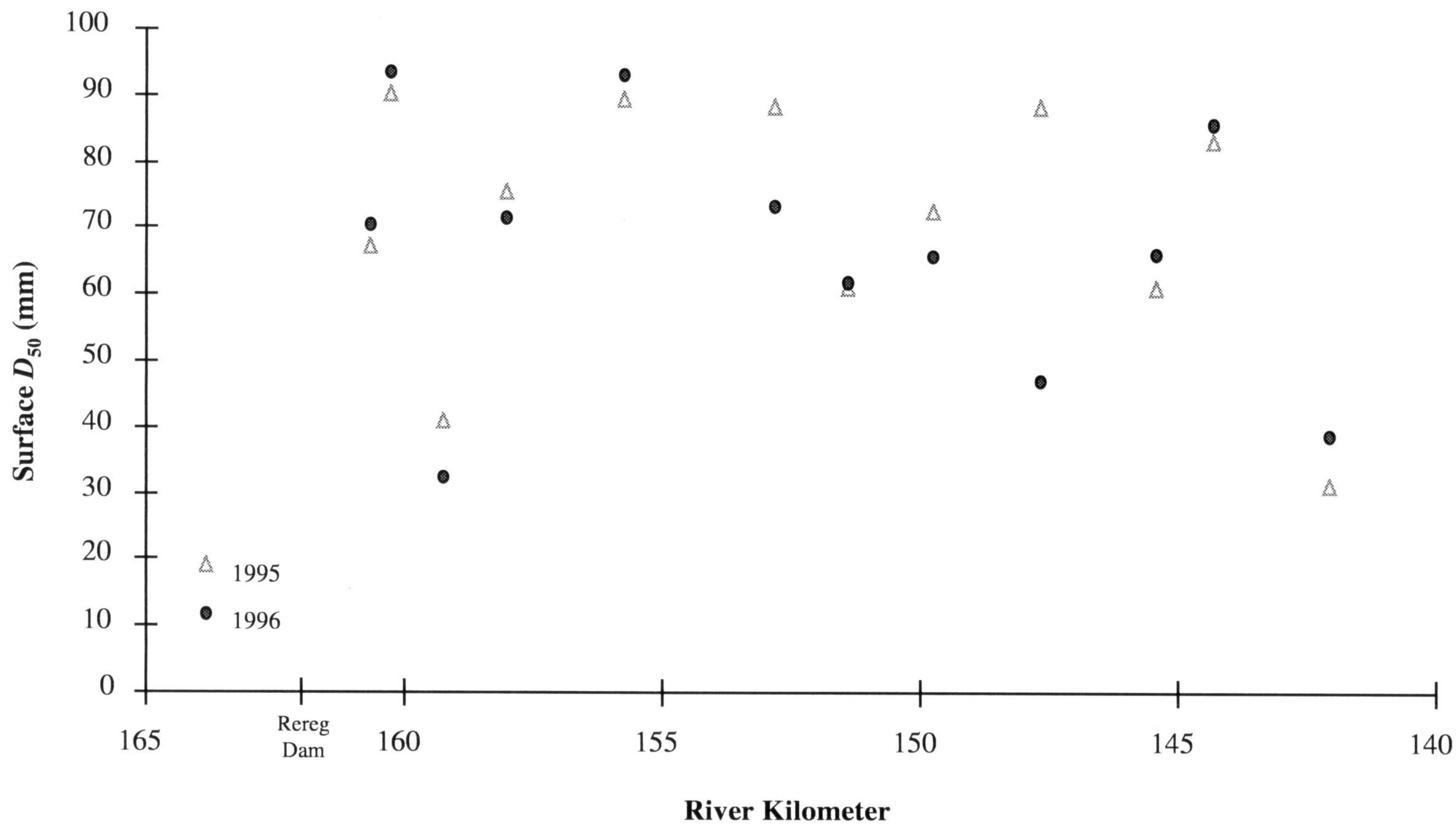

Figure 21. Surface D_{50} values for bar and island heads sampled in the primary study reach in 1995 and 1996.

In addition, the Trask sorting coefficient shows very little difference in surface particle sorting between sites (Figure 22). The coefficient generally ranged between 1.3 and 2.7, but reached 5.9 at the island at RK 142.1 (RM 88.3) in 1995. Better sorting within surface deposits was not observed close to the Project.

Spatial variations in grain size between sites were strongly influenced by abundance of *C. demersum*. The four lowest D_{50} values represent two sites [islands at RK 142.1 (RM 88.3) and RK 159.3 (RM 99.6), Figure 21] where macrophyte levels were especially high for both years. D_{50} was strongly associated with the amount of *C. demersum* (p-value = 0.006; extra sum of squares F-test) in the primary study reach. In particular, high levels of *C. demersum* are strongly significant in lowering the median grain size (Table 8).

There was also little change in surface grain size as a whole between years at each site (Figure 23). Even after accounting for the effects of *C. demersum*, there was no statistical evidence for an overall change in surface D_{50} following the 1996 flood (Table 8).

Bed-subsurface Particle Size

The bed subsurface D_{50} in the primary study reach was finer than the surface and ranged from 5 mm to 50 mm (average 20 mm, Figure 24). There was also no clear trend in subsurface median grain size with distance from the Project (Figure 24). The final statistical model showed no evidence for a longitudinal trend in subsurface D_{50} values when year and the abundance of macrophytes were accounted for in the primary study reach (Table 8).

The final statistical model showed no evidence for a temporal change in subsurface D_{50} in the primary study reach (Table 8). The data point representing the bar at RK 144.3 (RM 90.2) was influential in the regression, however. When removed from the analysis for comparison, the overall decrease in subsurface D_{50} between years was

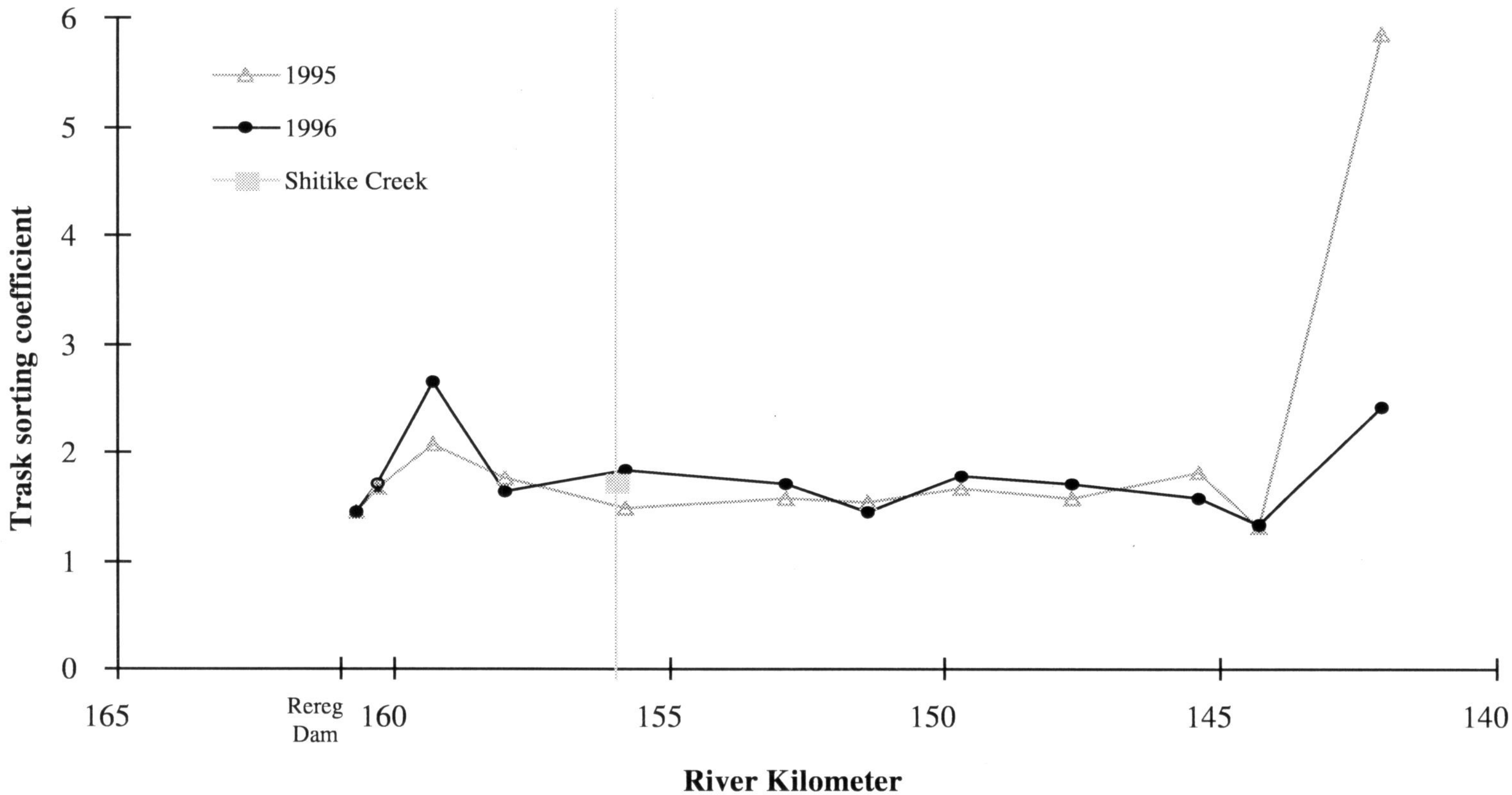

Figure 22. Trask sorting coefficients for surface bed material at bar and island heads sampled in the primary study reach. Higher coefficients indicate poorer sorting. The large square represents the value of sorting coefficient for Shitike Creek at its confluence.

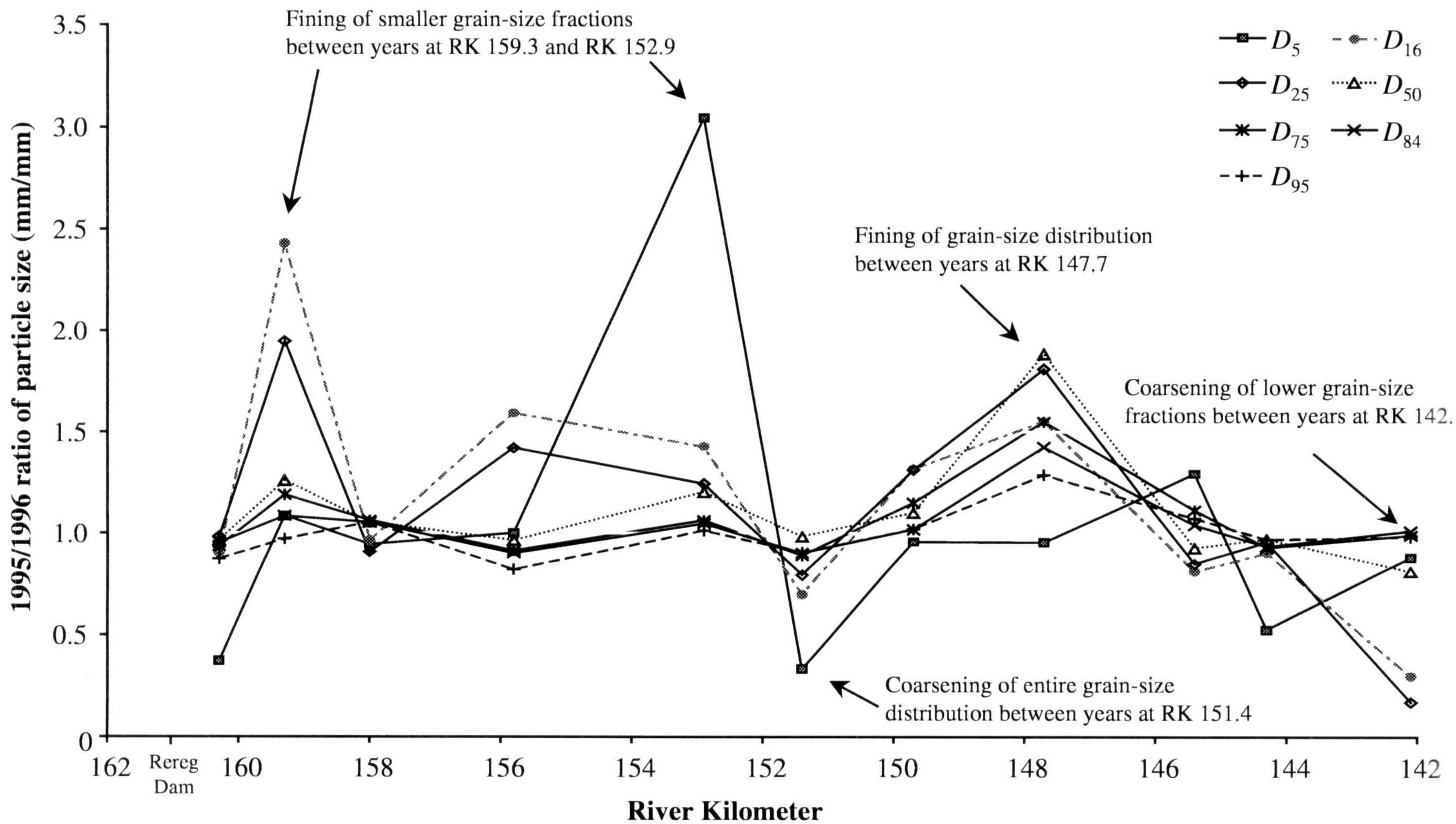

Figure 23. Surface grain-size distribution ratios $D_{x(1995)}/D_{x(1996)}$ for bar and island heads in the primary study reach.

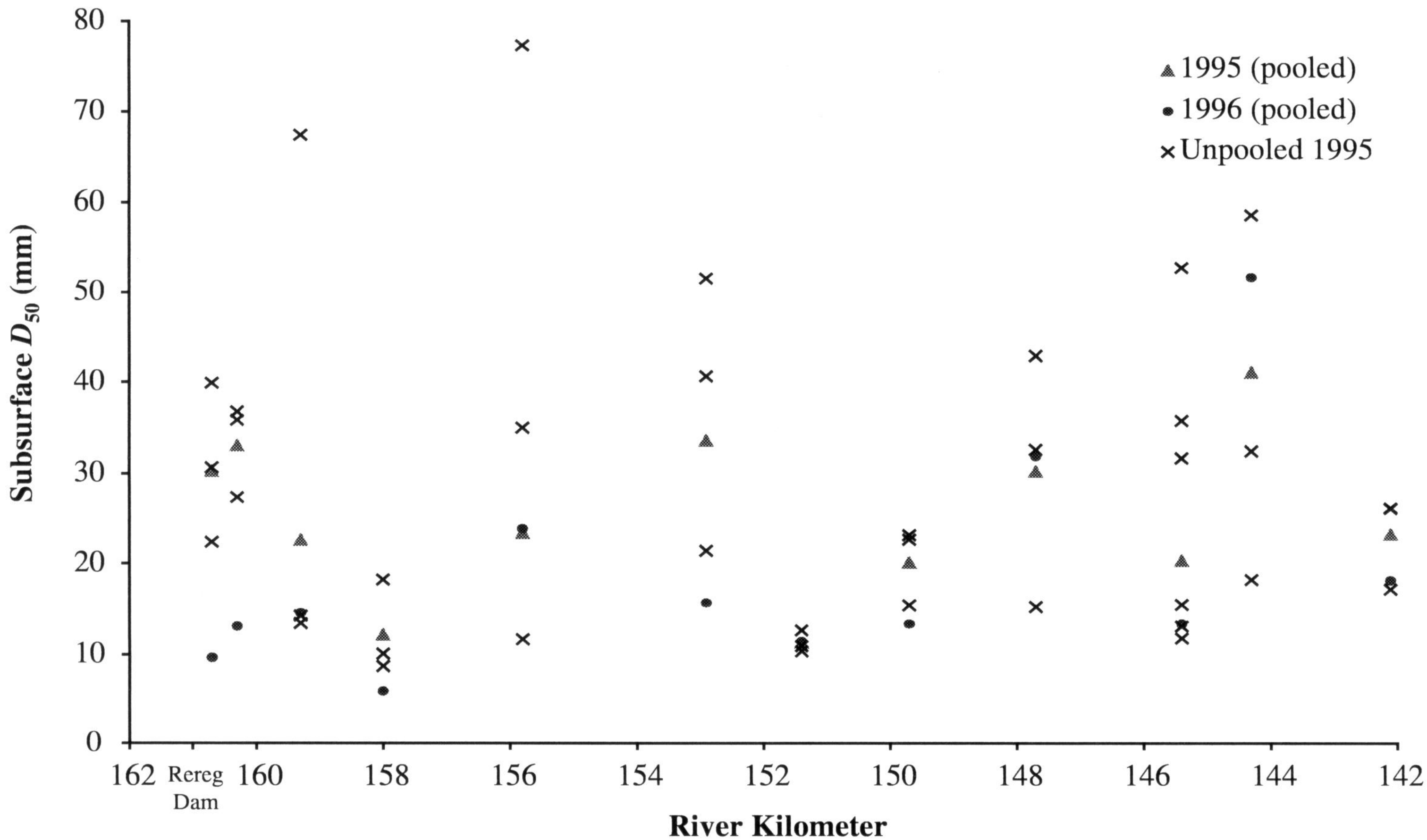

Figure 24. Subsurface D_{50} values for bar and island heads in the primary study reach. Pooled samples underwent statistical analysis. D_{50} values for unpooled 1995 samples (volumetrically comparable to 1996 samples) are shown for comparison.

significant (2-sided p-value = 0.012), suggesting that the subsurface may have fined somewhat in response to fine sediment inputs during the flood of February 1996.

Armoring

Armoring ratios ranged from 1.3 to 11.9 (average 4.0) and generally declined with distance from the Project (Figure 25). Multiple linear regression showed that the longitudinal trend in armoring was statistically significant (Table 8). The mean armoring ratio is estimated to be 0.16 less with each kilometer from the Project (95% confidence interval between 0.013 and 0.30). Although not statistically significant at $p = 0.05$, the results indicated that there may also have been an increase in armoring following the February 1996 flood (Table 8). Three of the four sites closest to the Project show the largest increases in armoring between years (Figure 25).

Data points representing the bar at RK 160.3 (RM 99.6) and the island at RK 158.0 (RM 98.1) in 1996 are influential in this regression. When the two points are removed separately or in combination (constituting three different scenarios of outlier removal), the decrease in armoring with distance from the Project remains significant at the 0.05 level. In two of these scenarios, there is strong evidence for an increase in armoring between 1995 and 1996. However, when only the point from the island at RK 158.0, RM 98.1) in 1996 is removed, the temporal change is not significant at even the 0.1 level. Thus, the model is greatly influenced by these points and the increase in armoring with time cannot be shown conclusively.

PARTICLE-SIZE TRENDS OVER THE ENTIRE STUDY AREA

Multiple linear regression models constructed for the entire study area showed no evidence for a longitudinal trend in surface D_{50}, subsurface D_{50}, or armoring (Table 8, Figure 26). In addition, the Trask sorting coefficient shows very little difference in

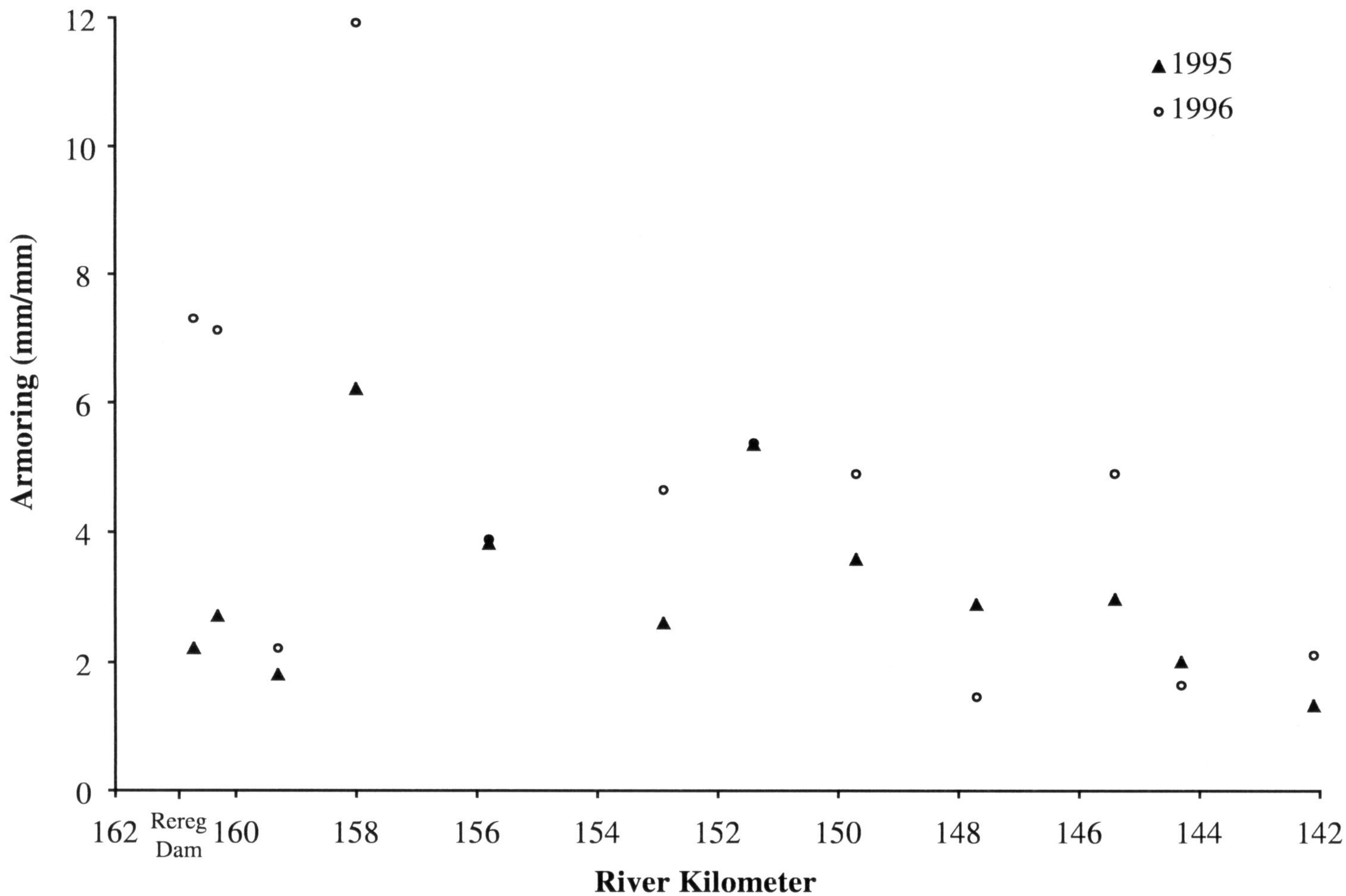

Figure 25. Armoring ratios for bar and island heads in the primary study reach for 1995 and 1996.

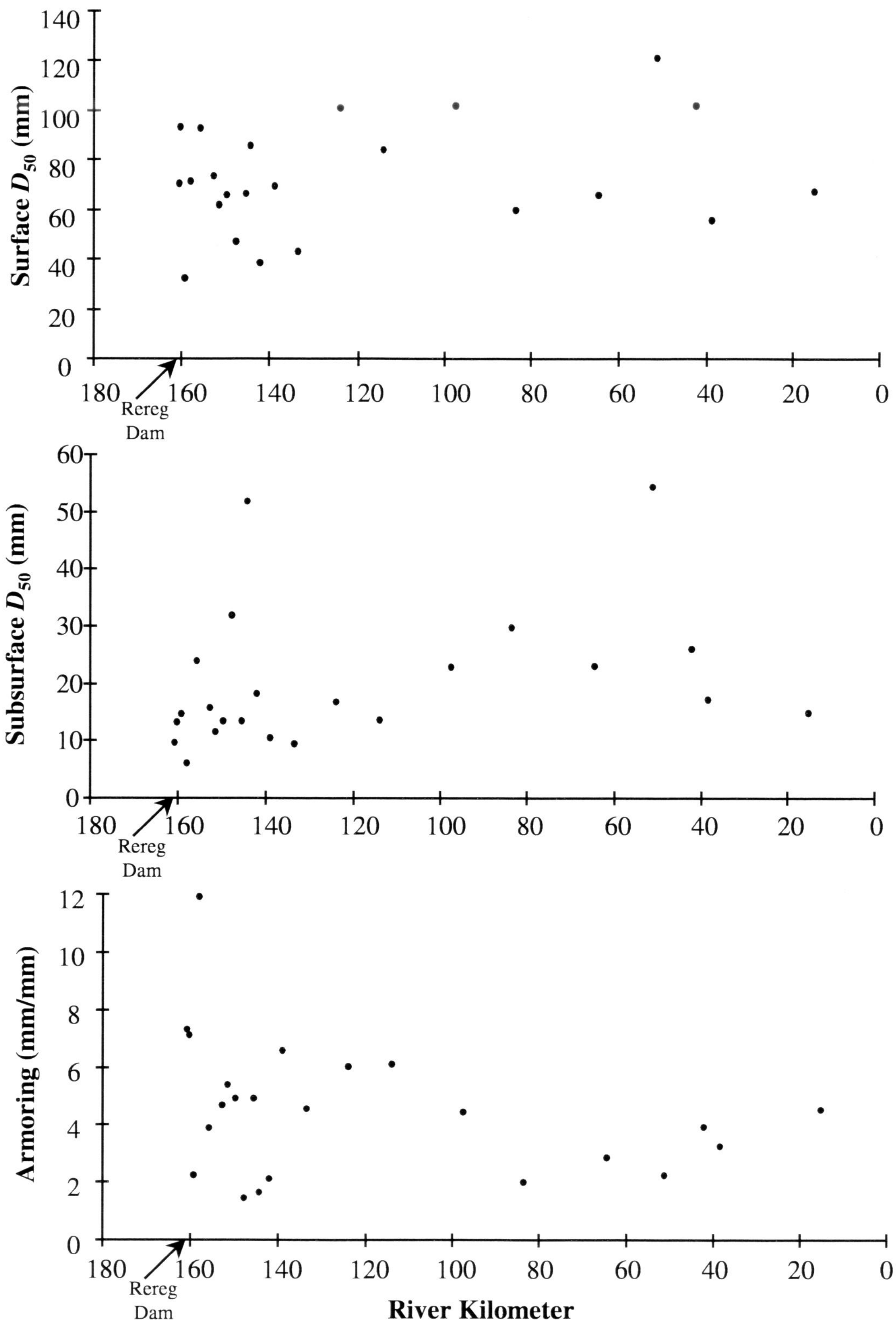

Figure 26. Surface D_{50} values, subsurface D_{50} values, and armoring ratios for bar and island heads along the entire study area in 1996.

surface particle-sorting between sites at this largest spatial scale (Figure 27). Thus, bed coarsening or greater sorting was not observed in the primary study reach relative to the lowermost river.

TRIBUTARY PARTICLE SIZES

Tributary D_{50} values were generally finer than mainstem values. Of the sampled tributaries, only the Warm Springs River had a coarser grain-size distribution than the mainstem (Figure 28). In general, grain-size distributions from tributaries exhibited similar sorting compared with the mainstem surface bed material (Figure 28).

Most grain-size distributions from the fourteen sampled tributaries were remarkably similar to each other (Figure 28), with D_{50} values averaging 50 mm (range 10–105 mm) and Trask sorting coefficients of about 2.4 (range 1.4–11.6). However, the two largest tributaries, the Warm Springs and White Rivers, did have particularly distinct grain-size distributions. The White River showed a strongly bimodal distribution, with a high proportion of material less than 2 mm in diameter (Figure 28), presumably sandy material derived from reworked lahar and glacial deposits from Mt. Hood provenance. However, there was no apparent trough in D_{50} values in the mainstem Deschutes directly downstream of the White River confluence (Figure 29). The Warm Springs River had a relatively coarse grain-size distribution (Figure 28). Despite this, mainstem D_{50} values registered no coarsening downstream of the Warm Springs River confluence (Figure 29). Thus, even where tributaries input the most distinctive bed material to the mainstem, distinctive shifts in the mainstem bed material size did not occur.

For example, grain-size distributions from Shitike Creek (RK 156.1, RM 97.0) and the nearby downstream sample site at the island at RK 155.8 (RM 96.8) were compared to assess the linkage of tributary and mainstem bed-material size. The overall surface grain-size distribution measured in 1995 just below Shitike Creek at the island at RK 155.8 was distinct from the grain-size distributions of Shitike Creek (Figure 30). Following the 1996 flood, mainstem gravels at the island at RK 155.8 showed a relative

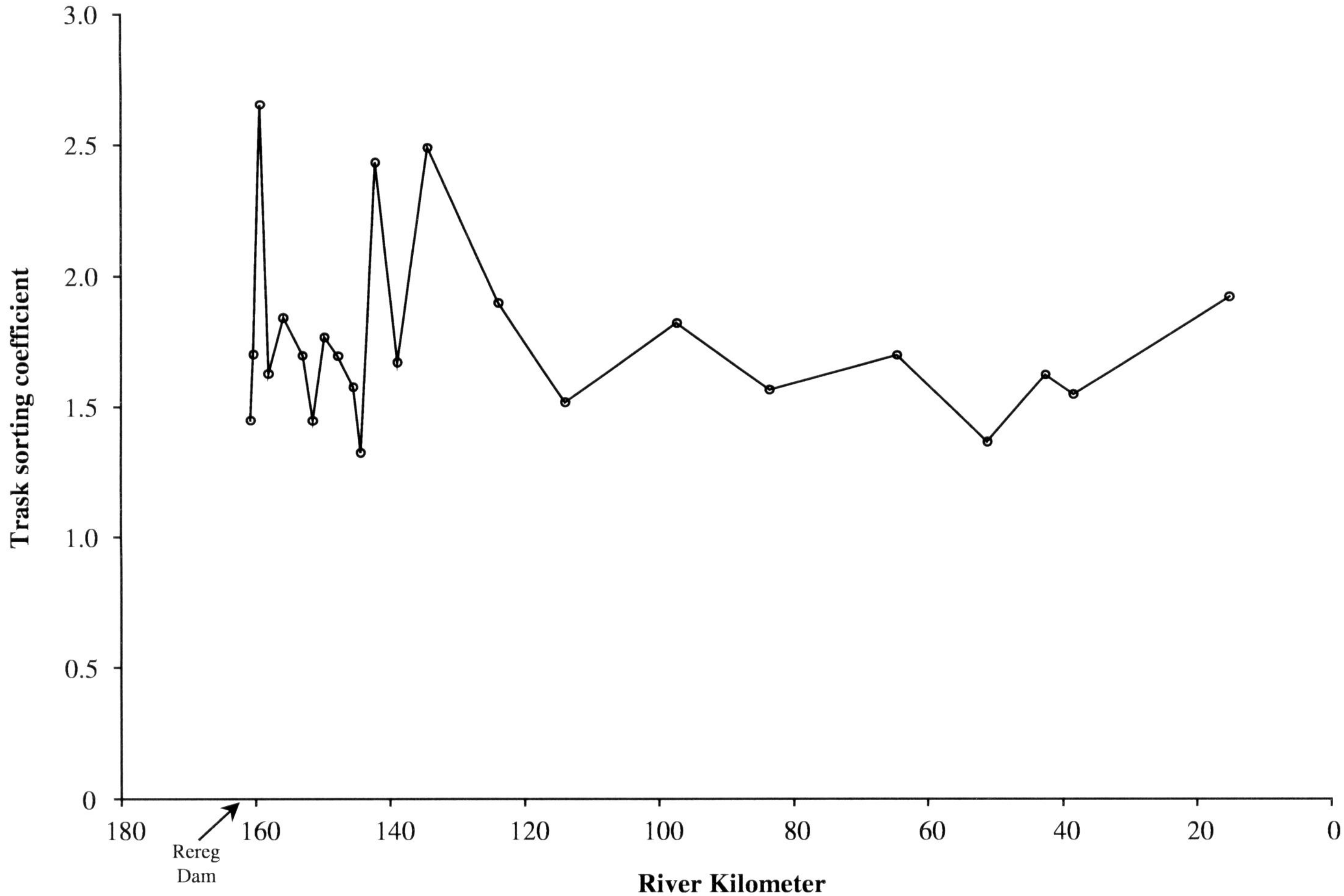

Figure 27. Trask sorting coefficients for surface bed material at bar and island heads in 1996 along the entire study area. Higher coefficients indicate poorer sorting.

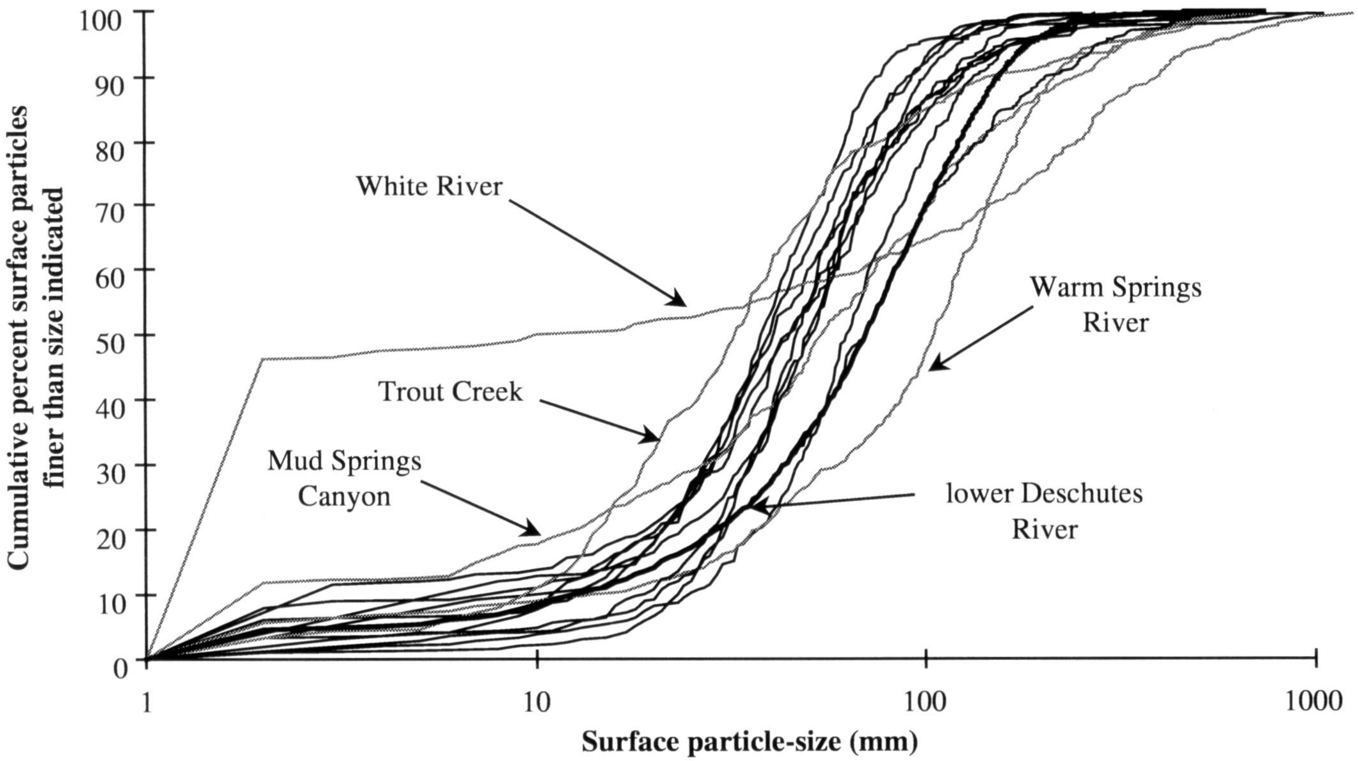

Figure 28. Surface grain-size distributions of 14 sampled tributaries of the lower Deschutes River. Dashed curves indicate the most distinctive grain-size distributions. Surface grain-size distribution of the mainstem Deschutes (based on pooling of all 1996 samples from bar and island heads) shown for comparison.

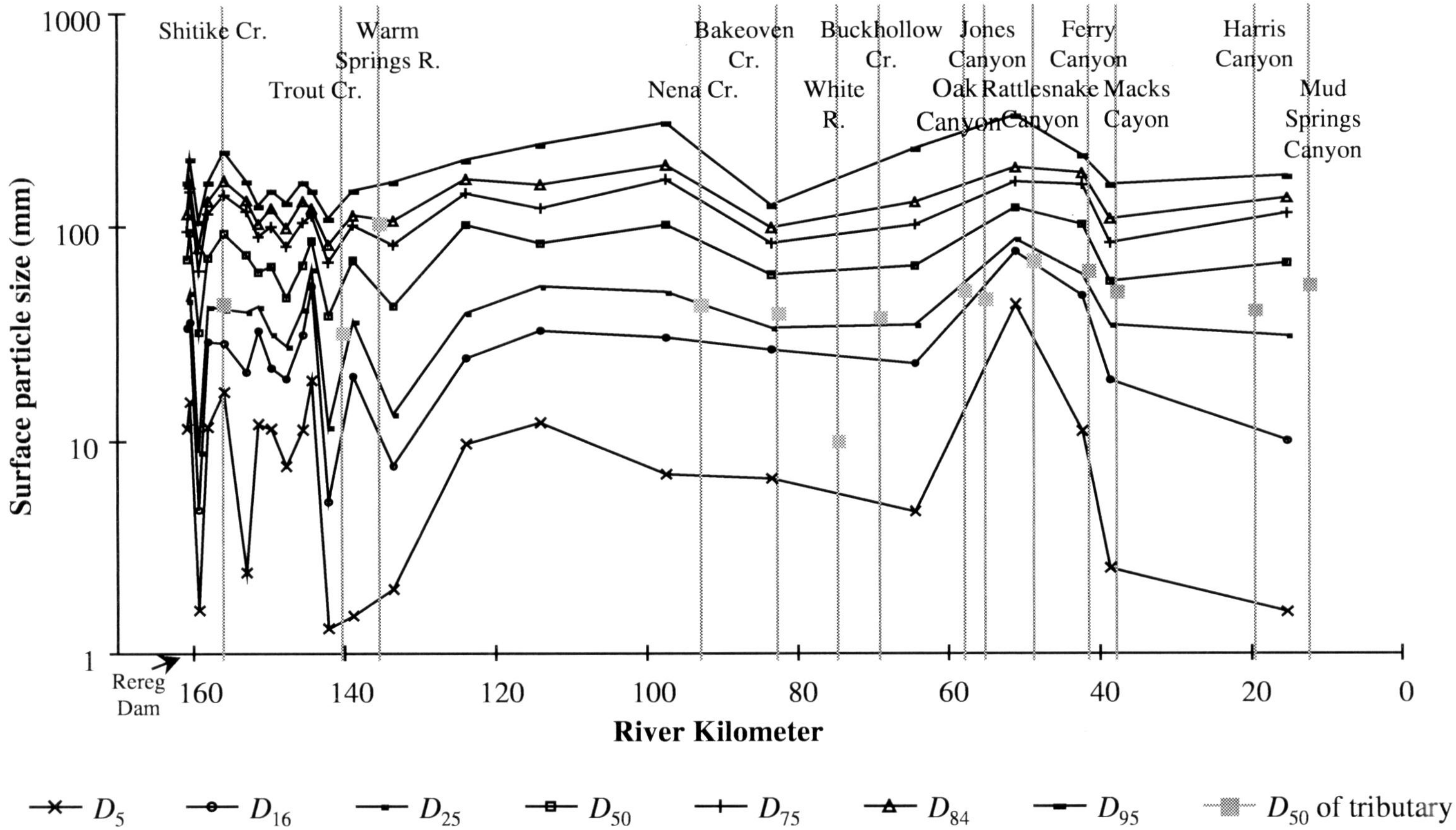

Figure 29. Surface grain-size percentiles of sample sites over the entire study area in 1996 relative to tributary confluences. Location of tributaries indicated by vertical lines. D_{50} values of tributaries shown by large squares.

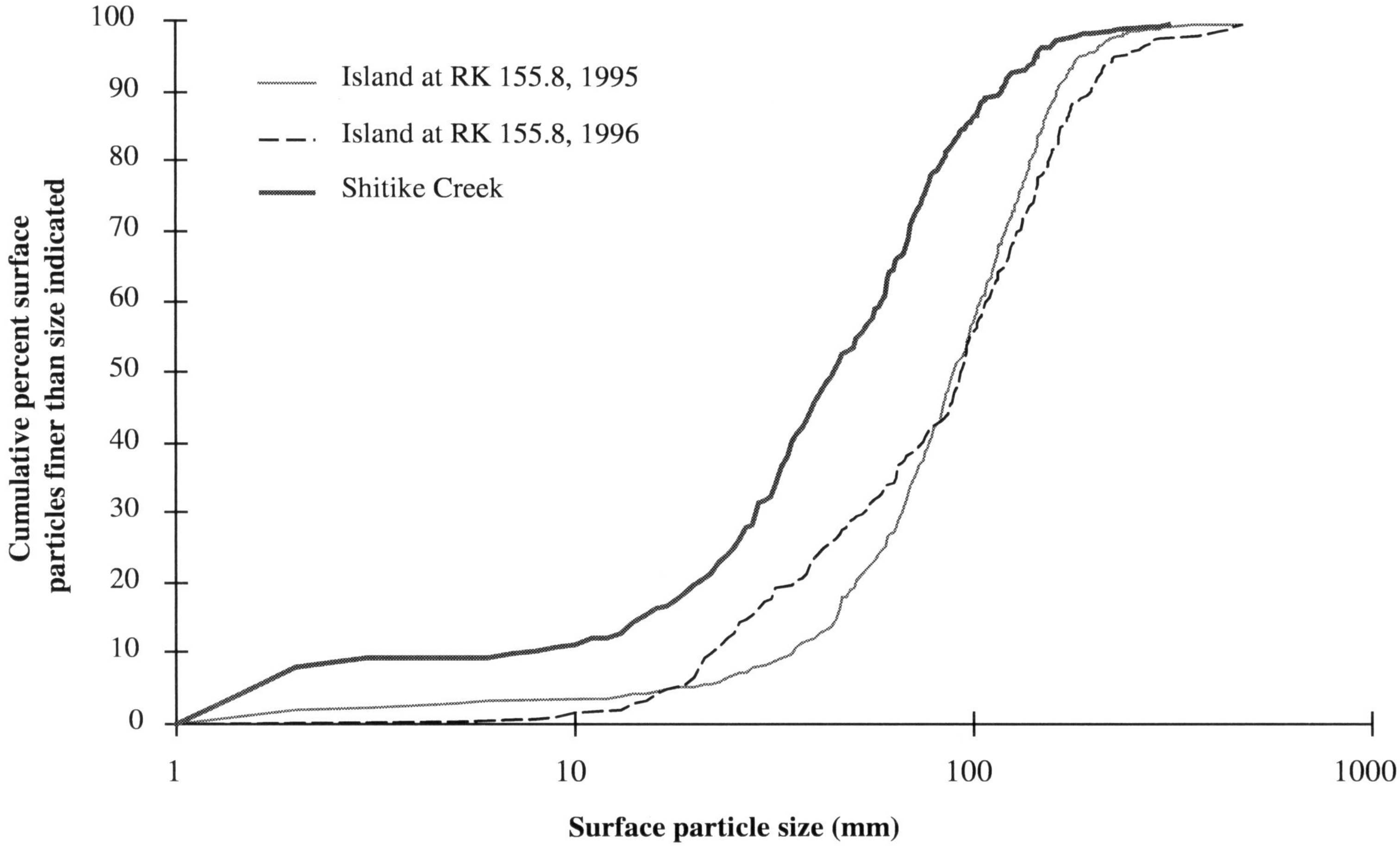

Figure 30. Surface grain-size distributions from Shitike Creek and the island head at RK 155.8.

increase in the predominance of particles in the 5 to 30 mm range, which corresponded with mid-range grain sizes for Shitike Creek (Figure 30). Sorting coefficients for the island at RK 155.8 were more similar to those of Shitike Creek (1.76) following the flood (1.48 in 1995 compared with 1.84 in 1996). These factors suggested that inputs of bed materials from Shitike Creek may have caused a local shift in mainstem grain-size distributions. However, the mixing of bed material from Shitike Creek with that being transported within the mainstem channel dampened the sedimentologic signal of the tributary in the gravels of island at RK 155.8. Thus, even where sediment had most likely been contributed to the mainstem from a tributary, the signal of the tributary grain-size distribution in the mainstem gravels was substantially dampened just a short distance downstream.

DISCUSSION

These analyses of bedload transport, historical channel changes, and longitudinal patterns of grain size all consistently characterize the Deschutes as an unusually stable alluvial river. That stability is reflected in the infrequency of bedload transport events, both prior to and following dam construction, the paucity of features exhibiting morphologic change on decadal time scales, the uniformity of grain size along the channel, and the absence of pronounced morphologic or textural change following the record flood in February 1996. Here we consider some aspects of that stability in detail and discuss its causes and implications for assessing the effects of the Project.

Evidence for Channel Stability

FREQUENCY AND MAGNITUDE OF BEDLOAD TRANSPORT

Modeled estimates of critical discharge were generally consistent across sites (Table 4), giving some confidence in results of the hydraulic model. General mobility of the channel bed was predicted to begin at discharges of around 340 m^3/s (12,010 ft^3/s) or, incorporating the results of the sensitivity analysis, between 270 and 460 m^3/s (9,530 and 16,240 ft^3/s) for primary study reach sites. These model results were evaluated against a detailed analysis of long-term cross-section change in relation to discharge. The historical cross-section analysis (1957–present) showed general mobility of the channel bed beginning around 250 m^3/s (8,830 ft^3/s), near the lower end of the predicted range (Figure 18). Furthermore, the dates over which bedload transport was predicted to occur (post-1957) coincide with the lowest measured elevations of the channel thalweg at the USGS measurement cross section (Figure 15), indicating that channel scour did occur during these events, as predicted.

Bedload transport at sites in the primary study reach was predicted to occur less than 1% of the time over the period of record for the critical discharge of 340 m^3/s (12,010 ft^3/s). The combined effects of reasonable uncertainties of parameters used in the hydraulic modeling did not substantially alter these results; predicted transport frequency remained at less than 1% for critical discharges of 270 m^3/s and 460 m^3/s (9,530 and 16,240 ft^3/s). This frequency is much lower than that in other gravel-bedded rivers where studies have shown that bed material is typically moved about 5–10% of the time, or several times per year, at flows close to bankfull (Andrews and Nankervis, 1995). The extremely low frequency of bedload transport in the Deschutes River appears to result from the very uniform flow regime and absence of high flows, coupled with a coarse gravel-to-cobble substrate with a relatively high entrainment threshold.

The volume of bed material moved was also predicted to be low, generally between 2,000 and 3,000 m^3/year (2,620 and 3,920 yd^3; Figure 13). In comparison, the Kemano River in British Columbia, Canada, a river with similar discharges and particle size to the Deschutes, has an estimated mean annual bedload transport rate of about 50,000 m^3/year (65,400 yd^3; Church, 1995). During water year 1996, the most active year on record, the Deschutes was predicted to have moved only around 14,900 m^3 (19,490 yd^3) of bed material.

To get a better sense of what these number mean in terms of channel morphological change, a rough estimate can be made of the quantity of channel-bed degradation required to supply the approximately 15,000 m^3 of material predicted to have been moved through Site B during the February 1996 flood (Table 7). There are no upstream or tributary sources of sediment in the 3.4 km reach between the Reregulating Dam and Site B, so all material predicted to have been transported by this event would have to be derived from within the channel. Determining the downstream distance over which bed material moves during a transport event is difficult (Hassan and Church, 1992) so we constrain the problem with two estimates of transport distance. In the first, we assume that bedload was derived from the entire reach between the Reregulating Dam and Site B. With an average river width for this reach assumed to be 75 m (250 ft) (the river is much wider upstream at several locations than at Site B) and channel-bed porosity estimated at 25%[1], the channel bed would undergo approximately 0.074 m (0.24 ft) of net degradation over the reach. This represents approximately $1*D_{50}$, indicating that, on average, only one "layer" of bed material need be stripped away from the entire cross section to supply the predicted bedload. The second estimate considers a more local source area for the bedload of five to ten channel widths directly upstream of Site B; this translates to300 to 600 m (980 to 1,970 ft) because the channel is 60 m (200 ft) wide at Site B. Again, taking into account porosity, the channel bed would undergo approximately 0.5 to 1 m (1.6 to 3.2 ft) of net degradation over the reach. This represents about 7 to $14*D_{50}$ or, in terms of averages, about 7 to 14 "layers" of bed material need be stripped away to supply the predicted bedload. This range encompasses the maximum degradation of 0.8 m observed at the USGS measurement cross section near Madras for

[1] Based on a value of 28% for uniform, coarse gravel (Todd, 1980). The reduction in porosity was made to take into account infilling of interstices in the coarse gravel by sand and finer gravel.

the February 1996 event (Figure 18e). For this reason, we believe this second scenario represents a more reasonable estimate of bedload travel distance.

This rough estimate assumes that transport and thus degradation would occur equally over the entire channel-bed surface in the reach supplying sediment. In reality, scour and transport may be locally concentrated, often in the deeper parts of the channel, and there may be little or no transport, or even deposition, elsewhere. In addition, this calculation does not take into account sediment derived from the channel banks or island perimeters. Field observations following the flood of February 1996 suggested this volume was small, however.

RATES OF SEDIMENT SUPPLY

Low predicted frequency and magnitude of bedload transport and no evidence for channel aggradation implies that the lower Deschutes River has historically been a sediment-poor system both prior to and following Project construction. This inference is supported by a calculation of sediment discharge rates into Lake Billy Chinook. Results from the sedimentation survey of this reservoir indicated that about 1,248,000 m^3 (1,633, 000 yd^3) of sediment had been captured by Round Butte Dam between 1964 and 1998 (Scott Lewis, PGE, written communication, 1998). This volume represents the total sediment input of all particle sizes from the Crooked and Deschutes Rivers to the mainstem lower Deschutes over 34 years. The Metolius River fan was smaller than the detection limits of the survey. Most of the sediment was fine-grained (sand and finer) with only minor gravel at fan apexes [Scott Lewis, oral communication, 1998, as cited in O'Connor et al. (in prep.)]. In contrast, about 27,300 m^3 (358,000 yd^3) of bedload was predicted to have been moved between 1964 and 1996. This amounts to approximately 2% of the total volume of the sediment fans in the reservoir, most of which would probably have been transported as suspended sediment prior to the Project.

The estimated 1,248,000 m^3 (1,633, 000 yd^3) of sediment captured behind Round Butte Dam in the 34 years since dam closure equals a sediment discharge rate of about

101,000 metric tons/yr (111,000 standard tons/yr) using an average sediment density of 2,740 kg/m^3 (5.32 slugs/ft^3; Fassnacht, 1998). For the 19,410 km^2 (7,490 mi.^{2}; Hubbard et al., 1997) basin above Round Butte Dam, this represents a unit sediment delivery of 5 metric tons/km^2/yr. The actual sediment discharge rate in the lower Deschutes River is certainly higher because the entire upstream basin does not contribute water and sediment to Round Butte Dam and because upstream dams on the Crooked and upper Deschutes Rivers trap sediment (O'Connor et al., in prep.). If we exclude the 1,300 km^2 (500 mi^2) Millican basin, which is not hydrologically integrated, and subtract drainage areas above upstream dams, this corresponds to an effective unit sediment supply rate of about 11 metric tons/km^2/yr (30 standard tons/mi^2/yr) for the 9,470 km^2 [3,650 mi^2; O'Connor et al. (in prep.)] drainage basin above Round Butte Dam that directly contributes sediment. For comparison, suspended sediment discharges alone in other rivers in North America are much higher than the *total* sediment discharge of the Deschutes River (Table 9).

These recent sediment surveys provide additional support of model predictions of low frequency and magnitude of bedload transport. If sediment supply is low and model predictions were incorrect (i.e., frequency and magnitude of transport were high), we would expect high rates of channel degradation and/or high armoring ratios directly downstream of the Project. Degradation rates just below the Project are about 2.2 mm/year both before *and* after dam closure (Figure 15). This rate of degradation is very low in comparison to those below dams from selected rivers around the United States (Table 9). Results from the channel-bed textural analysis also did not show any trends in armoring downstream of the Project (Figure 26).

EFFECTS OF A LARGE FLOOD

The flood of February 1996, with the highest peak discharge in the 72-year gaged record, was predicted to have produced transport rates much larger than those from any other recorded event. Subsequent field investigations in April, August, and September 1996, indicated that bedload transport *did* occur during the flood. This field evidence

Table 9. Suspended sediment discharges and channel-bed degradation rates below dams for selected rivers in North America.

River	Suspended sediment discharges of some major rivers in North America [a] Sediment discharges, metric tons/km^2/yr (std tons/mi^2/yr)
Columbia	13 (38)
Fraser (Canada)	90 (260)
Colorado (Mexico)	210 (600)
Copper	1,170 (3,330)
Eel	2,000 (5,710)
Deschutes	*total* sediment = 11 (30)

River	Channel-bed degradation below selected US dams [b] Average degradation per year, mm/yr (in/yr)
Arkansas	13 (0.53)
N. Platte	20 (0.79)
Missouri	28 (1.1)
Red	32 (1.2)
S. Canadian	120 (4.5)
Deschutes	2.2 (0.087)

[a] Milliman and Meade (1983)
[b] Leopold et al. (1964)

included new gravel deposits, bedload newly deposited on vegetated islands and floodplains, and the absence of former small islands in the lower river. Although the flood resulted in localized bedload transport and disturbance of vegetation, it did not substantially reorganize channel bars and other surfaces; its most visible effect was the uprooting and breaking of large riparian vegetation.

The occurrence of this large flood during the study period allowed us to examine whether the limited geomorphic change in the Deschutes was related to erosion thresholds not being exceeded since Project construction. Coarse-bedded rivers elsewhere have been shown to experience little or no degradation following impoundment because of the general infrequency of mobilizing flows (Petts, 1979; Church, 1995). Petts (1979) hypothesized that in such "non-mobile channels" a rare large flood, crossing some intrinsic threshold, may be required before adjustments will begin. Once that geomorphic threshold has been exceeded, a rapid phase of channel adjustment might ensue, redistributing channel and floodplain sediments. Critical discharge calculations predicted initiation of bedload transport at a discharge of about 340 m^3/s (12,010 ft^3/s) as measured at the Madras gage. The flood of 1996 had a maximum mean daily flow at the Madras gage of about 510 m^3/s (18,010 ft^3/s), a value exceeding the predicted critical discharge. Despite its 100-year return interval, the 1996 flood did not appear to be this kind of resetting flood, as it had little effect on the existing bars and islands. Apparently, larger and more infrequent events are responsible for shaping the primary channel features and morphology.

Channel Features, Vegetation Patterns, and Historical Channel Changes

Channel morphological features and vegetation patterns along the lower Deschutes River support the interpretation of general channel stability. Huntington (1985) identified chinook spawning dunes, biogenic features created by overlapping spawning redds, approximately 2 kilometers (~1.5 mi.) below the Project. Visual inspection indicates that these chinook spawning dunes still exist in the same location and are of comparable size and spacing, despite being abandoned by fish (D. Ratliff, PGE, oral communication, 1995). This suggests that the dunes have not moved in at least 15 years. The river contains very few meander bends and point bars — common features in active alluvial channels. Many of the existing meanders are deeply incised into the basalt flows that comprise the steep canyon walls. Tributary fans have built out into the river and constrained the channel. These fans appear to be old, judging from the age of their vegetation and the heavily weathered and desert-varnished boulders, and were not substantially modified by the February 1996 flood.

Channel stability is also implied by the scarcity of unvegetated deposits in the river. Islands, tributary fans, and floodplains are covered with grasses, sagebrush (*Artemesia spp.*), willows (*Salix spp.*), sedges, and alders (*Alnus rhombiofolia*). Alders on the order of 20+ years old can be found lining long stretches of channel banks and along the edges of many islands. These would be unlikely features if the Deschutes were an active alluvial river in which gravel and sand deposits were often reworked. Aerial photographs also illustrate stable channel boundaries and island locations. Changes that do occur in island and bar morphology tend to be associated with tributary confluences. One of the few islands that are not heavily vegetated is the first island downstream of the Shitike Creek confluence. New gravel was deposited on top and along the sides of this island by the February 1996 flood. Most of the vegetation on the island remained relatively undisturbed.

Analyses of historical cross sections and aerial photographs also suggest general channel stability. USGS cross section measurements for the Madras gage showed extremely limited channel bed degradation over the period of record (Figures 15 and 16). Lateral movement of the channel at the cross section was minimal (Figures 17 and 18). The majority of channel scour noted during high flow events was refilled in the weeks to months following the event, indicating quasi-equilibrium conditions (Figure 18).

Project Effects on the Geomorphology of the Lower Deschutes River

These results provide strong evidence for the intrinsic stability of the Deschutes River system. Here we evaluate the direct effects of the Project on the lower Deschutes River, within this context of a stable channel environment.

STREAMFLOW AND BEDLOAD TRANSPORT

The low frequency of discharges surpassing the predicted threshold for bedload transport provides a very small data set with which to evaluate the downstream effects of the Project on bedload transport frequency and magnitude. Only four transport events were predicted to have occurred over the 30+ years since Round Butte Dam was closed. A single high flow event can greatly affect the calculated frequency and magnitude of transport for a given time period (pre- or post-Project). Despite this, the results did not indicate any major natural or anthropogenic changes in either discharge (Figures 11 and 12) or the frequency and magnitude of bedload transport (Figure 13) in the primary study reach. Examination of individual events following Project construction did, however, suggest more subtle changes occurred in both discharge and bedload transport at this scale (Figure 14, Table 6). Low frequency of bedload transport, low sediment supply, and minimal Project-induced effects on streamflow suggest only limited channel degradation or morphological change should to be expected in the primary study reach following impoundment. The results of the historical cross-section and aerial photograph analyses bear this out.

CHANNEL-BED TEXTURE

The results indicate that there is no clear longitudinal trend in the surface and subsurface bed-material size distribution in either the primary study reach or the entire study area. Data points obtained from the same site for different years are generally similar to each other, except for local changes in D_{50} values at some sites in the primary study reach. For this reason, the finding of no longitudinal pattern in surface D_{50} values cannot be attributed to sampling error. Low adjusted R^2 values for all statistical models (0.02 to 0.23) suggest that factors other than downstream distance and year are much more important in determining bed material properties.

The marked uniformity of grain sizes and armoring over the extended river course partially reflects the lack of major changes in channel slope, the limited range of grain sizes introduced as bedload by tributaries, and minor hillslope inputs from bedrock canyon walls. No clear differences in grain size were noted upstream and downstream of major tributaries, where changes in longitudinal grain-size distribution patterns due to partially replenished sediment supply might be expected (Figure 29). Several factors account for this longitudinal uniformity: the similarity of bed-material size ranges between the main channel and tributaries; high transport efficiency of fine sediment by the mainstem; and opportunities for storage of tributary sediment in alluvial fans at tributary junctions. For example, much of the material transported by the White River during high flow events may be suspended sediment (U.S. Department of Energy, 1985), which is easily transported by the Deschutes out of the basin, so that the bed of the Deschutes is not noticeably finer downstream of the White River. Fine sediments not transported out of the drainage during high flow events are typically deposited as beaches and marginal deposits during flow recession. Coarser bed materials carried by the Warm Springs River are typically deposited within the extensive, coarse fan complex at its confluence with the Deschutes. Some inputs of gravel from Shitike Creek appear to be deposited locally within the mainstem Deschutes, inducing morphologic, but only minor textural, shifts in the mainstem.

High armoring ratios near the Project (up to 11.9 at RK 158.0, RM 98.1) and after the 1996 flood in the primary study reach appear to have resulted from subsurface fining, as the surface layer did not change significantly between years. This apparent increase in armoring via subsurface fining is contrary to most models of armor development (i.e., Parker et al., 1982, Dietrich et al., 1989). If sediment supply below the Project was substantially reduced, one would expect selective erosion to cause downstream winnowing of bed material. As our conceptual model (Figure 3) suggests, this would cause the surface grain size to coarsen with time near the dam and for the coarsening front to prograde downstream, particularly during high flow events. Such changes were not observed. Erosion of channel banks and islands by floodwaters may have introduced fine material into the bedload, although no apparent or adequate source of fine sediment exists in this reach. Fine sediment from sources upstream of Pelton Dam (i.e. Seekseequa Creek; Figure 1) may have contributed fine material to downstream sample sites through turbid water releases from the Project. The 1996 flood caused several large headcuts and tremendous erosion and sediment transport out of Seekseequa Creek into Lake Simtustus (Pelton Dam Reservoir) (C. Gannon, Confederated Tribes of the Warm Springs Reservation of Oregon, oral communication, 1999).

The most probable explanation for the fining of subsurface bed material between years, however, is a sampling artifact due to the reduction in volume of subsurface bed material sampled between years. Ferguson and Paola (1997) found that in small bulk samples, all percentiles, including the median, are underestimated, since it is less likely for large clasts to be included. While good precision in the sample mean can be achieved with sample sizes less than those suggested by DeVries (1970) and Church et al. (1987) for moderately sorted material, the phenomenon is especially serious for smaller samples of poorly sorted material like fluvial gravel (Ferguson and Paola, 1997). The relatively consistent lowering of all percentiles of subsurface material at sites in the primary study reach strongly suggests that the reduction of sample volume from an average of 60.9 kg to 20.3 kg may have caused the observed decrease in subsurface material size. To test this, multiple D_{50} estimates taken from unpooled bulk samples at a site in 1995 were compared to samples taken in 1996, since they were equivalent volumetrically. If there is indeed bias resulting from the change in sample volumes between years, then the multiple D_{50} values estimated individually from each bulk sample from a site in 1995 should be less than the one D_{50} estimated from pooling of these same bulk samples. Although this test was inconclusive (Figure 21), most D_{50} values from samples taken in 1996 fall within the range of comparably-sized, unpooled 1995 D_{50} values, so there is no clear evidence for subsurface fining between years. For this reason, the three high armoring ratios measured near the Project may not be correlated with the Project itself. In support of this, when only the 1996 data are considered over the study area, (so that subsurface samples are of comparable volumes), neither surface D_{50} values, subsurface D_{50} values, or armoring ratios illustrate a longitudinal trend (Figure 26, Table 8).

Following the criteria of Church et al. (1987), the requisite size of a representative bulk sample of the subsurface material may be *estimated* by the largest particles in the surface population, as long as the surface constitutes the same deposit. Using the average surface D_{95} value of 150 mm for sites in the primary study reach, the proposed 0.1% of sample size for the largest clast would then require a sample weighing about 5,000 kg per site. Even using a relaxed criterion of 5% would still require 100 kg of bed material. The substantial labor involved in transporting this sediment from a wilderness river and laboratory time required to process such samples is daunting. A precise description of grain-size distributions of bulk samples remains a difficult problem in such studies of gravel-bedded rivers.

Geomorphic Implications of Channel Stability

Within the context of downstream response of the channel, there are at least two implications of a stable river on river regulation. A stable river might be able to withstand a relatively wide range of change in flows with little effect on channel morphology and bed texture because the channel bed, for the most part, remains immobile. This may represent the current situation, where most fluctuations in streamflow occur at discharges that are less than critical (Figure 14). Even very large flows are apparently unable to substantially rework the channel, perhaps because of the very low volume of sediment available for transport.

The second implication is that the imprint and consequences of whatever changes do occur in the channel may persist for a very long time. For example, if reservoir operations further reduced the already infrequent occurrence of flows near the threshold for bed material transport, textural changes such as increased compaction, cementation, or cohesion of bed materials could result, further reducing bed mobility. Here, not having a disturbance event can be a disturbance event itself (Junk et al., 1989). On the other hand, changes to the channel morphology induced by surpassing high geomorphic thresholds, such as appears to have occurred during rare and exceptionally large paleofloods, could persist for geologically long periods of time until the next large-scale disturbance event. Field evidence suggests that there have been mechanisms for generating floods much larger than anything recorded over the last 72 years (O'Connor et al., in prep.). Mechanisms include outburst floods from large landslide dams, debris flows, and glacially dammed lakes (O'Connor et al., in prep). The legacy of these floods persist in the major rapids and slope profile breaks at Whitehorse, Buckskin Mary, and Boxcar, all of which were only slightly modified by the 1996 flood (O'Connor et al., in prep).

Review of Conceptual Model

In this study, it was hypothesized that the historically low sediment supply and transport rates would limit textural and morphologic adjustments of the lower Deschutes River. Our results strongly support an inference of low sediment supply and bedload transport. They also confirm very limited textural and morphologic change (Figures 2 and 3). The minor hydrological changes noted in the flow record since regulation suggest little change in the frequency of bed-mobilizing flows, and the results of the historical cross-section analysis show no change in the trend of minor channel-bed degradation that preceded Project construction. In other words, both the ratio of post- to pre-Project frequency of mobilizing flows and the ratio of sediment supply following impoundment to that before impoundment may be close to 1. Thus, as proposed by the conceptual model (Figure 3), the Deschutes falls squarely in Type B, where morphologic and textural response downstream from the Project should, for the most part, be small. While it is possible that the morphological manifestations of a reduced sediment supply (i.e., degradation and coarsening of the channel bed) due to gravel being trapped behind the

Project have not had a chance to occur, the very modest change over the 30+ year history, which includes some major storms, argues against dramatic changes in the near future.

Other studies of large dammed river systems also tend to support this conceptual model (Figure 3). Among these rivers, however, the lower Deschutes River apparently represents an unusual case. Because dams on most rivers markedly impact either the frequency of competent flows or the sediment load, or both, morphologic and grain-size responses such as those in Types A, C, and D are well documented, while there are many fewer cases of Type B adjustments like the Deschutes.

For example, the Peace River in British Columbia and Alberta may represent end-member Type A in the conceptual model. Before impoundment, the majority of bed material in the Peace River entered below the current point of regulation. Since dam construction, peak flows have been dramatically decreased, but the supply of sediment has not been reduced except for that derived from the mainstem bed and banks upstream of the dam (Church, 1995). There has been no degradation (because flow is no longer competent to move the gravel and cobble bed), aggradation is apparent at tributary junctions, and fine sediments supplied from tributaries are being deposited along the channel perimeter (Church, 1995).

Type D is exemplified by the Snake River. Annual flood series below the Hells Canyon Complex show no significant change in the size or frequency of floods (Collier et al., 1996); however, the winnowing of finer bed material has led to bed degradation and the loss of 75% of the surface area of sand beaches in the 241-km reach between the dams and the Salmon River tributary (Grams, 1991, as cited in Collier et al., 1996).

Most commonly, dramatic reductions occur in both sediment supply and competent flows, leading to armoring, coarsening, and degradation of the channel bed in the reaches closest to dams, as in Type C. In this case, reduced flows are still able to entrain channel bed material (Williams and Wolman, 1984; Galay et al,. 1985). For example, in the first two months following closure of the dam at Cochiti on the Rio Grande River, most bed material less than 1 mm in diameter was eroded (Dewey et al., 1979). Three years later, increases in the median diameter of the surface bed material ranged between about 2 and 5 times pre-dam sizes and extended 19 km downstream

(Lagasse, 1994). Within seven years, this front of coarsened surface bed material extended another 13 km downstream with local increases in D_{50} exceeding a factor of 20.

Rivers such as the Colorado below Glen Canyon Dam also fit within the conceptual model but in a more complex manner, with multiple responses observed on the same river. In the case of the Colorado, sediment supply has been greatly reduced and the range of annual peak discharges has decreased, but the range of daily flows has increased (Schmidt and Graf, 1990). The particle size distribution on this river is bimodal, with a large supply of sand-sized material coming in from tributaries and the upstream river, although most of this is now trapped behind the dam, and a supply of cobbles and boulders coming from tributary debris flow fans. In the reach closest to the dam before any tributary inputs of sediment, the Colorado River's transport capacity exceeds the sediment supply despite large reductions in both. The result has been channel-bed degradation and armoring (Pemberton, 1976). Farther downstream, and despite tributary sediment inputs, the Colorado River continues to erode fine sand beaches and channel margins because the larger flows responsible for depositing sand channel margins no longer occur, while the frequency of smaller but still competent mean *daily* flows has increased (Schmidt and Graf, 1990). The large cobbles and boulders from tributaries can only be moved during large discharge events, so these deposits have become more stable post-dam (Kieffer, 1985). Although this array of observed channel responses is complex, it is consistent with the conceptual model (Figure 2; Fassnacht, 1998).

CONCLUSIONS

Independent analyses of hydraulics and bedload transport, historical streamflow, morphologic change, and channel-bed texture all paint a convincing picture that the Pelton Round Butte Hydroelectric Project appears to have done little to alter the Deschutes River's naturally low frequency and magnitude of bedload transport. In a system with low sediment supply, this has resulted in little apparent morphologic or textural response downstream of the Project. The river downstream of the Project appears to be astonishingly stable within its current flow regime and sediment supply, with the low rates of sediment transport keeping pace with the modest inputs of sediment. Overall, this study suggests that armoring, degradation, and morphologic change below dams may be limited where sediment transport rates and sediment supply are low.

Channel responses to dams are complex in time and space, and are typically studied on a case-by-case basis. While specific impacts following river impoundment have been described, there has been much less synthesis of how channels can be predicted to respond to changes in sediment supply and the frequency of bed-mobilizing flows. The conceptual model suggested here successfully predicts a range of responses to channel impoundment in a geomorphic context. Many studies of other rivers document armoring and degradation of the channel bed due to reduced sediment supply where flows are still competent to move a large portion of the bed material. In contrast, the Deschutes River represents a unique hydrologic and sedimentologic environment where sediment supply and transport may be limited within time scales defined by the historical flow record.

[Blank]

ACKNOWLEDGMENTS

The authors gratefully acknowledge the many people who aided in logistics, field work, and/or field data collection, including Don Ratliff (PGE); Chris Zimmerman (Oregon State University); Scott McCollister (PGE); Eric Schulz (PGE); PGE surveyors Bob Buckley, Jim Tejcka, Gary Reynolds, Larry McGinnis, and Jeff Danielson; Tom Herrett (USGS); Tony Sorano (USGS); and PGE support personnel. A special thanks to the Confederated Tribes of the Warm Springs Reservation of Oregon, Jan Luelling, the Deschutes Club, Buck Ho, and Kenny Buck Sr., who allowed access to the river via private property. Larry Chitwood (Deschutes National Forest) graciously offered use of field equipment as well as laboratory equipment for processing subsurface samples. This work benefited greatly from discussions with Jim O'Connor (USGS), Julia Jones (OSU), and Bob Beschta (OSU). Lisa Ganio and Barbara Marks assisted in the statistical data analysis. Diana Surgeon (North Unit Irrigation District), Larry Zakrajsek (U.S. Bureau of Reclamation), and Scott Lewis (PGE) provided historical information on dams in the Deschutes River basin. Roy Wellman (USGS) and Tom Herrett were of great help in processing ADCP data. Local offices of the Bureau of Land Management and the Oregon Department of Fish and Wildlife served as excellent resources for information and assisted with accessing some study sites.

This material is based upon work supported under a National Science Foundation Graduate Research Fellowship to Heidi Fassnacht, and by funding provided by Portland General Electric to both Heidi Fassnacht and Ellen McClure. Any opinions, findings, conclusions or recommendations expressed in this publication are those of the authors and do not necessarily reflect the views of the National Science Foundation or Portland General Electric.

[Blank]

GLOSSARY

alluvial — pertaining to or composed of alluvium, or deposited by a stream or running water*

alluvium — a general term for detrital deposits made by streams on river beds, flood plains, and alluvial fans; esp. a deposit of silt or silty clay laid down during time of flood. The term applies to stream deposits of recent time. It does not include subaqueous sediments of seas and lakes*

anthropogenic — caused or produced by humans#

armoring ratio — ratio of the median channel-bed surface particle diameter to the median channel-bed subsurface particle diameter, i.e., $D_{50\ surface}/D_{50\ subsurface}$

average annual active storage — average maximum volume of water used or stored per year for the years examined (here 1965–1998). Calculated by subtracting the minimum volume of water stored in a reservoir from the maximum volume stored in a reservoir each year and averaging this value over the years of interest

b-axis — intermediate axis of a particle, where the a, b, and c axes are the longest, intermediate, and shortest mutually perpendicular axes through a particle, respectively)&

basalt — a dark colored igneous rock, commonly extrusive, composed primarily of calcitic plagioclase and pyroxene minerals*

bed-mobilizing flows — streamflows that are able to entrain channel bed material

bed material — material of which the streambed is composed*

bedload — the part of a stream's load that is moved on or immediately above the streambed, such as the larger or heavier particles rolled along the bottom; the part of the load that is not continuously in suspension or solution*

benthic — pertaining to the benthos (those forms of marine life that are bottom-dwelling; certain fish associated with benthos may be included); also, said of that environment*

boulder — clast whose intermediate diameter, or b-axis, is 256 to 4,096 mm%

bulk sample — sample in which all particles within an area has been retained rather than randomly selected individual particles within that area

capacity — the ability of a current of water or wind to transport detritus, as measured by the quantity it can carry past a given point in a unit of time*

cementation — the process by which clastic sediments are converted into rock by precipitation of a mineral cement among the grains of the sediment*

Cenozoic — The latest of the four eras into which geologic time is divided (Cenozoic, Mesozoic, Paleozoic, Precambrian); it extends from the close of the Mesozoic Era about 65 million years ago, to the present.*

channel capacity — the maximum flow which a given channel is capable of transmitting without overtopping its banks*

channel morphology — channel shape

clast — an individual constituent, grain, or fragment of a detrital sediment or sedimentary rock, produced by the physical disintegration of a larger rock mass*

clear water release — water devoid, or almost devoid of sediment due to the sediment being deposited/trapped behind a dam

cobble — clast whose intermediate diameter, or b-axis, is 64 to 256 mm[%]

compaction — tighter packing of sedimentary particles resulting in a decrease in porosity*

competence — the ability of a current of water or wind to transport detritus, in terms of particle size rather than amount, measured as the diameter of the largest particle transported. It depends on velocity*

competent flows — streamflows that are able to entrain channel-bed material

confluence — the point where two streams or glaciers meet*

critical discharge — in this paper, the discharge needed to initiate general mobility of channel-bed material

critical shear stress — in this paper, the shear stress at which threshold transport conditions are exceeded and general mobility of channel-bed material occurs

cross section — diagram showing the features transected by a vertical plane* With rivers, generally a diagram of channel bed and bank elevation with distance

degradation — the general lowering of the surface of the land by erosive processes, especially by the removal of material through erosion and transportation by flowing water*

density — the mass or quantity of a substance per unit volume*

detrital — Pertaining to or formed from detritus (loose rock and mineral material produced by mechanic means, e.g., disintegration or abrasion, and removed from its place of origin)*

discharge — rate of streamflow (or sediment transport) at a given instant in terms of volume per unit of time*

drainage network (drainage system) — surface stream, or a body of impounded surface water, together with all other such streams and water bodies that are tributary to it and by which the region is drained*

dynamic (or kinetic) **coefficient of friction** — forces of friction are forces resisting motion; forces of friction acting on an object that is in motion, or forces of dynamic (or kinetic) friction, are proportional to the normal force acting on an object; the proportionality constant is the dynamic (or kinetic) coefficient of friction; i.e. $f_k = \mu_k N$ where f_k = force of dynamic friction, μ_k = dynamic coefficient of friction, and N = the normal force acting on the object[##]

energy slope — slope of the total energy line, $S_f = - dH/dx$, where H is the amount by which the water surface rises from upstream to downstream (hence -H) and x is the distance downstream being considered[@]

entrainment — process of picking up and carrying along, as the collecting and movement of sediment by currents*

exceedance probability — percent of time a certain discharge is equaled or exceeded

falling limb of hydrograph — portion of a hydrograph where discharge is decreasing

fine material — also "fines," very small particles in a mixture of various sizes*

flood peak — the point in a hydrograph of maximum discharge

floodplain — that portion of a river valley, adjacent to the channel, which is built of sediments deposited during the present regimen of the stream and is covered with water when the river overflows its banks at flood stages*

flow duration curve — graph of frequency of flows at a station which shows proportion of time that discharge is equaled or exceeded over a specified period of time

flow parallel axis (of island or bar) — line bisecting island or bar and parallel to main direction of streamflow

fluvial — of or pertaining to rivers; growing or living in a stream or river; produced by the action of a stream or river*

geomorphology — the science that treats the general configuration of the earth's surface; specifically the study of the classification, description, nature, origin, and development of landforms and their relationships to underlying structures, and the history of geologic changes as recorded by these surface features*

gradient — degree of inclination of a part of the earth's surface; steepness of slope. It may be expressed as a ratio (of vertical to horizontal), fraction, percentage, or angle*

grain — a mineral or rock particle with a diameter of less than a few millimeters, such as a sand grain; also, a general term for particles of all sizes, as in the expressions "fine-grained" and "coarse-grained."* Used here as a general term, without regard to size of diameter of particle.

grain-size — see particle size

gravel — clast whose intermediate diameter, or b-axis, is 2.00 to 64.0 mm[%]

headwaters — the upper tributaries of a stream[#]

hydraulic environments — in this paper, locations in the river with similar flow patterns / flow characteristics often induced by similar channel planform geometry

hydraulic mean depth — also "hydraulic depth," ratio of cross-sectional area of streamflow in a channel (A) to top width (T) where top width is the width of the free surface of the fluid at the top of the channel [♉]

hydrograph — graph of discharge versus time

hydrology — the science that deals with global water (both liquid and solid), its properties, circulation, distribution, on and under the earth's surface and in the atmosphere, from the moment of its precipitation until it is returned to the atmosphere through evapotranspiration or is charged into the ocean. In recent years the scope of hydrology has been expanded to include environmental and economic aspects.*

hyperconcentrated flood flows — extremely clast-rich (characteristically volcaniclastic) flood that can result, for example, when a lahar enters a stream [$]

impoundment — dam

in-stream sediments — sediment that is stored in the bed or banks of a stream channel

incise — cut down into, as a river cuts into a plateau*

inflow hydrograph — a hydrograph of streamflow entering the Pelton Round Butte Project

infrared photographs — photographs taken with color infrared film, which is manufactured to record green, red, and the photographic portion (0.7 to 0.9 μm) of the near infrared scene energy[+] Vegetation is highly reflective of near infrared energy and shows up as red in a color infrared photograph. Objects reflecting green and red show up as blue and green, respectively[+]

intermediate axis — the middle-length axis of three mutually perpendicular axes through a rock (the three being the longest, middle, and shortest axes)

intermittent stream — a stream that flows only at certain times of the year, as when it receives water from springs or from a surface source, or a stream that does not flow continuously, as when water losses from evaporation or seepage exceed the available streamflow*

interstice — an open space, void

lag (of coarser material) — coarse-grained material that is rolled or dragged along the bottom of a stream at a slower rate that the finer material, or is left behind after currents have washed away the finer material*

lahar — a landslide or mudflow of pyroclastic material on the flank of a volcano; also the deposit produced*

longitudinal — said of an entity that is extended lengthwise *(e.g. longitudinal stream profile - profile of a stream that extends lengthwise down the stream i.e., from upstream to downstream or vice versa

macrophyte — a plant, especially a marine plant, large enough to be visible to the naked eye#

mainstem — main channel of a river

marginal (deposit) — deposit along the banks/sides of a channel

meander — one of a series of sinuous curves or loops in the course of a mature stream, produced as the stream swings from side to side in flowing across its floodplain or shifts in its course laterally toward the convex side of an original curve.

outflow hydrograph — a hydrograph of streamflow exiting Pelton Round Butte Project

particle — a general term, used without restriction as to shape, composition, or internal structure, for a separable or distinct unit in a rock. * Used in this paper the same as grain.

particle hiding — location of one particle downstream from another particle, in such a way as to protect the downstream particle from the full force exerted by streamflow.

particle size — the general dimensions, such as average diameter or volume, of the particles in a sediment based on the premise that the particles are spheres or that the measurements made can be expressed as diameters of equivalent spheres. It is commonly measured by sieving, by calculating settling velocities, or by determining areas of microscopic images.* In this study, for larger particles, measurements were made in the field using rulers or calipers.

particle-size distribution — the percentage, usually be weight, of particles in each size fraction in which a disaggregated sample of a soil,

pebble — rock, clast, particle, grain, etc.

perennial stream — stream that flows throughout the year; permanent stream*

phi unit (phi grade scale) — a logarithmic transformation of the Wentworth grade scale in which phi = $-\log_2$(particle diameter in mm). Wentworth diameter class limit of 32 mm = -5 phi, 1024 mm = +10 phi

planform — the outline of an object as viewed from above#

Pleistocene — an epoch in the Quaternary period. It began two to three million years ago and lasted until the start of the Holocene some 8,000 years ago.*

Pliocene — An epoch of the Tertiary period*

point bars — one of a series of low, arcuate ridges of sediment developed on the inside of a growing meander by the slow addition of individual accretions accompanying migration of the channel toward the outer bank.*

porosity — measure of the volume of voids per unit volume of sediment

post-dam events — storm events that occurred following construction of Pelton, Round Butte, and the Reregulating Dams

post-filling event — storm events that occurred following the filling of Round Butte Reservoir

prograde — move or build forward or outward

pyroclast — an individual particle ejected during a volcanic eruption. It is usually classified according to size.*

pyroclastic — pertaining to clastic rock material formed by volcanic explosion or aerial expulsion from a volcanic vent; also pertaining to rock texture of explosive origin. It is not synonymous with the adjective "volcanic."*

pyroclastic flow — surface flows of solid fragments of volcanic rock in a fluid (gas or liquid) matrix away from a volcano[&&]. they are gravity controlled, hot, and in some instances, may be partially fluidized[^]

Quaternary — The second period of the Cenozoic era, following the Tertiary. It began 2 to 3 million years ago and extends to the present. It consists of two grossly unequal epochs: the Pleistocene, up to about 8,000 years ago, and the Holocene since that time.*

reservoir inflow — streamflow entering the Pelton Round Butte Project

reservoir outflow — streamflow exiting the Pelton Round Butte Project

riparian — pertaining to or situated on the bank of a body of water, especially of a river* or functionally as the three-dimensional zones of direct interaction between terrestrial and aquatic ecosystems[**]

rising limb of hydrograph — portion of a hydrograph where discharge is increasing

River Kilometer (RK) — distance (in kilometers) from a specified point measured following the course of a river; in this paper, the specified point is the mouth of the Deschutes River, so RK 24 would be 24 km as traveled along the river, upstream from the mouth of the Deschutes

river left — the left bank/side of a river as viewed while looking downstream

River Mile — same as River Kilometer but distance is measured in miles instead of kilometers

river right — the right bank/side of a river as viewed while looking downstream

rotational failure (rotational landslide) — a slide in which shearing takes place on a well defined, curved surface, concave upward, producing a backward rotation in the displaced mass*

roughness element — object that resists streamflow e.g. boulder, vegetation, dune etc.

sampling grids — ten meter by ten meter grids used to conduct the Wolman pebble count technique of determining the particle size distribution of the channel bed surface

sand — clast whose intermediate diameter, or b-axis, is 0.0625 to 1.68 mm[%]

sediment discharge — the amount of sediment moved by a stream in a given time, measured by dry weight or by volume; the rate at which sediment passes a section of stream*

sediment rating curve — graph that relates sediment discharge to water discharge

sediment transport — movement of particles especially in a river

selective erosion — see winnowing

shear stress — the component of stress which acts tangential to a plane through any given point in a body; any of the tangential components of the stress tensor* in the case of sediment transport it is the component of stress tangential to a particle and parallel to flow

silt — clast whose intermediate diameter, or b-axis, is 3.9 to 52.6 μm[%]

sinuosity — (channel length) / (straight-line valley length) [%%]

skin resistance — the frictional resistance between a fluid and the surface of a solid* over which the fluid is moving (i.e. the resistance between the water and the channel bed)

sorting — a measure of the spread of the particle-size distribution on either side of an average*

specific weight — weight per unit volume[&]

stadia rod — a graduated rod used with an instrument having stadia hairs to measure the distance from the observation point to the place where the rod is positioned*

static coefficient of friction — forces of friction are forces resisting motion; forces of friction acting on an object that is stationary, or forces of static friction, are proportional to the normal force acting on an object; the proportionality constant is the static coefficient of friction; i.e. $f_s \leq \mu_s N$ where f_s = force of static friction, μ_s = static coefficient of friction, and N = the normal force acting on the object[##]

substrate — in this paper, subsurface bed material

subsurface bed material — sediment in the channel bed that underlies the surface armor layer

surface armor layer — the layer of particles extending to the depth of the largest surface particle

surface bed material — sediment in the channel bed that are exposed at the bed surface; sediment exposed to streamflow

suspended load — the part of the total stream load that is carried for a considerable period of time in suspension, free from contact with the stream bed*

temporal variability in resistance to transport — a concept discussed in Reid et al. (1985) in which the resistance of the channel bed to transport by streamflow varies depending on the timing of the high streamflows with respect to other bedload transport events and on the position in the storm hydrograph.

Tertiary — The first period of the Cenezoic era (after the Cretaceous of the Mesozoic era and before the Quaternary), thought to have covered the span of time between 65 million and 2 million years ago*

textural patterns — spatial or temporal pattern of channel-bed particle size

thalweg — the line connecting the lowest points along a stream bed or valley,* the point of lowest elevation in a channel cross section

threshold transport conditions — conditions under which bedload transport begins to occur, in this paper, when bedload transport begin to occur over the channel bed as a whole

total volumetric bedload transport rate (per unit gravel-bed width) — the total volume of bedload moved per unit time (per unit width of the channel bed that is composed of gravel-sized or coarser material)

total storage capacity — the total volume of water that a dam stores or is able to store

transects — something that cuts across, here, a straight line cross cutting the river perpendicular to the main direction of streamflow (i.e. cross section) or a straight line (delineated by a survey tape) stretched parallel to streamflow and along which particles were measured

transport days — days during which bedload transport was predicted to have occurred

transport events — a series of "transport days"

transport rates — the total quantity (volume, weight, etc.) of material transported per unit time

Trask sorting coefficient — $[D_{75}(\text{mm})/D_{25}(\text{mm})]^{1/2}$

tributary — any stream that contributes water to another stream*

tributary fans — fan-shaped wedges of sediment deposited where a tributary joins a larger river

tributary junctions — the location at which a tributary joins a larger river

water discharge — the volume of water flowing past a certain point per unit time

water year — the 12 month period between October 1 and September 30

Wentworth scale — an extended version of the Udden grade scale; the scale ranges from clay particles (diameter less than 1/256 mm) to bounders (diameter greater than 256 mm)*

winnowing — separation of fine particles from coarser ones by action of the wind* or water

[$] = Smith, G. A., 1987, The influence of explosive volcanism on fluvial sedimentation: The Deschutes Formation (Neogene) in central Oregon, *Journal of Sedimentary Petrology*, 57(4), 613-629.

* = Bates, R. L., and J. A. Jackson, 1984, *Dictionary of Geological Terms*, Third Edition, American Geological Institute, Doubleday, New York, 571 p.

[♉] = Mott, R. L., 1994, *Applied Fluid Mechanics, Fourth Edition*, Macmillan Publishing Company, New York,

[%] = Based on Wentworth grain-size classification as presented in Church, M. A., D. G. McLean, and J. F. Wolcott, 1987, River Bed Gravels: Sampling and Analysis, in *Sediment Transport in Gravel-bed Rivers*, ed. C. R. Thorne, J. C. Bathurst, and R. D. Hey, John Wiley and Sons, Ltd., 43-88.

[&] = Yang, 1996, *Sediment Transport Theory and Practice*, McGraw-Hill Series in Water Resources and Environmental Engineering, McGraw-Hill Companies, Inc., San Francisco, 393 p..

[&&] = Thorpe, R., and G. Brown, 1985, *The Field Description of Igneous Rocks*, Geological Society of London Handbook Series, John Wiley and Sons, New York, 154 p.

[^] = Cas, R. A. F, and J. V. Wright, 1988, *Volcanic Successions Modern and Ancient*, Chapman and Hall, New York, 528 p.

[#] = *Random House Webster's College Dictionary*, 1995, Random House, New York, NY, 1568 pp.

[@] = Henderson, F. M., 1966, *Open Channel Flow*, Macmillan series in civil engineering, Macmillian Publishing Co., Inc., New York, 522 p.

[+] = Lillisand, T. M., and R. W. Kiefer, 1994, *Remote Sensing and Image Interpretation, Third Edition*, John Wiley and Sons, Inc., New York, 750 p.

** = Swanson, F. J., S. V. Gregory, J. R. Sidell, and A. G. Campbell, 1982, Land-water interactions: the riparian zone, p. 267-291 in R. L. Edmonds ed. *Analysis of Coniferous Forest Ecosystems in the Western United States*, US/IBP Synthesis Series 14, Hutchinson Ross Publishing Co., Stroudsburg, PA

[%%] = Knighton, D., 1984, *Fluvial Forms and Processes*, Edward Arnold, New York, 218 p.

[##] = Serway, R. A., 1986, *Physics for Scientists and Engineers, with Modern Physics*, Second Edition, Saunders Golden Sunburst Series, Saunders College Publishing, New York, 1108 p.

REFERENCES

Andrews, E. D., and J. M. Nankervis, 1995, Effective discharge and the design of channel-maintenance flows for gravel-bed rivers, *Natural and Anthropogenic Influences in Fluvial Geomorphology, American Geophysical Union Monograph 89*, 151-164.

Aney, W. W., M. L. Montgomery, and A. B. Lichens, 1967, Lower Deschutes River, Oregon: Discharge and the fish environment, Lower Deschutes Flow Study Final Report, Oregon State Game Commission, Portland, Oregon, USA.

Appel, E. P., 1986, Oregon Fishing Map: Lower Deschutes River, Frank Amato Publications, Portland, Oregon, USA.

Bonneville Power Administration, 1985, White River Falls Fish Passage Project Final Report, Vol 1, Final Technical Report, p. 24.

Chien, N., 1985, Changes in river regimes after the construction of upstream reservoirs, *Earth Surface Processes and Landforms*, *10*, 143-159.

Church, M., 1995, Geomorphic response to river flow regulation: Case studies and time-scales, *Regulated Rivers: Research and Management*, *11*, 3-22.

Church, M., and R. Kellerhals, 1978, On the statistics of grain size variation along a gravel river, *Canadian Journal of Earth Sciences*, 15, 1151-1160.

Church, M. A., D. G. McLean, and J. F. Wolcott, 1987, River bed gravels: sampling and analysis, in *Sediment Transport in Gravel-Bed Rivers*, ed. C. R. Thorne, J. C. Bathurst, and R. D. Hey, John Wiley and Sons Ltd., 43-88.

Collier, M., R. H. Webb, and J. C. Schmidt, 1996, Dams and rivers: Primer on the downstream effects of dams, *U.S. Geological Survey Circular 1126*, 94 pp.

DeVries, M., 1970, On the accuracy of bed-material sampling, *Journal of Hydraulic Research*, 8, 523-533.

Dewey, J. D., F. E. Roybal, and D. E. Funderburg, 1979, Hydrologic data on channel adjustments, 1970-1975, on the Rio Grande downstream from Cochiti Dam, New Mexico, before and after closure, *United States Geological Survey Water-Resources Investigations 79-70*, 531 pp.

Dietrich, W. E., J. W. Kirchner, H. Ikeda, and F. Iseya, 1989, Sediment supply and the development of the coarse surface layer in gravel-bedded rivers, *Nature*, 340, 215-217.

Fassnacht, H., 1998, Frequency and magnitude of bedload transport downstream of the Pelton-Round Butte Dam Complex, Lower Deschutes River, Oregon, M. S. thesis, Oregon State University.

Ferguson, R.I., and C. Paola, 1997, Bias and precision of percentiles of bulk grain size distributions, *Earth Surface Processes and Landforms*, 22, 1061-1077.

Galay, V. J., R. S. Pentland, and R. A. Halliday, 1985, Degradation of the South Saskatchewan River below Gardiner Dam, *Canadian Journal of Civil Engineering*, 12, 849-862.

Gannett, M. W., D. S. Morgan, and K. E. Lite, 1996, Groundwater/surface water interactions in the upper Deschutes basin, central Oregon, [abs.] *EOS Transactions*, 77(46), F265.

Gilvear, D. J., and S. J. Winterbottom, 1992, Channel change and flood events since 1783 on the regulated River Tay, Scotland: Implications for flood hazard management, *Regulated Rivers: Research and Management*, 7(3), 247-260.

Grams, P. E., 1991, Degradation of alluvial sand bars along the Snake River below Hells Canyon Dam, Hells Canyon NRA, Idaho: Middlebury, Vermont, Middlebury College, unpublished senior paper, 98 p., as cited in, Collier et al., 1996.

Grant, G.E., 1997, A geomorphic basis for interpreting the hydrologic behavior of large river basins, in *River Quality: Dynamics and Restoration*, ed. A. Laenan, CRC Lewis Publishers, 105-116.

Grant, G. E., H. Fassnacht, and E. M. McClure, 1995. *Deschutes River Geomorphology Study, Final Study Plan* - May 12, 1995, FERC No. 2030, prepared for Portland General Electric Company, Portland, Oregon, USA.

Haslam, S.M., 1987, *River plants of Western Europe: the macrophytic vegetation of watercourses of the European Economic Community*, Cambridge University Press, Cambridge, U.K., 512 pp.

Hassan, M. A., and M. Church, 1992, The movement of individual grains of the streambed, in *Dynamics of Gravel-bed Rivers*, ed. P. Billi, R. D. Hey, C. R. Thorne, and P. Tacconi, John Wiley and Sons Ltd., 159-175.

Henshaw, F. F., J. H. Lewis, and E.J. McCaustland, 1914, Deschutes River, Oregon, and its utilization, *U.S.G.S. Water Supply Paper 344*.

Hubbard, L. E., T. A. Herrett, J. E. Poole, G. P. Ruppert, and M. L. Courts, 1997, Water Resources Data, Oregon, Water Year 1996, U.S. Geological Survey Water Data Report OR-96-1, U.S. Geological Survey Water Resources Division Portland, Oregon, USA, 432 pp.

Huntington, C. W., 1985, Deschutes River Spawning Gravel Study, Volume I, Final Report, prepared for U.S. Department of Energy Bonneville Power Administration Division of Fish and Wildlife, Portland, Oregon, USA, 179 pp.

Junk, W. J., P. B. Bayley, and R. E. Sparks, 1989, The flood pulse concept in river-floodplain systems, in *Proceedings of the International Large River Symposium*, ed. D. P. Dodge, Can. Spec. Publ. Fish. Aquat. Sci., 106, 110-127.

Kieffer, S. W., 1985, The 1983 hydraulic jump in Crystal Rapid – Implications for river-running and geomorphic evolution in the Grand Canyon, *Journal of Geology*, 93, 385-406.

Kondolf, G. M., 1997, Application of the pebble count: notes on purpose, method, and variants, *Journal of the American Water Resources Association*, 33, 79-87.

Krumbein, W. C., and F. J. Pettijohn, 1938, *Manual of Sedimentary Petrography*, Appleton-Century Company, New York, NY, 549 pp.

Lagasse, P. F., 1994, Variable response of the Rio Grande to dam construction, in Schumm, S.A., and Winkley, B.R. (Eds), *The Variability of Large Alluvial Rivers*, ASCE Press, New York, NY, 395-420.

Leopold, L. B., and T. Maddock Jr., 1953, The hydraulic geometry of stream channels and some physiographic implications, U. S. Geological Survey Professional Paper 252, 57 pp.

Leopold, L.B., Wolman, M.G., and Miller, J.P., 1964, *Fluvial Processes in Geomorphology*, Freeman, San Francisco, CA, 522 pp.

Manga, M., 1996, Hydrology of spring-dominated streams in the Oregon Cascades, *Water Resources Research*, 32, 2435-2439.

McClure, E. M., 1998, Spatial and temporal trends in bed material and channel morphology below a hydroelectric dam complex, Deschutes River, Oregon, M. S. thesis, Oregon State University.

Meyer-Peter, E., and R. Mueller, 1948, Formulas for bed-load transport, *Proceedings of the 2nd Meeting of the International Association for Hydraulic Structures Research*, 39-64, International Association for Hydraulic Research, Stockholm.

Milliman, J. D., and R. H. Meade, 1983, World-wide delivery of river sediment to oceans, *Journal of Geology*, 91(1), 1-21.

Nehlsen, W., 1995, Historical Salmon and Steelhead Runs of the Upper Deschutes River and Their Environments, Portland General Electric, 78 pp.

O'Connor, J.E., J. H. Hardison, III, and J. E. Costa, in press, Debris flows from failures of Neoglacial moraine dams in the Three sisters and Mt. Jefferson Wilderness areas, Oregon, U.S. Geological .Survey Professional Paper 1608.

O'Connor, J. E., G. E. Grant, J. H. Curran, and H. Fassnacht, in prep., Geomorphology of the Deschutes River canyon below Pelton and Round Butte Dams.

Parker, G., 1990, Surface-based bedload transport relation for gravel rivers, *Journal of Hydraulic Research*, 28(4), 417-436.

Parker, G., P. C. Klingeman, and D. G. McLean, 1982, Bedload and size distribution in paved gravel-bed streams, *Proceedings of the American Society of Civil Engineers Journal of the Hydraulics Division*, 108(HY4), 544-571.

Pemberton, E. L., 1976, Channel changes in the Colorado River below Glen Canyon Dam, *Proceedings of the Third Federal Inter-Agency Sedimentation Conference*, Denver, Colorado, USA., Water Resources Council, 5-61-5-73.

Petts, G. E., 1979, Complex response of river channel morphology subsequent to reservoir construction, *Progress in Physical Geography*, 3(3), 329-362.

Petts, G. E., 1980, Long-term consequences of upstream impoundment, *Environmental Conservation*, 7(4), 325-332.

Petts, G. E. 1984, Sedimentation within a regulated river, *Earth Surface Processes and Landforms*, 9, 125-134.

Portland General Electric, 1996, Portland General Electric Pelton Round Butte Hydroelectric Project Initial Consultation Document, FERC No. 2030, 849 pp.

Reid, I., L. E. Frostick, and J. T. Layman, 1985, The incidence and nature of bedload transport during flood flows in coarse-grained alluvial channels, *Earth Surface Processes and Landforms*, *10*, 33-44.

Rice, S. and M. Church, 1996, Sampling surficial fluvial gravels: the precision of size distribution percentile estimates, *Journal of Sedimentary Research*, 66, 654-665.

Schmidt, J. C., and J. B. Graf, 1990, Aggradation and degradation of alluvial sand deposits, 1965 to 1986, Colorado River, Grand Canyon National Park, Arizona, *U.S. Geological Survey Professional Paper 1493*, 74 pp.

Schumm, S. A., and R. W. Lichty, 1963, Channel widening and flood-plain construction along Cimarron River in southwestern Kansas: Erosion and sedimentation in a semiarid environment, *U.S. Geological Survey Professional Paper* 352-D, 88 pp.

Scott, W. E., T. C. Pierson, S. P. Schilling, J. E. Costa, C. A. Gardner, J. W. Vallance, and J. J. Major, 1997, Volcano Hazards in the Mount Hood Region, Oregon, U.S. Department of the Interior, U.S. Geological Survey Open-File Report 97-89, 14 pp.

Shields, I. A., 1936, Anwendung der Aehnlichkeitsmechanik und der Turbulenzforschung auf die Geschiebebewegung, Mitteilunguen der Preussischen Versuchsanstalt für Wasserbau und Schiffbau, translated by W. P. Ott and J. C. van Uchelen, U.S. Department of Agriculture Soil Conservation Service Cooperative Lab, California Institute of Technology, Pasadena, California, USA, 36 pp.

Smelser, M. G., and J. C. Schmidt, 1998, *An assessment methodology for determining Historical changes in mountain streams*, U.S.D.A. Forest Service Rocky Mountain Research Station General Technical Report RMRS-GTR-6, 29 pp.

Smith, G. A., 1987, The influence of explosive volcanism on fluvial sedimentation: The Deschutes Formation (Neogene) in central Oregon, Journal of Sedimentary Petrology, 57(4), 613-629.

Smith, G. A., 1991, A field guide to depositional processes and facies geometry of Neogene continental volcaniclastic rocks, Deschutes basin, central Oregon, *Oregon Geology*, 53(1), 3-20.

Swanson, Cameron, Evarts, Pringle, and Vance, 1989, IGC Field Trip T106: Cenozoic volcanism in the Cascade Range and Columbia Plateau, southern Washington and northernmost Oregon, *American Geophysical Union Field Trip Guidebook* T106.

U.S. Army Corps of Engineers, Flood Control Regulations for Prineville Dam and Reservoir, drawing number 113-D-39 (general plan and sections), district capacity table dated 1-13-59, 1959, data provided to author by Mr. Larry Zakrajsek, U.S. Bureau of Reclamation, Bend construction office, Bend, Oregon, USA.

U.S. Army Corps of Engineers, Flood Control Regulations for Prineville Dam and Reservoir - Final Construction Report, Specifications Number DC-5047, 1961, data provided to author by Mr. Larry Zakrajsek, U.S. Bureau of Reclamation, Bend construction office, Bend, Oregon, USA.

U.S. Army Corps of Engineers Hydrologic Engineering Center, 1995a, HEC-RAS River Analysis System, Hydraulic Reference Manual Version 1.0, 131 pp.

U.S. Army Corps of Engineers Hydrologic Engineering Center, 1995b, HEC-RAS River Analysis System, User' s Manual Version 1.0, 150 pp.

U.S. Department of Energy, 1985, *White River Falls Fish Passage Project, Tygh Valley, Oregon*, Bonneville Power Administration, Division of Fish and Wildlife Final Technical Report, Volume I of III, p. 24.

U.S. Department of the Interior, Bureau of Reclamation, 1966, Reclamation Project Data (supplement), Crooked River project, U.S. Government Printing Office, Washington, D.C., 275 pp.

U.S. Department of the Interior, Bureau of Reclamation, unpublished report, Project History - Deschutes Project - Oregon, Volume XX, 1967 - 1969, prepared for the North Unit Irrigation District, Madras, Oregon.

U.S. Department of the Interior, U.S. Geological Survey, Water Resources Division,1965, Water Resources Data for Oregon 1965 Part I: Surface Water Records, U.S. Geological Survey Water Resources Division, Portland, Oregon, USA, 359 pp.

U.S. Department of the Interior, U.S. Geological Survey, Water Resources Division, 1994, Description of gaging station 14-0925.00 Deschutes River near Madras, Oregon, 3 pp.

U.S. Department of the Interior, U.S. Geological Survey, 1997a, http://water.usgs.gov/swr/OR/data.modules/hist.cgi?statnum=14076500, October, 1997..

U.S. Department of the Interior, U.S. Geological Survey, 1997b, http://water.usgs.gov/swr/OR/data.modules/hist.cgi?statnum=14087400, October, 1997.

U.S. Department of the Interior, U.S. Geological Survey, 1997c, http://water.usgs.gov/swr/OR/data.modules/hist.cgi?statnum=14091500, October, 1997.

U.S. Department of the Interior Water and Power Resources Service, 1981, Water and Power Resources Service - Project Data, Deschutes River project, Government Printing Office, 1463 pp., Denver, Colorado, USA.

Williams, G. P., and M. G. Wolman, 1984, Downstream effects of dams on alluvial rivers, *U.S. Geological Survey Professional Paper 1286*, 83 pp.

Wolman, M. G., 1954, A method of sampling coarse river bed material, *Transactions of the American Geophysical Union*, 35(6), 951-956.

Xu, J., 1996, Underlying gravel layers in a large sand bed river and their influence on downstream-dam channel adjustment, *Geomorphology*, 17, 351-359.

Xu, J., 1997, Evolution of mid-channel bars in a braided river and complex response to reservoir construction: an example from the Middle Hanjiang River, China, *Earth Surface Processes and Landforms*, 22, 953-965.